Selection and Characterization of Synthetic Antibodies Against Human Rad51

A Thesis Submitted to the College of

Graduate Studies and Research

In Partial Fulfillment of the Requirements

For the Degree of Master of Science

In the Department of Biochemistry

University of Saskatchewan

Saskatoon

By

Yongpeng Fu

Permission to Use

In presenting this thesis in partial fulfillment of the requirements for a Postgraduate degree from the University of Saskatchewan, I agree that the Libraries of this University may make it freely available for inspection. I further agree that permission for copying of this thesis in any manner, in whole or in part, for scholarly purposes may be granted by the professor or professors who supervised my thesis work or, in their absence, by the Head of the Department or the Dean of the College in which my thesis work was completed. It is understood that any copying or publication or use of this thesis or parts thereof financial gain shall not be allowed without my written permission. It is also understood that due recognition shall be given to me and to the University of Saskatchewan in any scholarly use which may be made of any material in my thesis.

Requests for permission to copy or to make other use of material in this thesis in whole or part should be addressed to:

Head of the Department of Biochemistry

University of Saskatchewan

Saskatoon, Saskatchewan, S7N 5E5

Abstract

Chemotherapy is the predominant approach for treating cancer. However, disease relapse frequently occurs because chemotherapy often fails to eliminate all tumor cells due to intrinsic or acquired drug resistance. The failure of conventional chemotherapeutics regimes for cancer highlights the need for novel therapeutic interventions. Recent studies have shown that human Rad51, an evolutionarily conserved DNA recombinase required for homologous recombination, exhibits elevated expression in many cancer cells and is implicated in drug resistance after chemotherapy. Targeted inhibition of human Rad51 has been explored as a way to sensitize cancer cells to chemotherapy. Given the properties of antibodies and their fragments as high-affinity inhibitors, we used antibody phage display to generate antigen-binding fragments (Fabs) against human Rad51. We first isolated human Rad51 specific Fabs by screening a synthetic Fab phage display library against recombinant human Rad51. We isolated a human Rad51 Fab, referred to as Fab F_2, which bound human Rad51 with a K_D of 8.1 nM. Fab F_2 inhibited the DNA binding activity of human Rad51 but did not inhibit human Rad51 ATP hydrolysis activity. We converted Fab F_2 into an scFv-Fc fragment (scFv: single-chain variable fragment; Fc: glycosylated crystallizable fragment) for expression in human embryonic kidney 293T cells. Overexpression of scFv-Fc fragment in human embryonic kidney 293T cells increased 4.48-fold more sensitivity to the DNA-damaging agent methyl methanesulfonate in clonogenic survival assays. To enable the delivery of Fab F_2 into cells we fused it to a cell membrane import tag (FabItag I_2) based on a patent (WO 2014005219 A1) from iProgen Biotech Inc. We labeled FabItag I_2 with an 800CW fluorophore and showed that FabItag I_2 permeated human embryonic kidney 293T cells using fluorescence microscopy and flow cytometry. FabItag I_2 increased the sensitivity of human embryonic kidney 293T cells to methyl methanesulfonate by 2 folds in clonogenic survival assays.

Acknowledgements

I would like to take this opportunity to thank my supervisor Dr. Geyer for his guidance and support through my graduate studies. I enjoyed his passion and devotion he conveyed in regards to the research. I especially want to thank him for always trusting me and giving me freedom to learn and perform as many techniques as possible required for my project.

I would like to express gratitude to my committee members, Dr. Scot Stone and Dr. Scott Napper, whose feedback and suggestions were important for the accomplishment of my experiments and thesis.

I would like to thank current and past members from Geyer lab. In particular, I would like to thank Dr. Patricia González Cano and Dr. Landon Pastushok. Dr. Patricia González Cano not only taught me technical skills at the beginning of my program, but also responded to my endless questions with patience. Dr. Landon Pastushok provided many insightful ideas through my project and brought encouragement when experiments did not go well. I cannot complete Master studies without their help. Also, thanks to Dr. Luke Truitt and Karen Mochoruk for their helping in the cell biological portion of my project; Dr. Md Kausar Alam and Dr. Jianghai Liu, for their guide in general experiment procedures; Wayne I Hill and Lindsay Pelzer, for their technical assistance; Kevin Voth and Ashley Sutherland, for their proof-reading help.

In addition, I owe great thanks to my parents and my girlfriend Xue Li. It is their love, understanding and encouragement in these years, especially in the moment when I felt depressed, that endowed me with the strength to move forward. I will always be grateful.

Finally, I would like to thank CHINA SCHOLARSHIP COUNCIL for their financial support.

Table of Contents

List of Figures

List of Tables

List of Abbreviations

2xYT	2x Yeast extract and Tryptone Broth
BLI	Biolayer interferometry
Cap	Chloramphenicol
Carb	Carbenicillin
CCC-dsDNA	Covalently closed circular dsDNA
CDRs	Complementarity-determining regions
CFU	Colony-Forming Unit
CH	Constant heavy chain
CL	Constant light chain
DSB	Double-strand break
DSBR	Double-strand break repair
dsDNA	Double stranded DNA
dU-ssDNA	Uracil-containing ssDNA
ELISA	Enzyme-linked immunosorbent assay
Fab	Antigen-binding fragment
FBS	Fetal bovine serum
Fc	Crystallizable fragment
FTK	Fusion tyrosine kinase
G.A.	Gibson assembly
HEK	Human embryonic kidney
HJs	Holiday junctions
HR	Homologous recombination
hRad51	Human Rad51
IC_{50}	Half-maximal inhibitory concentrations
IgG	Immunoglobulin G
IPTG	isopropyl β-D-1-thiogalactopyranoside
IR	Ionizing radiation
Itag	Import tag
Kan	Kanamycin
LB	Luria Broth
MMC	Mitomycin C
MMS	Methyl methanesulfonate
NGS	Next generation sequencing
NHEJ	Non-homologous end joining
PBT	Phosphate buffered saline with BSA and tween 20
PTD	Protein transduction domain
ROS	Reactive oxygen species
scFv	Single-chain variable fragment
SDS-PAGE	Sodium Dodecyl Sulphate Polyacrylamide Gel Electrophoresis

SDSA	Synthesis-dependent strand annealing
SOC	Super Optimal Broth with Catabolic Repressor Medium
SP	Secretion signal peptide sequence
SSA	Single-strand annealing
ssDNA	Single stranded DNA
Tet	Tetracycline
VH	Variable heavy chain
VL	Variable light chain

Chapter 1 Introduction

Homologous recombination (HR) is used by cells to accurately repair DNA double-strand breaks (DSBs) using intact homologous DNA sequences (San Filippo *et al.*, 2008). The repair mechanism is defined by two main reactions, DNA strand invasion and joint molecule formation. These reactions are catalyzed by a class of conserved proteins, which includes the essential recombinase Rad51 (homolog of *Escherichia coli* RecA), an ATPase with DNA binding activity (Sung and Robberson, 1995). Rad51 polymerizes on resected single-stranded DNA ends to form a Rad51-DNA nucleoprotein filament (also referred to as presynaptic filament), promoting strand invasion and homologous pairing between two DNA duplexes (Benson *et al.*, 1994; Baumann *et al.*, 1996). The essential role of Rad51 in HR is supported by studies showing that the RAD51 deletion causes early embryonic lethality (Tsuzuki *et al.*, 1996), and that Rad51-deficident DT40 chicken cells accumulate chromosome breaks and aberrations resulting in cell lethality (Sonoda *et al.*, 1998). Rad51 expression and activity must be carefully regulated in normal cells to control HR and maintain genome integrity. In contrast, when Rad51 is deregulated it can lead to the loss of genomic rearrangements, which is central to the progress of carcinogenesis (Arias-Lopez *et al.*, 2006).

Chemotherapy is currently the predominant therapeutic strategy in many cancers. It damages the DNA of tumor cells by inducing adducts or single- or double-strand breaks in DNA. Disease relapse often occurs because chemotherapy fails to eliminate all tumor cells due to the intrinsic or acquired drug resistance. Chemoresistance can emerge because deregulated DNA repair removes chemotherapy-induced DNA damage in cancer cells (Vispe *et al.*, 1998). The failure of conventional chemotherapeutics regimes for treating cancer highlights the need for novel therapeutic interventions. Over-expression of human Rad51 (hRad51) and the resultant enhanced HR rates is described for a variety of cancer cells, including breast cancer, pancreatic, non-small cell lung carcinoma, and leukemia (Maacke, Jost*, et al.*, 2000; Maacke, Opitz*, et al.*, 2000; Bearss *et al.*, 2002; Raderschall *et al.*, 2002; Slupianek *et al.*, 2002). In these cancers, hRad51 over-expression gives rise to cancer resistance by promoting the repair of chemotherapy-induced DSBs (Vispe *et al.*, 1998). Targeted hRad51 inhibition using ribozyme or antisense treatments results in longer median survival after cancer treatment (Christodoulopoulos *et al.*, 1999; Collis *et al.*, 2001). Therefore, targeted inhibition of hRad51

using small molecule or biologic drugs is being explored as a way to sensitize cancer cells to chemotherapy.

Several small-molecule hRad51 inhibitors have been isolated using high-throughput drug screening (Ishida *et al.*, 2009; Huang *et al.*, 2011; Zhu *et al.*, 2013). However, many of these small molecules are limited by their specificity and cellular toxicity, which can cause side effects in cancer patients. As a result, most hRad51 small molecule inhibitors have only been used for *in vitro* studies to characterize hRad51 activities (Ward *et al.*, 2015). Thus, there is a need to develop more potent, specific, and less toxic anti-Rad51 drugs.

Here, we used an antibody phage display platform to generate "synthetic" antibodies against hRad51. In contrast to many chemical inhibitors, antibodies have the potential to neutralize antigen proteins *in vivo* (Antman and Livingston, 1980). However, application of antibody or antibody fragments for inhibiting intracellular targets is hindered by their inefficient delivery across the cell membrane. In this thesis, we used a membrane import peptide based on iProgen Biotech Inc. to facilitate the transport of antibody fragments across cell membrane (Patent: WO 2014005219 A1). This membrane import sequence consists of a secretion signal peptide sequence and a cleavage inhibition sequence, which exhibits efficient intracellular protein transduction efficiency. Fusing this membrane import sequence to Fab resulting in cell membrane internalization and sensitization of cells to DNA-damaging agent methyl methanesulfonate (MMS).

Chapter 2 Literature Review

2.1 Human Rad51 Recombinase

Homologous recombination (HR) is an essential mechanism for repairing a variety of DNA lesions in order to maintain genome stability. HR mechanism can be defined into two mechanistic steps, DNA strand invasion and joint molecule formation. Genetic and biochemical studies in *S. cerevisiae* showed that a class of enzymes known as recombinases, and their associated cofactors, catalyze these reactions. Of particular interest is Rad51, which is structurally and functionally homologous to the RecA recombinase in bacteria (Kowalczykowski, 1991; Radding, 1991; Conway *et al.*, 2004). The filament structure of RecA protein has been known for over a decade, however no complete crystal structure of Rad51 has been determined. NMR imaging and mutation analysis (Aihara *et al.*, 1999) have shown that Rad51 contains two domains, an N-terminal DNA binding domain, both single and double stranded DNA (ssDNA) (dsDNA) as well as a C-terminal ATP binding domain. Rad51 polymerizes on ssDNA to form a Rad51-ssDNA nucleoprotein filament (also referred to as presynaptic filament) in which homology search and DNA joint formation are catalyzed (Sung and Robberson, 1995). Although ATP binding is essential for Rad51 function in strand exchange, hydrolysis is not (Morrison *et al.*, 1999). The highest expression of Rad51 in proliferating cells is observed in S or S/G2 phase of the cell cycle, which correlates with high levels of HR observed in these stages of cell cycle (Yamamoto *et al.*, 1996; Chen *et al.*, 1997; Lundin *et al.*, 2003). The essential role of Rad51 in HR is supported by the Rad51 gene knockout in mice which leads to early embryonic lethality (Tsuzuki *et al.*, 1996), and by Rad51-deficident DT40 chicken cells that accumulate chromosome breaks and aberrations, resulting in cell lethality (Sonoda *et al.*, 1998).

2.1.1 Homologous Recombination

There are many endogenous and exogenous sources of DNA damage including reactive oxygen species (ROS), environmental exposure to irradiation, chemical agents, and ultraviolet light (UV). It has been estimated that a single human cell can suffer up to tens of thousands of DNA lesions per day (Jackson and Bartek, 2009). Among all types of DNA lesions, double-stranded break (DSB) is the most lethal as cells cannot circumvent even one unpaired DSB

(Jackson and Bartek, 2009). Fortunately, cells have evolved several mechanisms to repair DNA lesions.

Homologous recombination (HR) is an important mechanism for the repair of damaged chromosomes, particularly in DNA damage involving DSB (Moynahan and Jasin, 2010). At least two distinct HR pathways are accountable for DSB repair: double-strand break repair (DSBR) pathway (also referred to as double Holliday junction model) (see **Figure 2.1A**) and synthesis-dependent, strand-annealing (SDSA) pathway (see **Figure 2.1B**) (Sung and Klein, 2006). DSBR model was discovered in yeast, where it was shown that linear DNA containing ends that were identical in sequence to sections of a yeast chromosome could be specifically incorporated into the yeast chromosome at the site of identical sequence (Orr-Weaver *et al.*, 1981; Orr-Weaver and Szostak, 1983). Though different modifications may be adapted from its original conception, key features of this model are (see **Figure 2.1A**): (a) introduction of DSBs, (b) nucleolytic resection of DSBs to produce 3'-overhangs of ssDNA on either side, (c) formation of a recombinase filament on the ssDNA overhangs, (d) formation of a displacement loop (D-loop) following strand invasion into a homologous DNA, (e) extension of the 3'-overhangs to capture the corresponding end of DSBs, (f) generation of a DNA joint molecule harboring two Holliday junctions (HJ)s, and (g) resolution of the HJs to form non-crossover or crossover products. Unlike DSBR, which accounts for many observations found in meiotic recombination that are frequently associated with crossovers, SDSA explains mitotic DSBs repair, which is most frequently not associated with crossovers (Strathern *et al.*, 1982; Hastings, 1988; Nassif *et al.*, 1994; Ferguson and Holloman, 1996). The SDSA pathway is similar to the DSBR pathway in initial pathway reactions, including steps (a), (b), (c), and (d) in DSBR. In SDSA, however, a migrating D-loop never extends to capture the corresponding DSB end. Instead, the invading strand is displaced and re-anneals with the ssDNA tail on the other DSB end. Therefore, no HJs are produced in the SDSA pathway and consequentially only non-crossover products are made.

Not all DSBs associated with HR involve two DNA ends as described in DSBR and SDSA modes. A third pathway called break-induced replication (BIR) is more often evoked when there is only one DNA end (see **Figure 2.1C**) (Malkova *et al.*, 1996). The initiation of BIR is similar to that of DSBR pathway in steps (a), (b), (c), and (d). However, the single-stranded tail invades either a homologous DNA sequence present in a sister chromatid or a

repeated sequence on a different chromosome. When the sister chromatid is used in BIR, the copy is identical and DNA is accurately repaired. When a repeated sequence on a non-homologous chromosome is used in BIR, the result is a nonreciprocal recombination. With the exception of some forms of BIR, all of the above HR pathways require a recombinase. However, DSBs can also be repaired using non-HR pathways that do not involve a recombinase. One of these pathways is the single-stranded annealing (SSA) pathway, which does not require recombinase but still requires other HR factors to mediate annealing (see **Figure 2.1D**). In SSA, resected ends are closely flanked by direct repeats and can be annealed and ligated (Lin *et al.*, 1984). Protruding single-strand tails are then removed, resulting in deletion of one repeat and sequences between repeats. Another recombinase-independent pathway for DSB repair is non-homologous end joining (NHEJ), which ligates DSBs ends directly without requiring any homology between joining sequences (see **Figure 2.1E**) (Krogh and Symington, 2004).

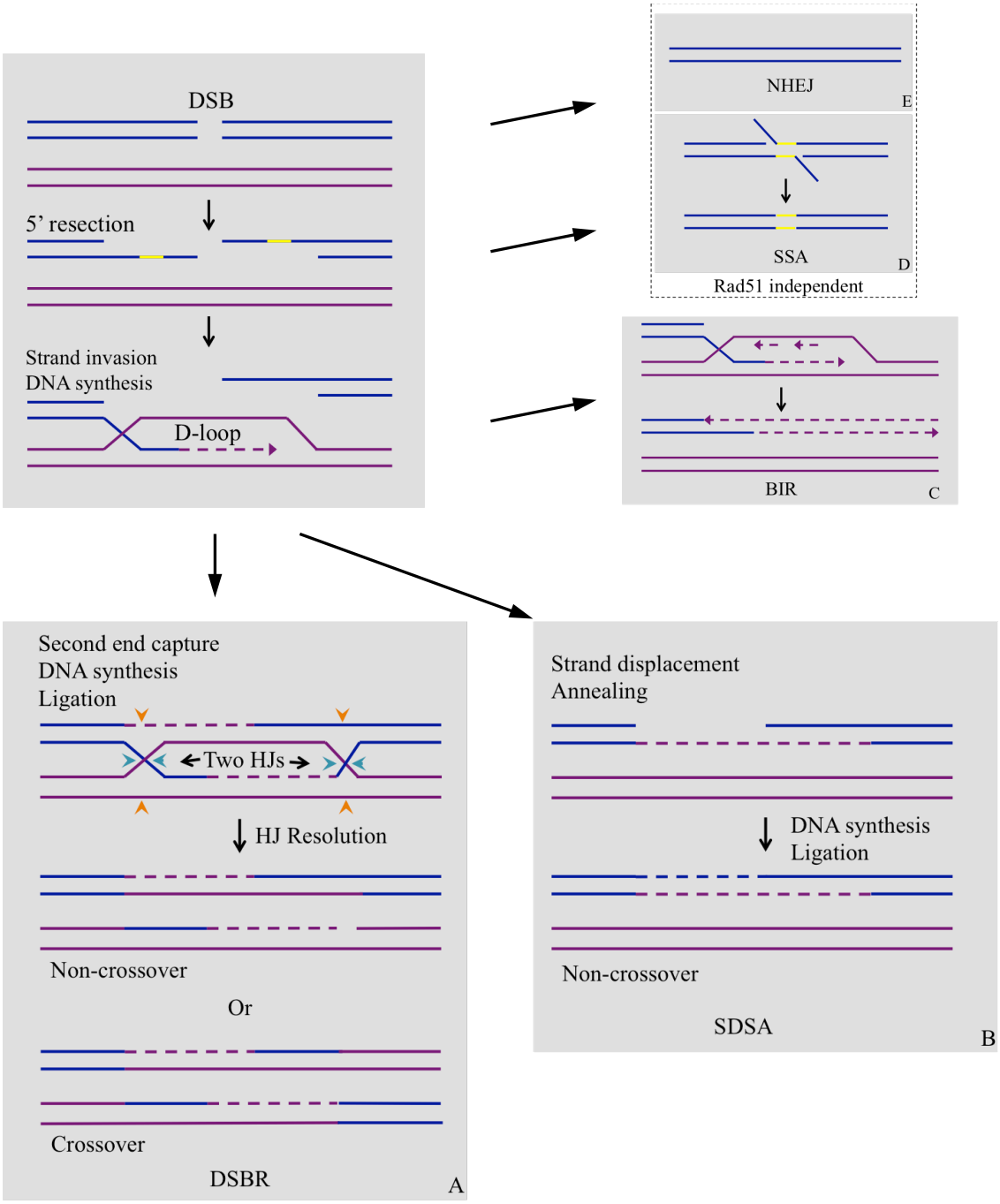

Figure 2.1 Pathways for Repairing DNA Double-strand Breaks
Double-strand breaks (DSBs) can be either repaired using Rad51-dependent pathways via homologous recombination (HR), which include double-strand break repair (DSBR), synthesis-dependent strand annealing (SDSA), and break-induced replication (BIR) or Rad51-independent pathways, which include single-stranded annealing (SSA) and non-homologous end joining (NHEJ). All pathways are initiated by nucleolytic resection of a DSB to produces 3'-overhangs. For Rad51-dependent pathways, a displacement loop (D-loop) is formed after these 3'-overhangs invade into a homologous sequence followed by DNA synthesis at the

invading end. In the DSBR pathway (A), the extension of the 3'-overhangs captures the second end of DSBs to form an intermediate with two Holliday junctions (HJs). Resolution of HJs can produce non-crossover (green arrow heads at both HJs) or crossover product (orange arrow heads one HJ and green heads at the other HJ). In the SDSA pathway (B), strand displacement occurs followed by annealing of the extended single-strand end to the ssDNA on the other break end, and by gap-filling DNA synthesis and ligation. In the BIR pathway (C), the reaction proceeds in the absence of the second DNA end. Both lagging and leading strand synthesis occur in the D-loop intermediate. For Rad51-independent pathways, no homologous sequence is involved. In the SSA pathway (D), direct repeats flanking the resected-ends anneal with each other and the protruding single-strand tails are removed. In the NHEJ pathway (E), DSBs ends are directly ligated. Dashed lines indicate the newly synthesized DNA. Yellow solid line indicates repeat sequence. Figure is adapted from (Krejci *et al.*, 2012)

2.1.2 Human Rad51 and Cancers

Accumulation of DNA damage is believed to eventually give rise to cancer (Hanahan and Weinberg, 2000), which is evidenced by the fact that DSBs and resultant genomic rearrangements are commonly found in cancer cells (Aplan, 2006). DNA repair, particularly HR, is essential for cells to maintain genomic integrity in response to various DNA damage caused by different sources. Although HR is considered to be an error-free rearrangement for DSB repair and for the maintenance of genome integrity, aberrant or dysregulated HR can cause genome rearrangement such as chromosomal translocation, deletions or amplification, which are strongly linked to carcinogenesis in humans (Richardson *et al.*, 1998; Richardson and Jasin, 2000; Bishop and Schiestl, 2003). Consistent with the importance of recombinase in the HR pathway, it is not surprising that altered expression of Rad51 is strongly correlated with genesis or progression of tumors (Kato *et al.*, 2000; Raderschall *et al.*, 2002; Blasiak *et al.*, 2003). Decreased levels of Rad51 have been observed in prostate cancer cells (Wang *et al.*, 2005), 30% of breast cancer cases (Yoshikawa *et al.*, 2000), and are associated with an increased risk of multiple myeloma (Munshi *et al.*, 2004). More importantly, increased Rad51 expression can lead to pathological recombination events between non-homologous or repetitive sequences, resulting in detrimental genome rearrangements (Lengauer *et al.*, 1998) (**Figure 2.2**), which is associated with treatment resistance (Short *et al.*, 2011; Kiyohara *et al.*, 2012), tumor relapse, and worse overall patient survival rate (Barbano *et al.*, 2011). Multiple immortalized and tumor cell lines show increased expression levels of Rad51 (Xia *et al.*, 1997; Raderschall *et al.*, 2002). However, elevated Rad51 expression is not due to gene amplification, but rather from increased transcription of the RAD51 gene. Rad51 promoter

activity, mRNA, and protein levels are increased an average of 840-, 4-, and 6-fold, respectively, compared to normal counterparts (Hine CM, 2008). Regulating the diphtheria toxin A with the Rad51 promoter is severely toxic to cancer cells while having minimal effect on normal cells, indicating Rad51 promoter hyperactivity is specific to cancer cells (Hine *et al.*, 2014). Several driver oncogenes activate the expression of Rad51 promoter gene in a gradual, step-wise manner as cells accumulate mutations and progress towards malignancy (Hine *et al.*, 2014). The ensuing overexpression of Rad51 causes illegitimate and hyper-recombination that may advance normal cells towards neoplastic transformation or further lead to cancer progression and metastasis (Nagathihalli and Nagaraju, 2011). A panel of cancers have been reported to exhibit elevated levels of Rad51 expression, including CML, breast cancer (Maacke, Opitz*, et al.*, 2000), pancreatic cancer (Maacke, Jost*, et al.*, 2000), head and neck (Connell *et al.*, 2006), invasive breast cancer (Maacke *et al.*, 2002), and non-small cell lung cancer (Qiao *et al.*, 2005). Elevated Rad51 expression and resultant enhanced HR rates correlate with high proliferation rate and radio- and chemo-resistance in cancer cells. On the contrary, *in vitro* and *in vivo* studies show that depletion of Rad51 by antisense RNAs attenuated radiotherapy resistance (Taki *et al.*, 1996; Ohnishi *et al.*, 1998) and intensified killing of cancer HeLa cells by cisplatin (Ito *et al.*, 2005). As such, being able to restore Rad51 to normal levels may sensitize cancer cells to DNA damaging treatments.

Aberrant levels of Rad51 alone may not be sufficient to initiate tumorigenesis. One study examined the potential for Rad51 to promote tumorigenesis at the earliest steps following injection of Rad51-transfected cells into athymic nude mice. It showed that the rate of tumor formation and size of tumor recovered 20 days post-injection is not elevated, indicating that overexpression of Rad51 alone in cells is not sufficient to progress normal cells to cancer cells *in vivo* (Bertrand *et al.*, 2003). It was recently found that Rad51 acts as a transcriptional co-factor to regulate metastatic gene expression in concert with c/EBPβ (Wiegmans *et al.*, 2014). Elevated expression of Rad51 promotes c/EBPβ transcription and upregulates subsequent metastatic genes that control cell mobility, proliferation, adhesion, and extra-cellular matrix. Therefore, cancer progression provoked by Rad51 can occur by two distinct mechanisms: (i) direct upregulation of pro-metastatic expression or (ii) aberrant HR pathway activation (Wiegmans *et al.*, 2014). Taken together, Rad51 is shown to be a clinically relevant biomarker

and an important target for the development of inhibitors to promote the efficiency of chemotherapy.

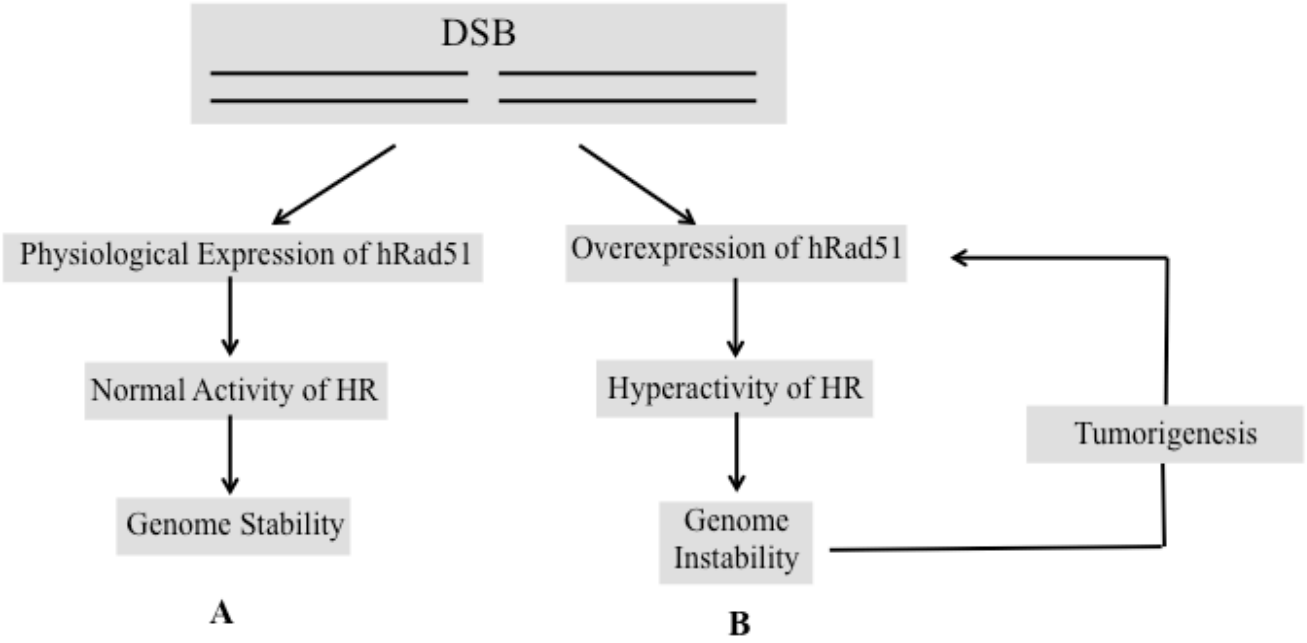

Figure 2.2 Effects of Rad51 Expression on Genome Stability
(A) In response to DSBs generated either from endogenous and exogenous sources or drug treatment, physiological expression of Rad51 maintains the normal activity of HR for DSB repair, maintaining genome stability. (B) Overexpression of Rad51 leads to hyperactivity of HR for DSB repair, which in turn results in genome instability. The loss of genome stability could advance normal cells towards neoplastic transformation ending up with tumorigenesis and along with selective pressure drive the accumulation of gene mutations and Rad51 expression.

2.1.3 Human Rad51 as a Therapeutic Target

Different molecular and cellular features between cancer and normal tissue are usually the basis for cancer therapy. Most cancer cells proliferate faster than their normal counterparts, making the cell cycle a potential therapeutic target. Efforts to inhibit the cell cycle have targeted mitotic spindle assembly in cell division, preventing equal division of DNA to progeny. Therapeutic antibodies and hormonal manipulation strategies have also been used to block growth signaling pathways intended for cell cycle initiation (Dickson and Schwartz, 2009). The most common means of targeting cell cycle is to introduce DNA damage into rapidly dividing cells using ionizing radiation (IR) and chemotherapy. DNA damage causes cell-cycle arrest and cell death directly or following DNA replication during the S phase of the

cell cycle. Because differentiated somatic cells of adult mammals generally replicate infrequently or not at all, DNA-damaging treatments are more toxic to cancer cells. Moreover, cancer cells are often addicted to a single DNA repair pathway whereas normal cells often possess two or more pathways. From a cancer risk perspective, an innate deficiency in DNA repair is undesirable, however, it can be exploited with chemotherapy to create synthetic lethality.

Synthetic lethality exists when a cell bearing mutations in two genes cannot survive whereas a mutation in only one of these two genes is not lethal to the cell (Jalal *et al.*, 2011). For example, DNA repair enzyme poly(ADP-ribose) polymerase 1 (PARP-1) and the BRCA (Breast Cancer Associated) proteins are both important players for cells to repair DSBs through HR (Farmer *et al.*, 2005; Ashworth, 2008). Inhibition of either (PARP-1) or BRCA cannot kill the cell, but the impairment of both is lethal to the cell. In fact, BRCA-deficient breast cancer cells exhibit extreme sensitivity to the inhibition of the PARP-1 (Farmer *et al.*, 2005; Ashworth, 2008). One study showed that the reason for PARP inhibition sensitivity is implicated with HR deficiency rather than a BRCA deficiency (McCabe *et al.*, 2006), which provides a sight to explore PARP inhibition in a wider range of tumors bearing HR deficiency. On the other hand, finding new strategies to inactivate specific proteins of the HR pathway in combination with DNA damaging agents can be an alternative therapeutic approach for clinical anti-cancer treatments. Because Rad51 plays an indispensable role in HR, approaches to target Rad51 expression in tumor cells have gained much interest.

Inhibition of Rad51 can be achieved by down regulating Rad51 expression, impairing the recombinase activity, or interfering with interactions between Rad51 and its partners. Depletion of hRad51 by siRNA has been successfully shown to attenuate radiotherapy resistance *in vitro* and *in vivo* for a variety of tumor cells (Taki *et al.*, 1996; Ohnishi *et al.*, 1998; Ito *et al.*, 2005; Kiyohara *et al.*, 2012). However, it is not without its limitations such as off-target effects, side effects, and delivery difficulties. Microarray gene analysis showed that the expression of dozens of non-targeted genes is modestly altered by siRNA transfection into cells (Jackson *et al.*, 2003). Side effects result from activation of the immune system in response to the exogenous RNA molecules or the delivery vehicle (Judge *et al.*, 2005). Difficulties associated with delivery include cellular membrane transport and accumulation of systemically delivered siRNAs in the liver (Jackson and Linsley, 2010).

Another indirect approach is targeting histone deacetylases (HDACs), which are a class of epigenetic regulators that control chromosome packing and transcription silencing. HDACs inhibition leads to chromatin reorganization, resulting in changes in expression profiles of cells. Expression of HR proteins, including Rad51, is repressed upon HDACs inhibition (Kachhap *et al.*, 2010). Several HDAC inhibitors (HDACi) have been shown to downregulate Rad51 (Kachhap *et al.*, 2010; Xie *et al.*, 2013) and exhibit synergistic effect in combination with PARPi and radiotherapy (Adimoolam *et al.*, 2007). However, the lack of specificity in epigenetic targeting limits clinical success for HDACi-mediated reduction of Rad51. In addition, a study conducted by Du *et al*., found that Rad51 foci formation is also inhibited by methotrexate, a molecule acting as an inhibitor of folic acid metabolism that is clinically used in the treatment of acute lymphoblastic leukemia and osteosarcoma cancers (Du *et al.*, 2012). Despite potential clinical application in combination therapies that induce DNA damage, the effect of methotrexate on HR requires more investigation in a variety of Rad51 overexpressing cancer cell lines.

Rad51 assembles on both ssDNA and dsDNA to form similar filaments for HR reactions (Ristic *et al.*, 2005). As a result of the affinity of Rad51 for DNA, Martinez *et al*., explored whether Rad51 could be directly inhibited by DNA aptamers, which consist of single-stranded oligonucleotides capable of entering tissues and binding a specific target (Martinez *et al.*, 2010). In this study, they isolated three specific DNA aptamers against Rad51 (see **Table 1**) using Systematic Evolution of Ligands by Exponential enrichment. These aptamers inhibited DNA strand exchange activity and ATP/Rad51/ssDNA filaments formation, however, more studies are required to investigate the therapeutic potential of these aptamers with respect to their effects on Rad51 focus formation, HR rate, and cell survival after DNA damaging treatment.

Small molecule modulators of Rad51 remain the most conventional and effective approach. These molecules act directly on the catalytic steps of Rad51 recombinase activity, including interference of Rad51 heptamer formation and ATP/Rad51/ssDNA filament formation (Arkin and Wells, 2004). The most extensively studied small molecule inhibitors of Rad51 are summarized in **Table 2.1**. Among them is a chemical compound 4'-Diisothiocyanostilbene-2, 2'-disulfonic acid (DIDS) that directly interacts with Rad51 close to the DNA-binding site thereby competing with DNA for Rad51 binding (Ishida *et al.*, 2009).

DIDS binds to Rad51 with K_D of 2 μM and the IC_{50} of DIDS on strand exchange activity is in 1-10 μM ranges when Rad51 is 6 μM (Ishida *et al.*, 2009). However, the effect of DIDS on the HR and DNA repair was not evaluated in human cells because DIDS exhibits high level toxicity on cells due to its ability to inhibit ionic channels and membrane transporters (Wulff, 2008).

Another Rad51 inhibitor compound **1** (RI-1) was isolated by performing high-throughput screening of a 10,000-compound pool (Chembridge DIVERSet^{TM}) using fluorescence polarization to assay nucleoprotein filament formation (Budke *et al.*, 2012). The IC_{50} of RI-1 inhibition of ssDNA binding is 5-30 μM with corresponding Rad51 in 0.2-0.4 μM ranges (Budke *et al.*, 2012). Even though consistent reduction in IR and mitomycin C (MMC) induced Rad51 foci formation is observed following RI-1 treatment, RI-1 may have limited therapeutic applications because RI-1 exhibits off-target effects and instability in biological systems (Budke *et al.*, 2012). Takaku *et al*., identified a compound halenaquinone that can impair D-loop formation and homologous pairing from 160 crude extract fractions of marine sponges (Takaku *et al.*, 2011). Interestingly, halenaquinone only inhibits strand exchange of nucleoprotein filament but not the formation of filament, which is because halenaquinone blocks Rad51 binding to dsDNA but not ssDNA. However, halenaquinone were reported to associate with toxic effects on cells, limiting its therapeutic applications (Budke *et al.*, 2013).

Huang *et al*., identified a small molecule B02 that inhibited Rad51 DNA strand exchange activity by screening >20,000 compounds from the NIH Small Molecule Repository (Huang *et al.*, 2011). B02 binds directly to Rad51 with a K_D of 5.6 μM and inhibits human Rad51 (1 μM) in a D-loop assay with an IC_{50} of 27.4 μM. B02 blocks the binding of ssDNA to Rad51 thereby disrupting the nucleoprotein filament formation, which subsequently inhibits ATP hydrolysis by Rad51 (Huang *et al.*, 2012). In mouse embryonic fibroblasts, a 17- and 5-fold increase in cell sensitivity to cross-linking agents cisplatin and MMC, respectively is observed following B02 treatment. However, inhibition of Rad51 by B02 exhibits little effect on the survival of MEF cells with DNA damage induced by MMS (Huang *et al.*, 2012).

Using yeast two-hybrid system, Zhe *et al*., isolated a small molecule IBR2, which mimics the interaction between Rad51 and BRC repeats (conserved domains of BRCA2) (Zhu *et al.*, 2013). Because BRC binding occupies the Rad51 hydrophobic pocket responsible for Rad51 multimerization, IBR2 binding inhibits HR by preventing Rad51 multimerization following

filament formation. Unexpectedly, IBR2 also increases proteasome-mediated degradation of Rad51 in cells. IBR2 was shown effectively inhibiting cell growth in a panel of cell lines (Zhu *et al.*, 2013).

Most small molecule Rad51 inhibitors are chemotherapeutic agents isolated by screening large collections of commercialized chemical compounds for their inhibitory effects on Rad51 recombinase activity. However, many of these small molecules have limitations such as non-specificity and high cellular toxicity, thereby causing significant side effects on cancer patients. Therefore, there is a need to develop more potent, specific, and less toxic anti-Rad51 agents. Because antibodies are highly specific for their targets both *in vitro* and *in vivo*, antibodies and their fragments have gained a lot interest for screening anti-Rad51 agents.

2.2 Phage Display

Antibody phage display is a library selection technology for isolating "synthetic" antibodies without using animals (Smith, 1985). Being the first artificial antibody selection platform, phage display has had a major impact on immunology, cell biology, pharmacology, and the development of therapeutic antibodies (Bradbury and Marks, 2004; Hoogenboom, 2005). In contrast to traditional methods of antibody generation, such as mouse hybridoma techniques (Watters *et al.*, 1997), antibody phage display can be readily modified to manipulate selection conditions and stringencies (Winter and Milstein, 1991; Watters *et al.*, 1997). In addition, antibody phage display obviates the disadvantage of hybridoma antibodies that may cause human anti-mouse antibody reaction (Courtenay-Luck *et al.*, 1986; Tjandra *et al.*, 1990). Both the hybridoma system and antibody phage display provide a means of selecting potential antibodies against specific antigens, but the latter one can be performed in a high throughout manner. Phage display allows antibody specificities to be obtained that would have otherwise been eliminated in animal expression system because of tolerance mechanisms (Roovers *et al.*, 2001). Further, phage display technique is inexpensive, simple, rapid to set up, and accessible to most molecular biology laboratories.

Table 2.1 Small Molecule Inhibitors of Rad51

Compound	K_d/IC_{50} values	Mechanism	Effects	Limitations	Reference
DIDS	K_d=2 μM; IC_{50}=1-10 μM/(6 μM Rad51)	Blocks Rad51 binding to ssDNA	↓Stand exchange reactions	High cellular toxicity	(Ishida *et al.*, 2009)
RI-1	IC_{50}=5-30 μM/(0.2-0.4 μM Rad51)	Inhibits Rad51 polymerization	↓IR and MMC induced Rad51 foci formation	Irreversibly binding to Rad51; long pre-treatment time (24h)	(Budke *et al.*, 2012)
Halenaquinone	IC_{50}=60 μM	Blocks Rad51-ssNDA filament binding to dsDNA	↓Exchange of nucleoprotein filament ↓IR induced Rad51 foci formation	High cellular toxicity because of Michael acceptor activity	(Takaku *et al.*, 2011)
B02	IC_{50}=27.4 μM/(1 μM Rad51)	Disrupts Rad51 binding to DNA	↓Rad51 DNA strand exchange activity ↓IR and cisplatin induced Rad51 foci formation ↑Sensitivity to MMC and cisplatin	Long pre-treatment time required to sensitize cells	(Huang *et al.*, 2011)
IBR2	IC_{50}=10 μM	Disrupts Rad51 binding to BRC2, prevents Rad51 multimerisation and filament formation; Increases proteasome-mediated Rad51 degradation	↓IR induced Rad51 foci formation; ↓Cell proliferation and tumor growth rate ↑Sensitivity to imatinib	Long incubation time with IBR2 required (32h)	(Zhu *et al.*, 2013)
Non-small molecule Rad51 inhibitor **DNA aptamers**	IC_{50}: A13=20 nM A30=22 nM A79=25 nM	Promotes dissociation of ATP/Rad51/ssDNA complex	↓Rad51 DNA strand exchange activity	Therapeutic potential needs to be investigated	(Martinez *et al.*, 2010)

Antibody phage display has provided approximately 30% of all human antibodies currently in clinical development. The clinically most advanced human antibody derived from phage display is the D2E7 anti-TNFα IgG1 antibody, adalimumab (den Broeder *et al.*, 2002). TNFα (tumor necrosis factor alpha) is a proinflammatory mediator implicated in autoimmune conditions. Adalimumab has been approved for the treatment of several conditions including rheumatoid arthritis, ankylosing spondylitis, chronic plaque psoriasis, and Crohn's disease, which was the first fully human antibody approved by the FDA in 2002. Another example of an antibody isolated by phage display against a cytokine target is the B-lymphocyte stimulator(Blys) blocking antibody, belimumab (Edwards *et al.*, 2003). Blys is a potent cytokine for B-cell proliferation and differentiation. Belimumab shows specificity for secreted Blys and was affinity matured and shown to be a potent inhibitor of Blys signaling (Baker *et al.*, 2003). The FDA has approved this antibody in March 2011 for use in treatment of systemic lupus erythematosus. A number of other antibodies against soluble ligands have been generated by phage display (Kabir *et al.*, 2009; Lloyd *et al.*, 2009; Moreland *et al.*, 2012).

Phage-derived antibodies have been selected that show high specificity for a chosen protein target. For example, selections have been carried out to identify antibodies with the ability to discriminate between chicken and quail lysozyme, which differ by only one surface amino acid (Ayriss *et al.*, 2007). Another example shows antibodies have been generated that distinguish between the SH2 domains of ABL1 and ABL2 tyrosine kinase (Mersmann *et al.*, 2010; Pershad *et al.*, 2010), which differ in sequence by only 11%. To generate antibodies with desired specificity in such studies, negative selection steps have been incorporated into phage display selections. Antibody phages binding to unrelated target are eliminated by preincubating the antibody phage library with the unrelated target prior to each round of selection against the expected target.

The pace of phage display development is largely encumbered by difficulties in producing antibodies in sufficient quantity and quality. Establishment of faster expression systems is needed to fully exploit the use of antibody phage display technology. Because *E. coli* enables rapid growth of expression cultures and permits efficient mutagenesis and DNA manipulation, antibody expression in bacterial host is of great interest. Despite the challenges faced in the development of efficient expression protocols in bacteria, researchers now have successfully developed efficient systems for displaying antigen-binding sites in antigen-binding fragment

(Fab) domain format (Schenone *et al.*, 2010; Cortes *et al.*, 2012). Fabs retain the antigen-binding specificity of IgG molecule necessary for effector functions (**Figure 2.3**). The development of methods for expressing Fabs in *E. coli* is a major progress in antibody research since it provides a way of purifying the antigen-binding fragment of antibodies in microbial systems (Better *et al.*, 1988), providing benefits regarding large scale and ease of manufacture (Humphreys, 2003). It has been reported that high-affinity Fab antibodies can be generated from Fab libraries with completely synthetic complementarity-determining regions (CDRs) displayed on a single scaffold (Lee *et al.*, 2004).

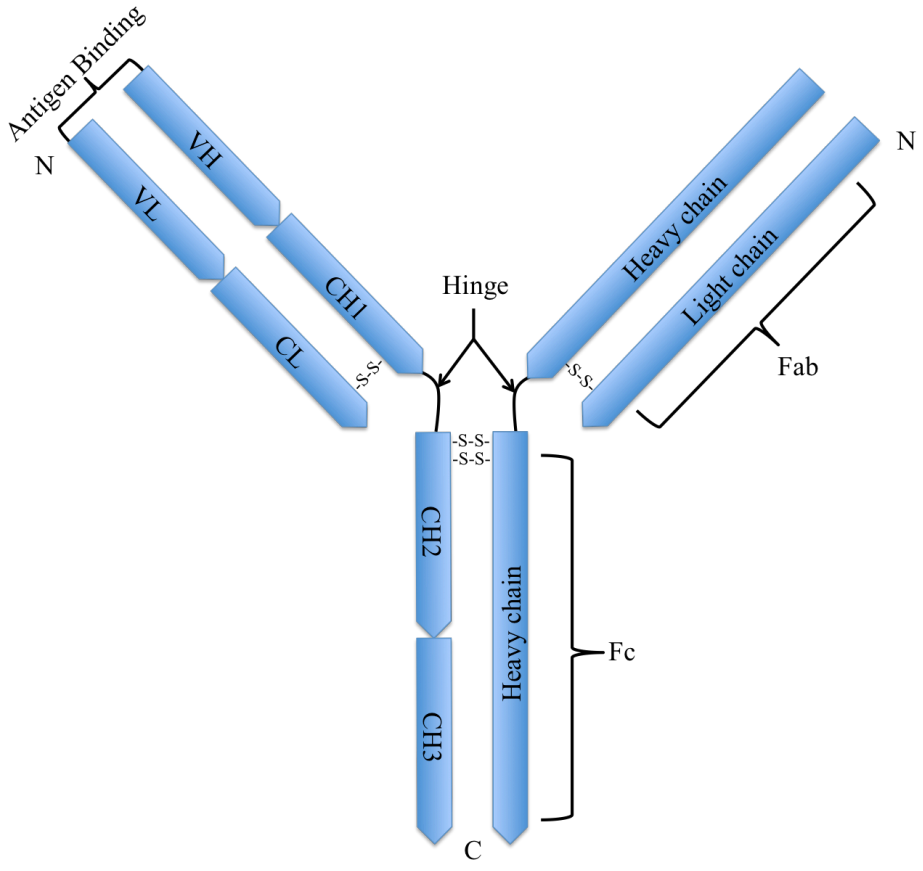

Figure 2.3 Schematic View of IgG Molecule
IgG molecule has a four-chain monomeric structure composed of two identical light chains and two identical heavy chains. The light chain contains one variable domain (VL) and one constant domain (CL). The heavy chain contains one variable domain (VH) and three constant domains (CH1, CH2, and CH3). The hinge connects the region between the CH1 and CH2. IgG molecule can be divided into two functional portions: antigen binding fragment (Fab), which is the antigen-binding site, and crystallizable fragment (Fc). N, N-terminus; C, C-terminus.

The development of phage display technology has made it possible to produce large *in vitro* antibody fragment libraries (Nelson and Sidhu; Marks *et al.*, 1991; Barbas *et al.*, 1992; Griffiths *et al.*, 1993; Nissim *et al.*, 1994; Barbas and Burton, 1996; Knappik *et al.*, 2000; Frisch *et al.*, 2003; Fellouse *et al.*, 2004; Jespers *et al.*, 2004; Lee *et al.*, 2004; Bond *et al.*, 2005). The design of these synthetic libraries is based on the knowledge of CDRs contained in Fabs, which determine the antigen-binding site (Hoogenboom and Winter, 1992; Winter, 1998). Introduction of diversity into only a subset of positions within four of the six CDRs (one is variable region of an antibody light chain V_{L3}; three are variable regions of heavy chain V_{H1}, V_{H2} and V_{H3}) can generate high-affinity antibodies (Birtalan *et al.*, 2008). In 1991, the Scripps group reported the first display and selection of human antibodies on phage (Barbas *et al.*, 1991). This initial study described the rapid isolation of a human antibody Fab that bound tetanus toxin and the method was then extended to rapidly clone human anti-HIV-1 antibodies for vaccine design and therapy (Barbas *et al.*, 1992; Barbas *et al.*, 1993; Barbas, 1995).

The central principle behind phage display relies on the expression of antibody fragments on the surface of phage particles (Willats, 2002) (**Figure 2.4**). This is accomplished by fusing DNA that encodes antibody fragments into filamentous phage coat protein genes. In this case, a physical link between the phenotype and genotype of the expressed protein fragments is established. Specific phage-displayed antibodies can be selectively enriched from library pools by exposing phage particles to an antigen immobilized on a solid support (e.g. microtiter plates, or magnetic beads) while weakly-or non-binding phage particles are removed by washing. However, the selection often yields non-specific phage binders or binders that interact with the solid support rather than the target, making it necessary for the introduction of negative selection steps (Menendez and Scott, 2005). Ultimately, the sequence of single phage populations with desired specificities can be deduced by sequencing the encapsulated DNA within phage particles.

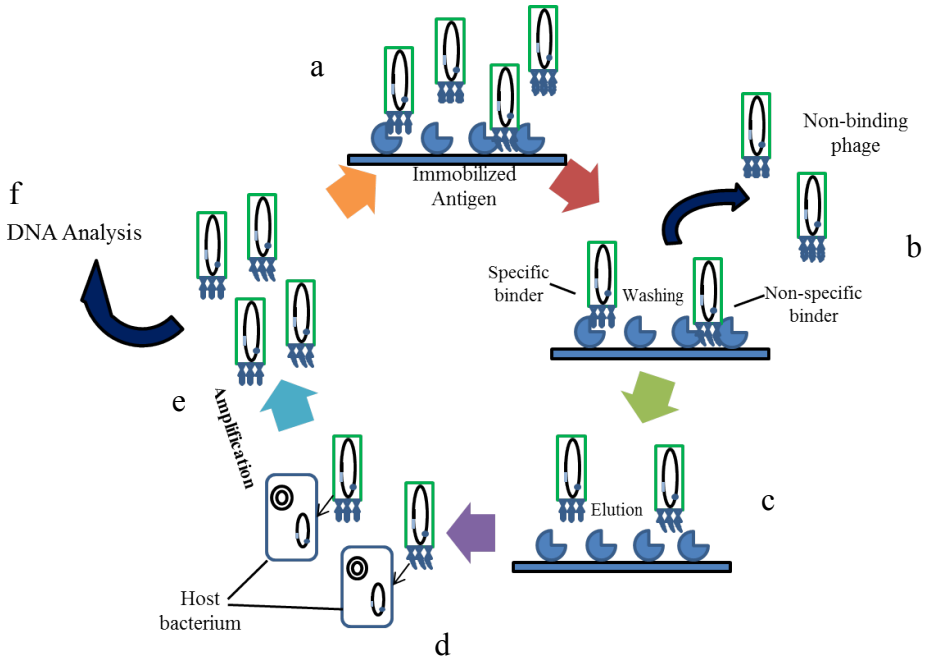

Figure 2.4 Phage Display Selection
(a) The phage library displaying variant peptides or proteins are exposed to target molecules and phages with appropriate specificity are captured. (b) Non-binding phage are washed off – although some non-specific binding may also occur. (c) Bound phages are eluted by conditions that disrupt the interaction between the displayed peptide or protein and the target. (d) Eluted phage are infected into host bacterial cells and thereby amplified. (e) This amplified phage population is in effect a secondary library that is greatly enriched in phage displaying peptides or proteins that bind to the target. (f) After several (usually three to five) rounds of selection monoclonal phage populations may be selected and analyzed individually.

2.2.1 Intracellular Antibody Delivery

Phage display is a powerful technology to produce antibodies specific for extracellular or cell-surface targets. However, if an intracellular target like hRad51 is of interest, then the antibody must across the cell membrane. In the late 1970s, investigators found microinjecting purified antibody into individual cells could block the function of intracellular target molecules (Antman and Livingston, 1980). However, examples published since the first report of this method are scarce, mainly is because of the very tedious process. For intracellular antibody to become a broadly applicable technology, it requires a means of expressing or introducing antibodies into large cell populations or in animals. Some success was made in the early attempts to express antibodies in the cytosol of cells (Biocca *et al.*, 1990; Carlson, 1993), but in general such antibodies or antibody fragments were found malfunctioning because they either failed to express or did not bind to their target in the context of intracellular environment.

In nature, antibodies are produced within B-cells, secreted into the extracellular space to be part of the body's defense system, and hence are capable of surviving in various harsh environments. Their resistance to denaturation is dependent on a rigid antiparallel β sheet core that is stabilized by disulfide bridges. However, when antibody fragments are expressed in cytosol, that is normally a reducing environment, this prevents the formation of disulfide bridges, which, in turn, compromises the structural integrity and function of antibodies. To overcome the problem of incorrect folding and reduced stability of antibodies expressed in the reducing environment, both new ways of designing antibody libraries and new methods of selecting from those libraries have been developed as outlined in the review by Stocks (Stocks, 2005).

Therefore, introducing antibodies into the cytosol from outside the cell would be highly desirable to meet the increasing demand of antibody fragments delivery. First, It would enable use of the increasing number of antibodies that target intracellular targets. Furthermore, intracellular delivery of antibodies to live cells may offer a convenient way to replace siRNA or gene transfections. However, efficient application of antibody fragments is limited by their inefficient delivery to the target sites. One major intracellular barrier is the cell membrane, which represents a non-permissive barrier for hydrophilic macromolecules. Therefore, delivery of macromolecules generally depends on endocytosis, which is the most common internalization pathway. After uptake, the macromolecules are still considered "extracellular" because they are trapped in endosomes where they are most likely destined for lysosomal degradation. In order to elicit effect, both cellular uptake and endosomal release have to occur.

One approach used in recent years to overcome the cell membrane barrier is to link the cargo macromolecule to one of the protein transduction domains (PTDs), which are a class of short peptide sequences that are capable of entering cells efficiently, either alone or lined to bulky cargos (Mae and Langel, 2006). The application of PTDs emerged from the discovery that the human immunodeficiency virus transactivator of transcription (HIV-TAT) protein was able to penetrate cells (Prochiantz, 2000). The most widely studied and used PTDs are a class of arginine-rich PTDs, which includes HIV1-TAT-PTD, nona-arginine and Antennapedia-PTD (Brooks *et al.*, 2005; Futaki, 2005; Torchilin, 2008). Although the exact internalization mechanism for PTDs is not known, it is widely accepted that PTDs are primarily taken up by

endocytosis (Richard *et al.*, 2003; Fuchs and Raines, 2004; Futaki, 2006; Duchardt *et al.*, 2007). The positive charge of the oligoarginine in PTDs may help to concentrate the peptide on the cell surface by electrostatic interactions with negatively charged lipids in the plasma membrane (Gump *et al.*, 2010). After endocytic uptake, the internalized PTDs (either alone or linked to cargos) should escape endosome/lysosome degradation, which is believed to be a bottleneck in the efficient intracellular delivery of macromolecules.

Some models have been proposed for the mode of endosomal escape for free PTDs. One model suggests that oligoarginine bound to membranes and rigidified the local area, resulting in leakiness and rupture of the membrane (Hitz *et al.*, 2006). In agreement with this, PTDs are reported in another model to form a nonpolar ion pair with negatively charged lipids and partition this ion pair to cell membranes (Rothbard *et al.*, 2004). Some other factors are stressed, including the importance of the pH gradient across the endosomal membrane (Bjorklund *et al.*, 2006) and the need for a minimum threshold concentration of PTDs for translocation across membranes (Magzoub *et al.*, 2005).

With our increasing understanding of PTDs mechanism of action, their potential application in various diseases has been exploited. In 2005, two groups of researchers independently claimed to have created cell-permeable antibodies (transbody) by linking an PTD to an antibody (Heng and Cao, 2005; Muller *et al.*, 2005). Afterwards, different antibody formats have been linked to PTDs for intracellular delivery as shown in **Table 2.3**. Tetanus in chromaffin cells and influenz a A viral activity were neutralized by antibodies or antibody fragments fused to PTDs (Stein *et al.*, 1999; Poungpair *et al.*, 2010). Transbodies have also been used to promote or suppress apoptosis (Cohen *et al.*, 1998; Zhao *et al.*, 2003). Further application include inhibition of cell cycle progression by an anti-cyclin D1 transbody (Chen and Erlanger, 2006). Tumor cell retention of a Fab fragment is enhanced by conjugating to a HIV1 TAT protein-derived peptide (Anderson *et al.*, 1993).

Table 2.2 Different Antibody Formats Linked to PTDs for Intracellular Delivery

Construct	PTD	Cell lines	Reference
scFv	HIV1 TAT (44-57)	HEK293 mice (injection)	(Niesner *et al.*, 2002)
scFv	MTS	293T, BT-474 and PyVmT cells	(Shin *et al.*, 2005)
Fab	HIV1 TAT (37-62)	A431 breast carcinoma cells	(Anderson *et al.*, 1993)
Fab	HIV1 REV peptide (positions 34–50) (TRQAR RNRRR RWRER QRGC)	HeLa, rats	(Kameyama *et al.*, 2006)
Whole IgG	R_{68}	HeLa cells MCF-7 cells SK-BR-3 cells Murine lung enthothelial line	(Chen and Erlanger, 2002)
Whole IgG	KGEGAAVLLPVLLAAPG ("MTS")	NIH 3T3 cells	(Zhao *et al.*, 2001)

PTD, protein transduction domain; scFv, single chain fragment variable; Fab, fragment antigen-binding; MTS, membrane transport sequence.

Chapter 3 Hypothesis and Aims

3.1 Hypothesis

We hypothesize that specific antibody fragments against hRad51 can be generated using phage display technology. These antibody fragments can be used as potential therapeutic agents to specifically inhibit the aberrant activity of hRad51. By linking them to a protein transduction domain, these antibody fragments can be delivered across cell membrane to sensitize cancer cells to chemotherapy.

3.2 Aims

1. To isolate Fabs against hRad51 from Fab phage display library.

2. To characterize anti-hRad51 Fab activities, including binding affinity, binding specificity, DNA-binding, and ATPase inhibitory activity.

3. To develop intracellular anti-hRad51 Fab and test its ability to sensitize cells to DNA damaging agent MMS.

Chapter 4 Materials and Methods

4.1 General Information

4.1.1 Reagents and Suppliers

Table 4.1 Reagents

Reagent	Supplier
PCR Purification Kit	Thermo Scientific
Plasmid Miniprep Kit	Thermo Scientific
QIAPrep Spin M13 Kit	Qiagen
BCA Protein Assay Kit	Thermo Scientific
Oligonucleotides	Integrated DNA Technologies
Nitrocellulose	Bio-Rad
Odyssey Blocking Buffer	LI-COR Biosciences
Fast SYBR® Green Master Mix	Thermo Scientific
Gibson Assembly® Master Mix	New England Biolabs
Nunc MaxiSorp® Flat-Bottom 96-Well Plate	Thermo Scientific
Tissue Culture Flat-Bottom 96-, 48- & 24-Well Microplates	Corning
Ultra Low Cell Culture Flask, 25 & 75cm^2	Corning
Pierce Zeba® Desalting Spin Columns	Thermo Scientific
IRDye® 800CW Protein Labeling Kit	LI-COR Biosciences
Dip and Read^{TM} Biosensors	ForteBio
Lipofectamine 2000® Regent	Invitrogen Life Technologies
MMS	Sigma-Aldrich
DMSO	Fisher Scientific
FBS	Invitrogen Life Technologies
DMEM	Invitrogen Life Technologies
Trypan Blue, 0.4%	Invitrogen Life Technologies

Table 4.2 Enzymes

Enzyme	Supplier
*Xho*I	Thermo Scientific
*Sac*I	Thermo Scientific
HotStarTaq® DNA Polymerase	Qiagen
Phusion High-Fidelity DNA Polymerase	Thermo Scientific
T4 DNA Ligase	New England Biolabs
T4 Polynucleotide Kinase (PNK)	New England Biolabs
T7 DNA Polymerase	New England Biolabs

4.1.2 Strains

Table 4.3 *E. coli* Strains and Genotypes

Strain	Genotype	Reference
XL1-Blue	*recA1 endA1 gyrA96 thi-1 hsdR17 supE44 relA1 lac (F′ proAB lacIqZΔM15 Tn10 (Tet^r))*	Stratagene
MC1061	F-*araD139 Δ(araA-leu)7697 galE15 galK16 Δ(lac)X74 rpsL (Strr) hsdR2 (rK-mK+) mcrA mcrB1*	(Wertman *et al.*, 1986)
SS320	*hsdR mcrB araD139 Δ(araABC-leu)*7679 Δ*lac*X74 *galUgalK rpsL thi*	Lucigen
CJ236	FΔ*(HindIII)::cat* (Tra$^+$ Pil$^+$ Cam^R)/ *ung-1 relA1 dut-1 thi-1 spoT1 mcrA*	New England Biolabs
BL21(DE3)	F-*omp*T *hsd*SB(r$_B^-$, m$_B^-$) *gal dcm* (*DE3[lacI lacUV5-T7 gene 1 ind1 sam7 nin5]*)	Novagen
Rosetta(DE 3)pLysS	F-*ompT gal dcm lon*? *hsdS$_B$*($r_B^- m_B^-$) λ(DE3 [*lacI lacUV5-T7 gene 1 ind1 sam7 nin5*]) [*malB*$^+$]$_{K-12}$(λ^S) pLysSRARE[*T7p20 ileX argU thrU tyrU glyT thrT argWmetT leuW proL ori*$_{p15A}$](Cm^R)	Novagen

Table 4.4 Mammalian Cell Lines

Strain	Disease	Description	Reference
HEK293T	Human embryonic adherent kidney cells	Application: Efficacy testing transfection host viruscide testing	ATCC-CRL1573

Table 4.5 Antibodies

Antibody	Supplier
Goat Anti-Human IgG IRDye 800CW	LI-COR Biosciences

4.1.3 Oligonucleotides

Oligonucleotides were obtained from Integrated DNA Technologies. Sequences are given in 5' to 3' direction. Serial numbers (S.No) are used as reference for oligonucleotides in the subsequent work. P1, P2, Seq, and Temp represent forward primer, reverse primer, sequencing primer, and template, respectively.

S.No	Name	Sequence (5'->3')
1	Rad51 P1	GCA ATG CAA ATG CAA CTG
2	Rad51 P2	GTC TTT AGC ATC GCC AAC
3	FS Temp P1	CCA TCT CAT CCC TGC GTG TCT CCG ACT CAG AAC CAT CCG CCC GGA AGA CTT CGC AAC TTA
4	FS Temp P2	CCT CTC TAT GGG CAG TCG GTG ATA CGG TGA CCA GGG TTC CTT G
5	TGS157	TCC AGATGA CCC AGT CCC CGA GCT CCC TG
6	TGS160	CAA ATC TTG TGA CAA AAC TCA CAC GGG TGG TTC GCA CCA CCA CCA CCA CCA CTG AG
7	TGS163	GGA AAC AGG ATC AGCTTA CTC C
8	TGS164	CTA AGA AAC CAT TAT TAT CAT GAC
9	Import Tag (Itag)	ATG GCC TTG GGC CCT TGC ATG TTG TTG TTG TTG TTG TTG TTG GGT TTG CGC CTG CCG GGT GTT TGG GCG CCG CCG CGT CGC CGC CGC CGT CGT CGC CGT CGT
10	L3-H3 Kunkel	ACG TTC GGA CAG GGT TAT TAT TGT GCT CGC

4.1.4 Plasmids

The following four plasmid maps were created from free online web source PlasMapper (http://wishart.biology.ualberta.ca/PlasMapper/) (Dong *et al.*, 2004).

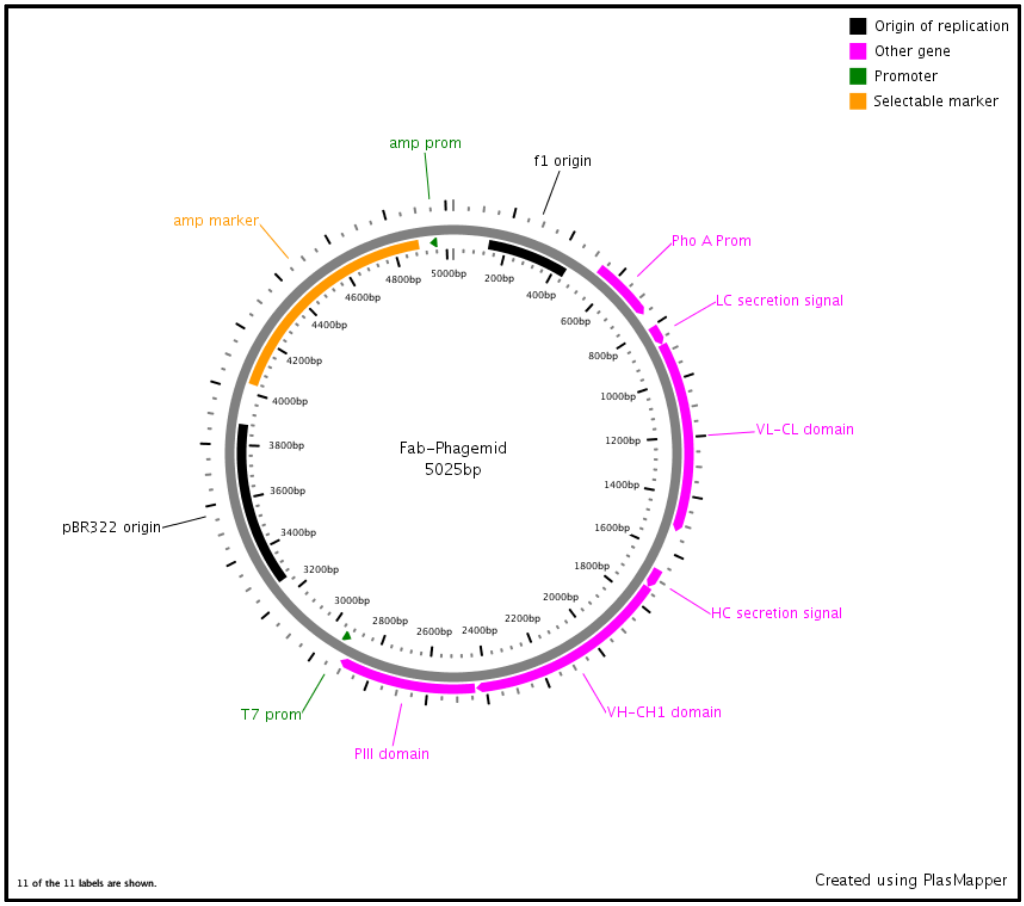

Figure 4.1 Fab-Phagemid

Fab-phagemid is used for Fab display. The phagemid backbone contains a single-stranded DNA filamentous phage origin of replication (f1 ori) to allow packaging into phage particles and a double-stranded DNA origin of replication (pBR322 ori) to enable replication as a plasmid in *E. coli*. A selective marker, β-lactamase gene (amp marker), was used to maintain plasmid in *E. coli*. For Fab display, a DNA cassette consisting of a promoter (Pho A Prom) was used to drive transcription of a bi-cistronic message that encodes for the light chain (VL-CL) as well as the variable and first constant domains of the heavy chain (VH-CH1). The N-terminus of each chain was fused to a Pel B secretion signal for directing expressed chains to the periplasm while the C-terminus of the heavy chain was fused to a phage coat protein (PIII domain). In the periplasm of *E. coli*, the light and heavy chains associated with each other to form intact Fab, which was incorporated into phage particles that were secreted from *E. coli* host.

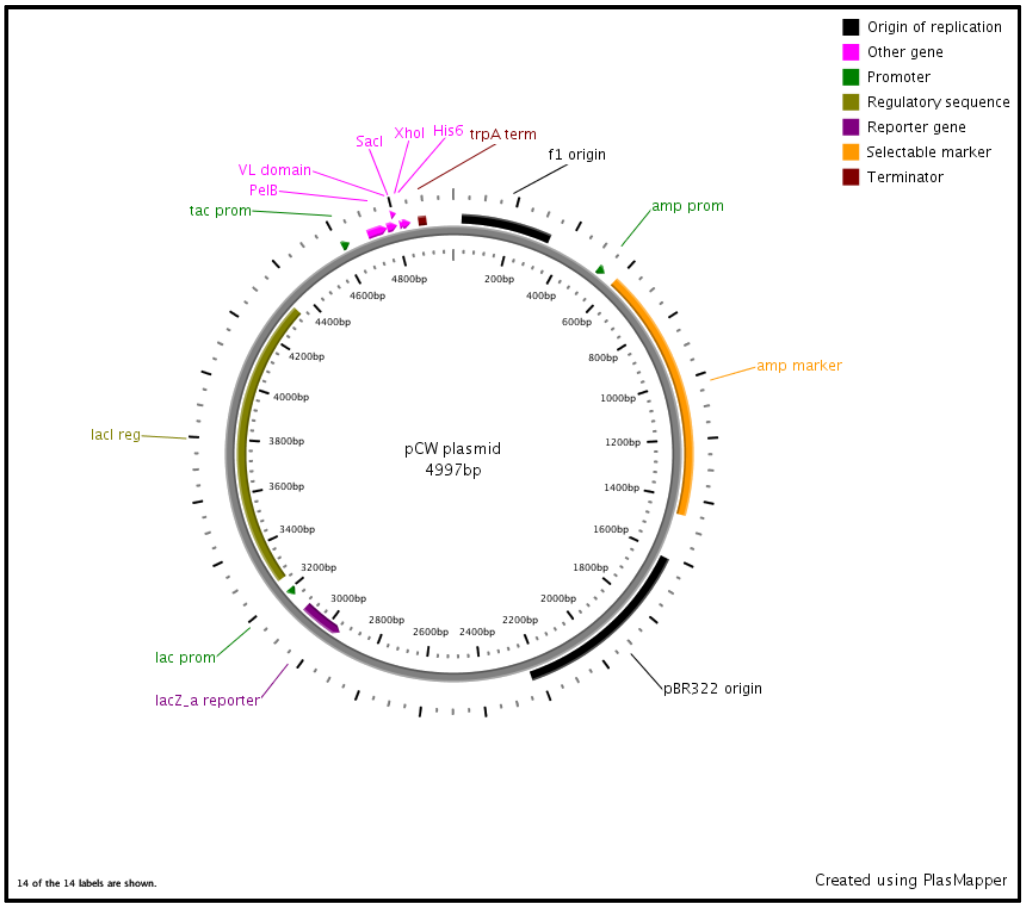

Figure 4.2 pCW Bacterial Expression Plasmid

pCW plasmid is used for expressing Fabs in *E. coli*. pCW was designed for receiving Fab (light and heavy chain) coding sequences from phagemid for bacterial expression. The expression and termination are tightly controlled by tac promoter (tac prom) and trpA terminator (trpA term), respectively. pCW contains a Pel B secretion signal on the light chain for directing expressed chain to the periplasm . Fabs were cloned between *Sac*I and *Xho*I sites using Gibson Assembly. pCW contains a double-stranded DNA origin of replication (pBR322 ori) to enable replication in *E. coli*. The ampicillin-resistance gene (amp marker) is used to maintain the plasmid in *E. coli*.

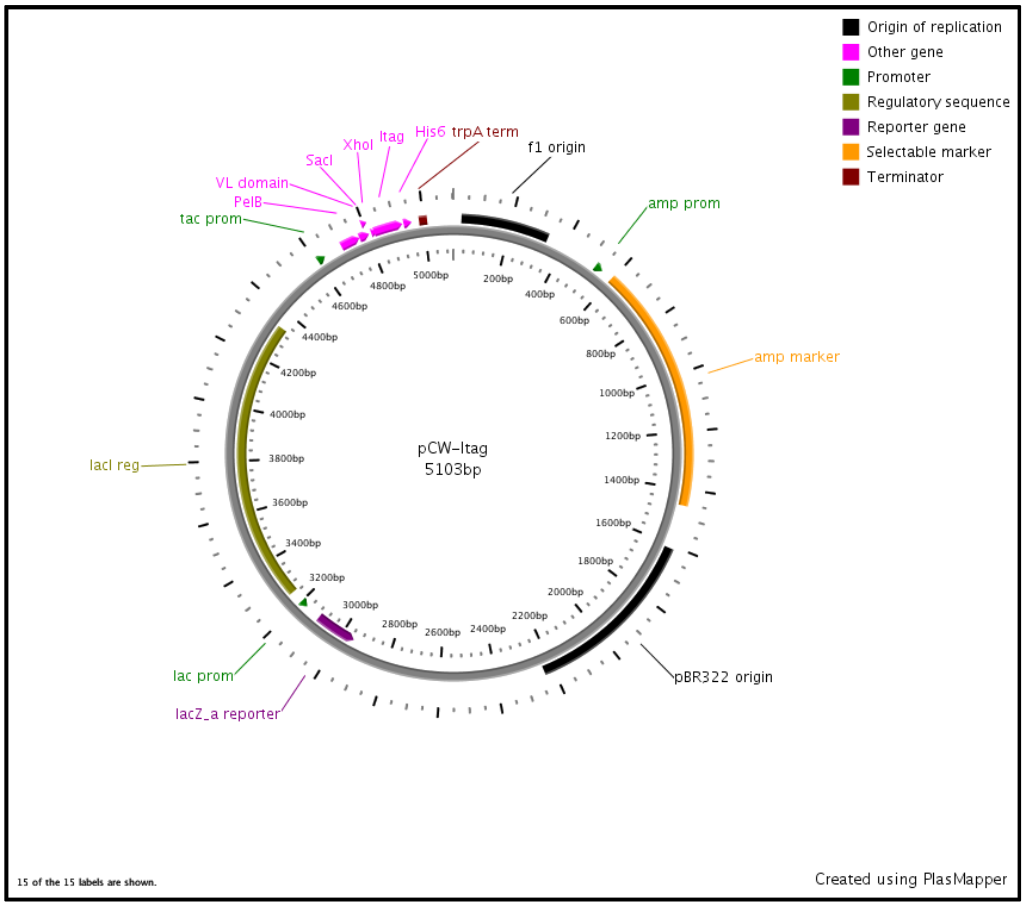

Figure 4.3 pCW-Itag Bacterial Expression Plasmid
pCW-Itag plasmid is based on pCW with the addition of an import tag (Itag) followed by a stop codon following the His6.

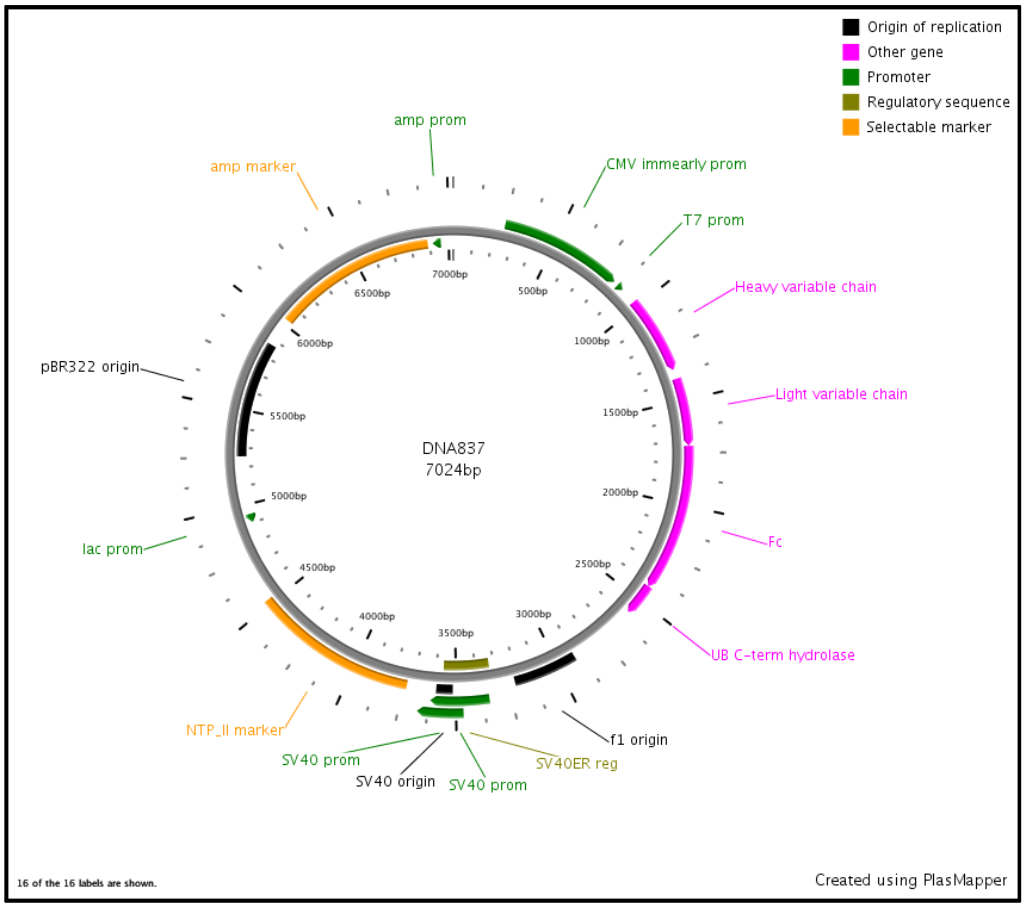

Figure 4.4 DNA837 Mammalian Cell Expression Plasmid

DNA837 plasmid was a reconstructed plasmid suitable for a mammalian expression system. It contains: (i) A double-stranded DNA origin of replication (pBR322 ori) to enable replication as aplasmid in *E. coli*. (ii) Selective marker (amp marker) to maintain plasmid in *E. coli*. For scFv-Fc expression in mammalian cells, a human CMV immediate-early promoter (CMV immearly prom) is used to drive transcription of the message that encodes for heavy and light chain variable regions followed by fragment crystallizable region (Fc region). C-terminus of Fc region was fused to ubiquitin carboxyl-terminal hydrolase to prevent ubiquitin-mediated degradation.

4.2 General Protocols

4.2.1 DNA Extraction and purification

Plasmid DNA was extracted from the cell lysate using a Plasmid Miniprep Kit (Thermo Scientific GeneJET™) as per manufacturer's instructions. ssDNA was extracted from phage particles using QIAPrep Spin M13 Kit (Qiagen) as per manufacturer's instructions. PCR products were purified using PCR Purification Kit (Thermo Scientific) as per manufacturer's instructions.

4.2.2 DNA Sequencing

Individual DNA samples were diluted to a concentration of 50 µg/mL in Milli-Q water (Millipore). DNA was sequenced using 3500 Genetic Analyzer (Thermo Scientific) or Next Generation Sequencing (NGS) (Ion Torrent™). Plasmid DNA, ssDNA and PCR products were prepared in an A260/280 ratio of 1.8-2, diluted to a concentration of 50-60 µg/mL in 10 mM Tris-HCl pH 8.5, 0.1% Tween 20.

4.2.3 Polymerase Chain Reactions

4.2.3.1 High Fidelity PCR

Gene amplification from high fidelity PCR was used for DNA sequencing. The PCR protocol was modified from "Phusion High-Fidelity DNA Polymerase" (Thermo Scientific) manufacture's condition. PCR (50-100 µL) contained the following reagents: 1x Phusion HF Buffer (60 mM Tris-SO_4 pH 8.9, 180 mM $(NH_4)_2SO_4$, 1.5 mM $MgSO_4$), 200 µM dNTPs, 1 µM of forward and reverse primers, 100-200 ng template DNA, and 1 Unit/50 µL of Phusion High-Fidelity DNA Polymerase. Reactions were performed under the following cycling conditions: initiation step at 98 °C for 30 seconds, 25-30 cycles of amplification with denaturation step at 98 °C for 10 seconds, annealing step at 55 °C for 15 seconds, extension step at 72 °C for 20 seconds per kilobase pair, final extension step at 72 °C for 5 minutes.

4.2.3.2 PCR Amplification of Kunkel Product

Kunkel product was amplified by high fidelity PCR to bring light and heavy chain complementarity-determining regions closer together for NGS analysis. PCR (50-100 µL) contained the following reagents: 1x Phusion HF Buffer (60 mM Tris-SO4 pH 8.9, 180 mM $(NH4)_2SO_4$, 1.5 mM $MgSO_4$), 200 µM dNTPs, 1 µM of forward and reverse primers, 100-200 ng Covalently Closed Circular dsDNA (CCC-dsDNA) (Section 4.4.1.2), and 1 Unit/50 µL of Phusion High-Fidelity DNA Polymerase. Kunkel PCR was performed under the following cycling conditions: initiation step at 98 °C for 30 seconds, 25-30 cycles of amplification with denaturation step at 98 °C for 10 seconds, annealing step at 56 °C for 10 seconds, extension step at 72 °C for 5 seconds, final extension step at 72 °C for 15 seconds.

4.2.3.3 *E. coli* Colony PCR

Colony PCR was used as a rapid test to verify the correct insertion of a DNA segment into a plasmid prior to plasmid purification and sequencing. From a fresh 2YT/Agar plate containing appropriate antibiotic, a single colony was picked and resuspended in 200 µL of sterile H_2O. One microliter of the colony suspension was used as the template for PCR reaction. If the PCR result was positive, the remaining colony suspension was used to inoculate 5 mL of 2YT buffer supplemented with appropriate antibiotic to maintain corresponding plasmid, followed by plasmid purification after a period of incubation.

4.2.3.4 Agarose Gel Electrophoresis

Agarose gel electrophoresis was used to visualize PCR products and plasmids based on their relative molecular size. Agarose gel was prepared in a mix of 1x TAE Buffer (40 mM Tris-acetate, 1 mM EDTA, pH 8.0), 0.5-1.0% (w/v) ultrapure agarose and 0.5 µg/mL ethidium bromide. Samples were mixed with 1x loading dye (10% (v/v) glycerol, 0.04 M EDTA pH 8.3, 0.01% (w/v) bromophenol blue). Following sample loading, gels were electrophoresed at 100 to 200V for 30 to 60 minutes in 1x TAE Buffer and photographed using a Gel-Doc Imager (Bio-Rad).

4.2.4 Sodium Dodecyl Sulphate Polyacrylamide Gel Electrophoresis (SDS-PAGE) and Western Analysis

SDS-PAGE was used to separate proteins based on their electrophoretic mobility. Protein samples were resuspend in final 1x SDS loading dye (60 mM Tris-HCl (pH 6.8), 5% (v/v) glycerol, 2% (w/v) SDS, 4% (v/v) 2-mercaptoethanol, 0.0025% (w/v) bromophenol blue). Homogenized *E. coli* samples containing protein mix were resuspended in 1x SDS loading dye for loading. Prior to loading, sample suspension was heated at 95 °C for 5 minutes and cooled.

The methodology of SDS-PAGE used in the thesis employed the Laemmli method (Laemmli, 1970) utilizing a 4-12% (stacking – separating) polyacrylamide gel. Sample fractions were resolved in this 4-12% polyacrylamide gel in 1x running buffer (25mM Tris-HCl pH 8.3, 190 mM glycine, 0.1% (w/v) SDS) at 150 V for 60 minutes using a Mini-Protean 3 electrophoresis unit (Bio-Rad).

For Western analysis, proteins in the SDS-PAGE gels were transferred to nitrocellulose membranes using Bio-Rad Mini Trans-Blot Cell (wet electrophoretic transfer cell) at 100 V with constant 350 mAmps for 1 hour in the presence of transfer buffer (48 mM Tris-HCl pH 8.3, 39 mM glycine, 20% (v/v) methanol). To develop the blot, membranes were blocked with Odyssey blocking buffer (LI-COR Biosciences) for 1 hour at room temperature, followed by incubation with a IRDye® 800CW dye-labeled antibody (diluted Odyssey blocking buffer, 0.2% Tween-20) for an additional 1 hour followed by washing with PBS for three times. Developed blots were visualized and scanned using an Odyssey infrared imager (Li-COR Biosciences).

4.2.5 Gibson Assembly Cloning Reactions

DNA encoding Fabs were PCR amplified using TGS150 and TGS160 primers from the Fab phagemid. pCW (or pCW-Itag) plasmid (**Figure 4.2 & 4.3**) for Gibson Assembly was digested using *Sac*I and *Xho*I restriction enzymes as per FastDigest's instruction (Thermo Scientific). PCR-generated insert was cloned into linearized pCW (or pCW-Itag) using Gibson Assembly® Master Mix (New England Biolabs) as per manufacturer's instructions.

4.3 General *E. coli* Protocols

4.3.1 Bacterial Media

2x Yeast Extract Tryptone (2xYT) Medium: 2xYT media was prepared in 1 L of the Milli-Q water (Millipore) with 31 g of BD Difco™ 2xYT. The media was mixed thoroughly with frequent agitation to completely dissolve the powder, followed by autoclaving at 121 °C for 15 minutes. Solid media contained 18 g/L of agar.

Luria Broth (LB) glucose Media: LB media was prepared in 900mL of Milli-Q water (Millipore) containing 10 g Bacto-tryptone, 5 g yeast extract, 10 g NaCl, and 3 g D-glucose. Media was prepared as previously described.

Super Optimal Broth with Catabolic Repressor (SOC) Medium: SOC media were prepared in 1 L of Milli-Q water (Millipore) with 20 g Peptone, 5 g Yeast Extract, 2 mL of 5 M NaCl, 2.5 mL of 1 M KCl, 10 mL of 1 M $MgCl_2$, 10 mL of $MgSO_4$, and 20 mL of 1 M D-glucose. Media was prepared as previously described.

Overnight Express™ Instant TB Medium (Novagen®): Instant TB media is a complete granulated culture medium for high-level protein production in the pET and other isopropyl β-D-1-thiogalactopyranoside (IPTG)-inducible bacterial expression systems without the need to monitor cell growth. The medium was prepared in 1 L of Milli-Q water (Millipore) with 60 g Overnight Instant TB Medium, supplement with 10 mL glycerol, followed by sterilization using Stericup® vacuum filtration system (Millipore).

Antibiotics: Antibiotic powder was resuspended in Milli-Q water (Millipore) at a 1000x stock and stored at -20 °C. The appropriate antibiotics were added into media at indicated concentration listed on Table 4.6.

Table 4.6 Antibiotic In-Use Concentration

Antibiotic	In-Use Concentration (µg/mL)
Carbenicillin (carb)	50
Kanamycin (kan)	25
Tetracycline (tet)	5
Chloramphenicol (cap)	5

2xYT/tet medium: 2xYT media containing 5 µg/mL tetracycline

2xYT/carb medium: 2xYT media containing 50 µg/mL carbenicillin

2xYT/carb/kan medium: 2xYT media containing 50 µg/mL carbenicillin and 25 µg/mL kanamycin

4.3.2 Preparation of Electrocompetent *E. coli* cells

E. coli were cultured as described using standard techniques (Elbing and Brent, 2001). Unless otherwise noted, *E. coli* in liquid media were grown at 37 °C with shaking (200 RPM). *E. coli* grown on solid media were incubated at 37 °C overnight.

Electrocompetent *E. coli* cells were optimized for high transformation efficiency by electroporation. A single *E. coli* colony was used to inoculate 500 mL 2xYT liquid medium followed by incubation. When the OD600 of the culture reached 0.35-0.4, the culture was immediately put on ice for 20-30 minutes with occasional swirling. Cells were harvested by centrifugation at 5,000 g at 4 °C for 10 minutes in a Sorvall GS-3 rotor. Cells were subsequently washed three times using ice-cold Milli-Q water (Millipore) and isolated by centrifugation at 5,000 g at 4 °C for 10 minutes. Cells were resuspended in 50 mL of ice-cold 10% ultrapure glycerol and stored at -80 °C.

4.3.3 Preparation of Plasmid DNA

Individual colonies were inoculated in 5-10 mL of 2xYT media containing appropriate antibiotic. Cells were collected by centrifugation at 5,000 g for 10 minutes. Plasmid DNA was extracted using Plasmid Miniprep Kit (Thermo Scientific) as per manufacturer's instructions. Plasmid concentration was determined by measuring the OD at 260 nm using a NanoDrop 2000c spectrophotometer (Thermo Scientific).

4.3.4 *E. coli* Electroporation

Electrocompetent DH10B *E. coli* cells were used in transformation of plasmids. 50 µL of frozen cells were thawed on ice and mixed with DNA solution (5-10 µL of a ligation reaction or 1 µL of 50-150 ng/µL plasmid DNA) and transferred to an ice-cold 0.2 cm gap electroporation cuvette. Cells were electroporated in field strength of 12.5 kV/cm (Ec2 on Bio-Rad Micro Pulser). Immediately following electroporation, 500-1,000 µL of SOC (no antibiotics) was added to cells with subsequent incubation in 37 °C shaker for 30-60 minutes. Finally, 10-100 µL cells were plated onto 2xYT agar plates containing appropriate antibiotics.

4.3.5 Storage of *E. coli* cells

Transformed cells were stored in -80 °C for long-term use. Briefly, individual colonies were picked from plate and grown overnight in 5 mL 2xYT media containing appropriate antibiotic(s). The next morning, 0.5 mL of the overnight culture was added into 0.5 mL of 80% sterile glycerol, followed by gentle vortexing. The glycerol *E. coli* stock was stored in -80 °C.

4.4 Phage Display

4.4.1 Kunkel Mutagenesis

4.4.1.1 Preparation of dU-ssDNA Template

A single colony of *E. coli* CJ236 harboring a Fab-phagemid was used to inoculate 1 mL of the 2xYT/carb/kan medium with $1x10^{10}$ phage/mL of M13K07 helper phage. After 2 hours, kanamycin was added (25 μg/mL) and the culture incubated for 6 hours. Then the culture was transferred to 30 mL of 2xYT/carb/kan medium supplemented with uridine (0.25 μg/mL) and incubated overnight at 37 °C.

Phages were purified from cell culture supernatant using PEG/NaCl precipitation as described (Rajan and Sidhu, 2012). Briefly, the culture supernatant was separated from cell pellet by centrifuging for 10 minutes at 16,000 g and the supernatant was added into a fresh tube containing 1/5 volume of PEG/NaCl. The mixture was incubated for 5 minutes at room temperature and centrifuged for 10 minutes at 12,000 g at 4 °C. The supernatant was removed, and the phage pellet resuspended in 1/25 volume of the overnight culture in PBT buffer. The suspension was centrifuged for another 5 minutes at 27,000 g to pellet the remaining insoluble matter. The phage concentration was estimated using NanoDrop 2000c spectrophotometer (OD_{280}=1.0 for a solution of $2.33x10^{12}$ phage/mL). Purified phage was immediately used for next round of selection or stored at -80 °C in 10% glycerol.

dU-ssDNA was extracted from above purified phage using QIAPrep Spin M13 Kit (Qiagen) as per manufacturer's instructions.

4.4.1.2 *In Vitro* Synthesis of Covalently Closed Circular dsDNA (CCC-dsDNA)

Mutagenic oligonucleotides were incorporated into heteroduplex CCC-dsDNA using a three-step procedure based on a published method (Kunkel *et al.*, 1987). First, mutagenic oligonucleotides were phosphorylated using 0.6 μg of the oligonucleotide, 2.5 μL of 10x TM buffer, 2.0 μL of 10 mM ATP, 1.0 μL of 100 mM DTT, and Milli-Q water to a total volume of

25 μL. T4 polynucleotide kinase was then added into the mixture followed by incubation for 1 hour at 37 °C. Following phosphorylation, the oligonucleotide was immediately used for annealing step in a PCR tube containing 1 μg of ssDNA, 2 μL of 10x TM buffer, 2 μL of the phosphorylated oligonucleotide, and Milli-Q water to a total volume of 20 μL. To obtain optimum annealing, the molar ratio of oligonucleotide to ssDNA template was 3:1. The reaction mixture was then incubated in a thermocycler at 90 °C for 3 minutes, 50 °C for 3 minutes, and 20 °C for 5 minutes. Following annealing, primer extension occurred in the annealed oligonucleotide/template mixture by adding 1 μL of 10 mM ATP, 1 μL of dNTPs, 1.5 μL of 100mM DTT, 3 units of T4 DNA ligase, and 3 units of T7 polymerase. The reaction mixture was incubated overnight at 20 °C. CCC-dsDNA was affinity purified and desalted using the QIAquick DNA purification kit (Qiagen) as per manufacturer's instructions.

4.4.1.3 Phage Display Library Construction

The heteroduplex CCC-dsDNA was introduced into *E. coli* SS320 strain (*E. coli* MC1061 strain with F' episome from XL1-blue) to convert CCC-dsDNA into a phage-displayed Fab library. Briefly, 350 μL of electrocompetent SS320 cells were thawed on ice and mixed with 20 μg CCC-dsDNA and transferred to an ice-cold 0.2 cm gap electroporation cuvette. Cells were electroporated using a BTX ECM-600 electroporation system with the following settings: 12.5 kV/cm field strength, 129 ohms resistance, and 50 μF capacitance. Immediately following electroporation, 1mL of SOC (no antibiotics) was added to cells and the cells then transferred to 22 mL of SOC medium in a 250-mL baffled flask. The cuvette was rinsed twice with 1 mL SOC media and transferred to the flask to a final volume of 25 mL followed by subsequent incubation for 30 minutes. To determine the library diversity, serial dilutions were plated on 2xYT/carb plates and incubated overnight to select for the phagemid. The remaining culture was transferred to a 2 L baffled flask containing 500 mL of 2xYT/carb/kan/ medium supplement with M13K07 helper phage followed by overnight incubation. The phage library was purified using PEG/NaCl precipitation protocol (Section 4.4.1.1).

4.4.2 Phage Display Selection Against Immobilized hRad51

The following is a general procedure of phage display selection that was performed. 5 μg/mL of hRad51 (dissolved in 100 μL of phosphate-buffered saline [PBS] buffer) was used to coat Maxisorp plates (Nunc) at 4 °C overnight or room temperature for 2 hours. hRad51 that

was not absorbed to the plates was removed and wells were blocked with 0.5% BSA (resolved in 200μL of PBS buffer) for 1.5 hours at room temperature. In parallel, an equal number of uncoated wells were blocked BSA as a negative control. BSA blocking solution was then removed and wells were washed 4 times with PT (0.05% Tween20 in PBS) buffer. One hundred microliters of the library FS phage solution was added to each coated well in a concentration of 1 x 10^{10} phage/mL in PBT buffer (0.5% BSA and 0.05% Tween20 in PBS), and incubated for 2 hours at room temperature, followed by 10 washes (6 washes for 1st round) with PT buffer to eliminate unbound phages. Bound phages were eluted using 100 mM HCl for 5 minutes and neutralized with 1.0 M Tris–HCl (pH 8.0). Half the eluted phage solution was added to 10 volumes of actively growing *E. coli* XL1-Blue (OD_{600} ~0.8) in 2xYT/tet medium and incubated for 30 minutes. To determine the enrichment, 10-fold serial dilution of the infected *E. coli* culture was plated on 2xYT/carb plates followed by overnight incubation. The remaining culture was infected with M13K07 helper phage in a final concentration of 10^{10} phage/mL followed by incubation for 45 minutes. The culture was then transferred to 25 volumes of 2xYT/carb/kan medium and incubated overnight. The amplified phage was extracted and used for next round of selection. This selection cycle was repeated until the enrichment ratio reached a maximum. Typically, enrichment is first observed in round 3 or 4, sorting beyond 6 is seldom necessary.

4.5 General Protein Protocols

4.5.1 Protein Purification

4.5.1.1 hRad51 Purification

Human Rad51 (hRad51) was overexpressed in *E. coli* Rosetta(DE3)pLysS cells and purified using a combination of ammonium sulfate precipitation and Ni-chelating chromatography. More specifically, Rosetta(DE3)pLysS cells containing hRad51 plasmid were inoculated in 10 mL of LB glucose media containing kanamycin and grown overnight. The next morning, 5 mL of overnight culture was inoculated 900 mL of LB-glucose media containing Kanamycin. Culture was grown to an $OD_{600\ nm}$ of 1.2 at 37 °C. Cells were induced with 0.25 mM IPTG and cultured for an additional for 4 hours at 37 °C. Cells were harvested by centrifugation at 5,000 g for 10 minutes at 4 °C, resuspended in binding buffer (20 mM sodium phosphate, 0.5 M NaCl, 25 mM imidazole at pH 7.4) for immediate purification. Cells

were lysed by sonication using two pulse sequences under the following conditions: 3-second pulse, 6-second rest, 90-second total pulse time. Cell debris and inclusion bodies were removed by centrifugation at 12,000 g for 15 minutes at 4 °C.

Ammonium sulfate was added to the supernatant to a final concentration of 0.35 g/mL with constant stirring at 4 °C for overnight. The proteins were precipitated by centrifugation at 12,000 g for 15 minutes at 4 °C. The protein pellet was dissolved in binding buffer, filtered through 0.22 micron filter, and passed through DE52 anion exchange column (Sigma-Aldrich) to remove bound DNA. The resuspended proteins were loaded onto a 1 mL HiTrap Ni-chelating column (GE Healthcare) using an ÄKTAprime plus system (GE Healthcare). After washing with at least 30 mL of binding buffer, hRad51 was eluted in buffer containing 500 mM imidazole. Elution fractions were analyzed by SDS-PAGE. Fractions containing hRad51 protein were dialyzed against 300 volumes of PBS buffer overnight at 4 °C with a 10-kDa molecular weight cutoff membrane (Amicon® Ultra Centrifugal Filter). Protein concentration was determined using Pierce™ BCA Protein Assay Kit as per manufacturer's instruction.

4.5.1.2 Fab Purification

BL21-DE3 containing the pCW-Fab plasmid was inoculated in 10 mL of 2xYT/carb medium and grown overnight at 37 °C. The following morning, 1 mL of overnight culture was used to inoculate 1L of Overnight Express™ Instant TB Medium (Novagen®), supplemented with carbenicillin. The culture was then incubated for 18-24 hours at 30 °C. Cells were harvested by centrifugation at 5,000 g for 10 minutes at 4 °C and resuspended in binding buffer (20 mM sodium phosphate pH 8.0, 0.15 M NaCl) for immediate purification. Cells were homogenized using French press disrupter (Constant Systems LTD) as per manufacturer's instruction. Cell debris was removed by centrifugation at 12,000 g for 15 minutes at 4 °C.

Fab was purified from supernatant as described in hRad51 purification except that a 1 mL HiTrap Protein L-affinity column (GE Healthcare) was used. Fab was eluted in elution buffer (0.1 M glycine pH 2.5) and neutralized in neutralization buffer (1 M Tris-Amino pH 8.5). A 30-kDa molecular weight cutoff membrane (Amicon® Ultra Centrifugal Filter) was used to dialyze Fab solution against PBS buffer.

4.5.1.3 Quick Protein Extraction from Bacteria

Soluble protein is extracted from small-scale culture using B-PER® Bacterial Protein Extraction Reagent (ThermoScientific). Bacterial cells were harvested by centrifugation at 5,000 g for 10 minutes at 4 °C. Cell pellet was resuspended in 4 mL of B-PER Reagent per gram of cell pellet. The suspension was incubated at room temperature for 10 minutes and the supernatant containing soluble proteins was separated from insoluble lysate by centrifugation at 12,000 g for 5 minutes at 4 °C. Supernatant was used for crude estimate for binding in biolayer interferometry analysis.

4.5.2 Bio-layer Interferometry Analysis

Octet® biolayer interferometry (BLI) platform (ForteBio Inc) was used to measure binding to the sensor tip as a wavelength shift (in nm) in real time. All the steps were performed at 25 °C with a stirring speed at 1000 RPM in a tilted-bottom 384-well plates (ForteBio Inc) containing 80 μL of solution. PBS buffer (pH 7.4) containing 0.1% (v/v) Tween 20 and 10 mg/mL bovine serum albumin (BSA) was used to dilute analytes and to wash the sensors. Purified Fab was loaded onto a Protein L biosensor (ForteBio) from a 0.5 μM solution until a wavelength shift of 0.5 nm had been achieved. 5'-biotinylated oligo$(dT)_{36}$ was loaded onto a streptavidin biosensor from a 1 μM solution until a wavelength shift of 1 nm had been achieved. Association rates were obtained by monitoring changes in wavelength shift for indicated concentration of hRad51 for 2-3 minutes. Dissociation rates were obtained by placing the loading biosensors from the association step into wells containing blank buffer and changes in the wavelength shift (nm) were monitored until the wavelength shift was stable. Association and dissociation rates and dissociation constants were calculated by Data Analysis software (version 7.1-Forte Bio, 1:1 (Langmuir) binding model) where a buffer blank was used as a reference cell subtraction.

4.5.3 ATPase Assay

hRad51 (2 μM) was incubated with Fab F_2 in different ratios in 100 μL of 50 mM HEPES buffer (pH 7.4), containing 1 mM $MgCl_2$, 45 mM NaCl, 3% glycerol, 0.6 mM 2-mercaptoethanol, 1 mM dithiothreitol, 30 μM EDTA and 0.1 mg/mL bovine serum albumin (BSA), in the presence of 20 μM oligo$(dT)_{36}$. The reaction was performed in a 37 °C water bath. After 10 minutes pre-incubation, the reaction was initiated by addition of 50 mM ATP.

After 20 minutes of incubation, 30 μL of 100 mM EDTA was mixed with a 20 μL aliquot of the reaction mixture to quench the reaction. The release of inorganic phosphate by ATP hydrolysis was determined using the malachite green assay. Briefly, 50 μL of the quenched sample solution was incubated for 1 min with a 470 μL aliquot of malachite green dye (0.034% (w/v) malachite green oxalate, 1.05% (w/v) hexaammonium heptamolybdate tetrahydrate, and 0.1% (w/v) polyvinyl alcohol in 1 M HCl). Color development was stopped by addition of 50 μL of 34% (w/v) sodium citrate dehydrate. The absorbance was measured at 620 nm with a spectrophotometer. 1 mg/mL NaH_2PO_4 was used to prepare phosphate standard. The reaction is in a linear range for up to 30 minutes.

4.5.4 Protein Labeling

Fab and anti-IgG antibody were labeled with IRDye® 800CW dye for in-cell imaging and Western analysis. Briefly, 500 μg of protein was dissolved in 600 μL of PBS buffer at room temperature and mixed with 1.35 μL of 10 mg/mL IRDye® 800CW dye. The reaction mixture was incubated at room temperature for 2 hours with mild rotation followed by overnight incubating at 4 °C with mild rotation, in the absence of UV light. The next morning, the free IRDye® 800CW was separated from the protein conjugates using Piece Zeba® Desalting Spin Columns (Thermo Scientific) as per manufacturer's instruction. IRDye® 800CW/Fab ratio and Fab concentration were determined by measuring the absorbance of the conjugate at 280 nm and 780 nm using UV-Vis spectrophotometer, and calculated using the formula provided by IRDye® 800CW Protein Labeling Kit.

4.6 Mammalian Cell Studies

4.6.1 Tissue Culture

Mammalian cell cultures were maintained at 37 °C with 5% CO_2. HEK293T cells were cultured in Dulbecco's Modified Eagle's Medium (DMEM). Cells were passaged at a ratio of 1:10 to 1:20 for general maintenance when the confluence reached 80-90%.

4.6.2 Transient HEK293T Cell Transfection

DNA837 (expressing anti-hRad51 scFv-Fc) plasmid was transfected into HEK293T cells using Lipofectamine 2000® Regent (Invitrogen Life Technologies). HEK293T cells were seeded onto 10 cm tissue culture dishes at densities of 4 x 10^6 cells/dish and incubated

overnight in DMEM supplemented with 10% FBS. Following removal of media and replacement with fresh media, 500 μL of room-temp Opti-MEM® and 5μg plasmid was mixed with a solution containing 500 μL Opti-MEM® and 20 μL Lipofectamine 2000® regent. After incubating for 5 minutes at room temperature, the above mixture was added to seeded cells in drop-wise manner. Cells were cultured for 48 hours, collected and a portion of the sample was lysed for Western analysis as descried in Section 4.2.5 to confirm the presence of scFv-Fc expressed from DNA837.

4.6.3 Clonogenic Survival Assay

A clonogenic survival assay was used to test the sensitivity of HEK293T cells to increasing doses of DNA-damaging agents in the presence of Fab or scFv-Fc, (Essers *et al.*, 1997). HEK293T cells were trypsinized and reseeded in a 6-well tissue culture plate at 200 cells/well. After culturing overnight, cells were treated with indicated concentrations of MMS alone, or in combination with indicated amount of Fab F_2 or FabItag I_2. For scFv-Fc, DNA837 transfected 293T cells (Section 4.6.2) were seeded in a 6-well tissue culture plate at 200 cells/well. After culturing overnight, MMS was added to cells in indicated concentrations. After 7 days, cells were fixed and stained using staining solution (0.3% crystal violet, 50% methanol in PBS). Colonies were counted using light microscopy (EVOS® FL Cell Imaging System, ThermoFisher Scientific). Cells treated with PBS and DMSO, or empty vector transfected cells were used as negative controls, respectively.

4.6.4 Fluorescence Imaging and Flow Cytometry

The ability of Fabs to internalize in HEK293T cells was analyzed using fluorescent microscopy (EVOS® FL Cell Imaging System, ThermoFisher Scientific). Cells were seeded in a 48-well plate at $5x10^4$ cells/well, and IRDye® 800CW dye-labeled Fab (Section 4.5.4) was added to cells. Cells were incubated for indicated hours followed by imaging. Briefly, cells in each well were washed using 300 μL of PBS. Fluorescence images were obtained with a fluorescent microscopy using Cy7 channel (EVOS® FL Cell Imaging System, ThermoFisher Scientific). Image optimization of contrast and brightness was performed to the same extent for respective panels. For quantitative analysis of uptake cells were detached from the walls after incubating for indicated hours. The cells were washed twice with PBS and the internalized fluorescence signal was immediately measured using Gallios Flow Cytometry (Beckman

Coulter, Inc.). For excitation of IRDye® 800CW dye the 640 nm laser was used and fluorescence emission was monitored through 755 LP filter. Five thousand cells were analyzed. Untreated cells were used to set the gate on live cells (FSC/SSC). Mean fluorescence intensity are reported for gated cells in each sample.

4.6.5 Statistical Analysis

P-values for clonogenic survival assay were determined by performing an unpaired *t* test using SPSS 16.0 (SPSS, USA). Data were represented by the mean ± S.D. (Standard Deviation) based on at least three independent experiments. A *p* value of less than 0.05 was considered significant (*$p<0.05$, **$p<0.005$).

Chapter 5 Results

5.1 Specific Aim 1: Isolation of Fabs Against hRad51 using the Fab Phage Display Library

5.1.1 Expression and Purification of hRad51 Protein

In order to isolate antibody fragments specific to human Rad51 (hRad51), we used recombinant hRad51 as the target antigen. hRAD51 gene (GenBank: CAG38796.1) was isolated from a testis cDNA library by the polymerase chain reaction (PCR) and cloned into the *EcoR*V and *Xho*I site of pET28a expression vector. The resulting plasmid, designated pET28a-hRad51 was provided by Dr. Luo (University of Saskatchewan). To optimize the condition for hRad51 expression, cell cultures were grown either at 18 °C for 16 hours or 37 °C for 4 hours post IPTG induction. We observed that the 4-hour IPTG induction at 37 °C was sufficient to induce high levels of hRad51 expression. Using this protocol, we obtained a yield of 4.7 mg hRad51 protein per 1 L of culture compared to 2.7 mg of hRad51 protein when the culture was incubated at 18 °C for 16 hours (**Figure 5.1**).

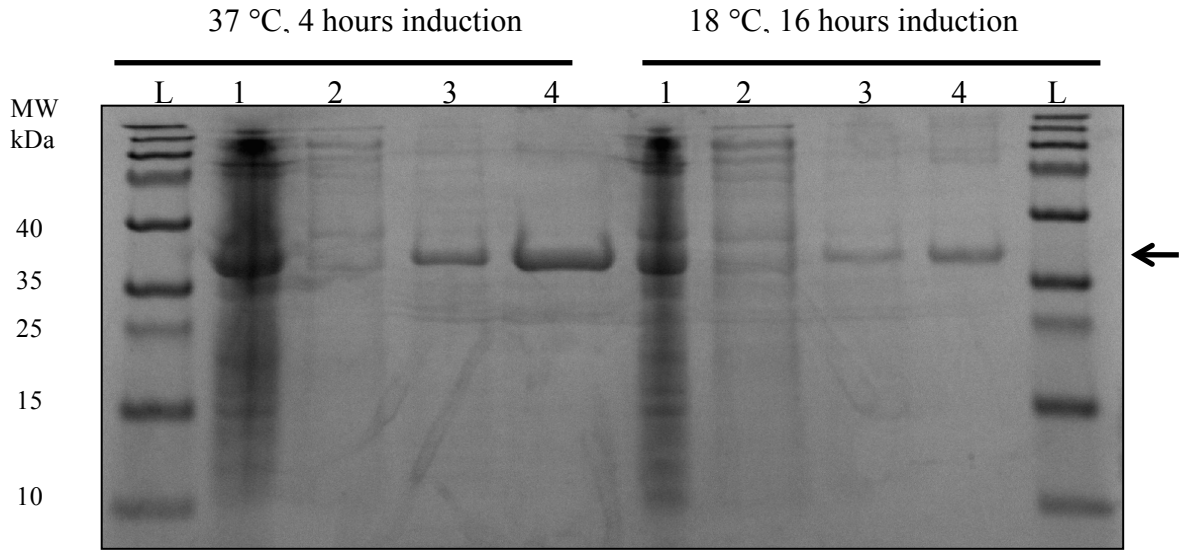

Figure 5.1 Comparison of hRad51 Expression Levels Using Different Induction Conditions
E. coli Rosetta (DE3) pLysS cells were cultured at 37 °C for 4 hours or at 18º for 16 hours following IPTG induction. His-tagged hRad51 was purified using nickel-affinity chromatograph, analyzed by polyacrylamide gel electrophoresis, and visualized by Coomassie blue staining. (Lane L) Protein molecular weight (MW) ladder; (Lane 1) whole-cell lysate; (Lane 2) soluble protein; (Lane 3) flow-through of Ni-affinity resin; (Lane 4) elution from Ni-affinity resin. Arrow indicates the expected MW (37kDa) of the hRad51 protein.

5.1.2 Antibody Phage Display Against hRad51 Using Fab-Phage Library

We performed phage display selection as outlined in Section 4.4.1. Based on several published protocols (Tonikian *et al.*, 2007; Rajan and Sidhu, 2012), we chose 5 μg/mL of purified hRad51 to coat maxisorp plates for phage display selection using a Fab-phage library. The Fab-phage library was constructed by V.M. Bharathikumar in Dr. Geyer's lab and contains $1x10^{10}$ diversity in complementarity-determining region of light and heavy chain 3 (L3 and H3) (**Figure 5.2**). To isolate a hRad51 binding Fab, the Fab-phage library was incubated with immobilized hRad51 and non-binding phage were washed away. Bound phage were eluted and amplified for next round of selection. The number of phage eluted after each round of selection was calculated based on the number of colonies formed after reinfection of the eluted phage particles in the host bacteria. After four rounds of selection, an increase in the enrichment of the number of hRad51-bound phage relative to BSA-bound phage was observed (**Figure 5.3**).

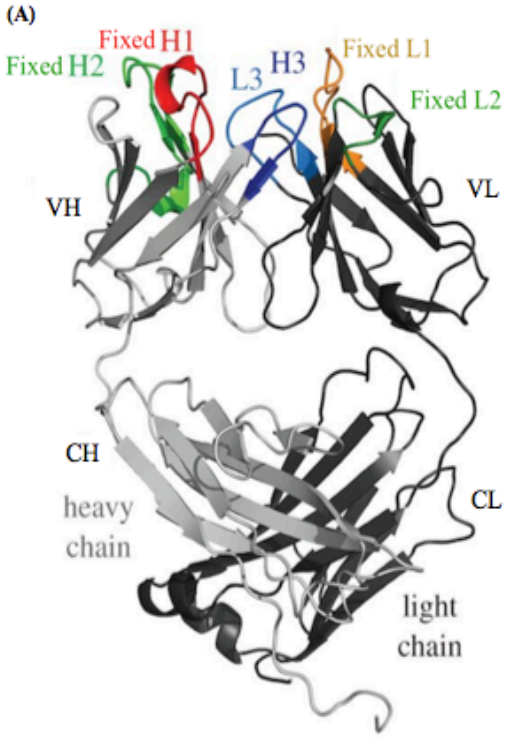

(B)

L3

Q	Q	Z_4	P	L	T

H3

A	R	Z_{1-10}	A	G	D	Y	F	D	Y
A	R	X_{7-15}	Y_4	G	Y	M	F	D	V

(C)

Theoretical Diversity							Actual Diversity
L1	L2	L3	H1	H2	H3	Total	
1	1	$2.9x10^4$	1	1	$2.6x10^{14}$	$7.4x10^{18}$	$1.0x10^{10}$

Figure 5.2 L3 and H3 Diversity in Fab-phage Library
(A) Fab framework used for library construction is shown in carton representation. The framework is composed of a light (heavy grey) and a heavy (light grey) chain. Six complementarity-determining regions (CDRs) are colored and located in the variable light (VL) and variable heavy (VH) chains. Fab-phage library contains four fixed CDRs: L1 (orange), L2 (light green), H1 (red) and H2 (heavy green) and two diversified CDRs: L3 (blue) and H3

(teal). (B) Library diversity designs in L3 and H3 regions. Z denotes any of the following thirteen amino acids introduced at different proportions: Y (20%), S (20%), G (20%), T (6.5%), A (6.5%), P (6.5%), H (3.5%), R (3.5%), E (3.5%), F (2.5%), W (2.5%), V (2.5%) or L (2.5%). X denotes any of the following nine amino acids introduced at different proportions: Y (25%), S (20%), G (20%), A (10%), F (5%), W (5%), H (5%), P (5%) or V (5%). The lengths of L3 and H3 are varied by altering the number of Z and X. (C) Theoretical diversity represents the number of combinatorial possibilities. Actual diversity represents the sequence composition determined by next generation sequencing.

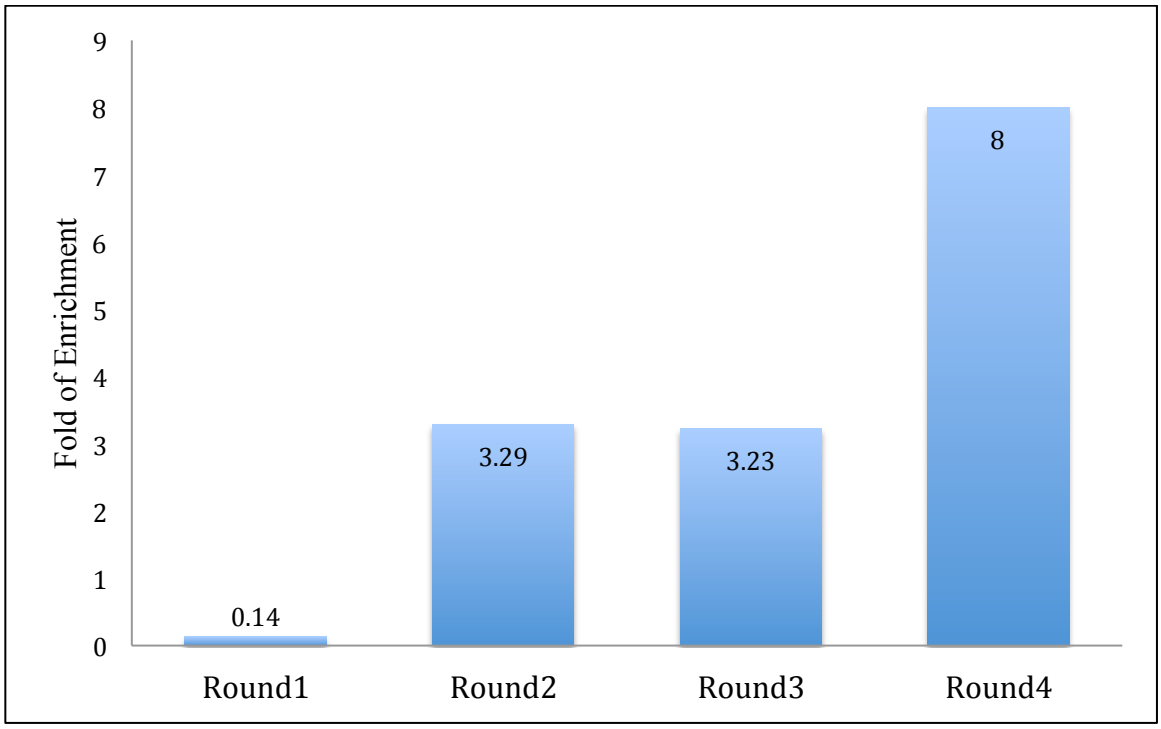

Figure 5.3 Enrichment of Phage-Displayed Fabs During Rounds of Phage Display Selection

The library of Phage-displayed Fabs were selected against hRad51 (5 μg/mL). After each round of selection, number of eluted phage were calculated. The enrichment after each round was determined by dividing the number of hRad51-bound phage eluted by the number of eluted phage from a control plate containing immobilized BSA.

5.1.3 Next Generation Sequencing of the Enriched Fab-Phagemid Pool

Enrichment in the number of target-bound phage is a suitable indicator to monitor the progress of selection for antibody phage display. However, it does not provide sequence information on changes in the antibody repertoire after each round of selection. Next Generation Sequencing (NGS) technologies have been used to monitor phage display selections and to speed up the identification of specific antibodies by monitoring enrichment of antibody

sequences during successive rounds of selection (Fischer, 2011). However, NGS read lengths using ion torrent sequencing technology are limited to 50-400 continuous base pairs.

LCDR3 and HCDR3 in variable regions in the Fab-phage Library (i.e. LCDR3 and HCDR3) are separated by ~ 928 base pairs. Therefore, in order to retain information on specific pairings of LCDR3 and HCDR3 in a given antibody fragment, we used the Kunkel protocol to bring LCDR3 and HCDR3 closer together in DNA sequence space (**Figure 5.4**). To do this, we extracted ssDNA from third and fourth round phage pools (Section 4.4.1.1) and used them as templates for Kunkel reaction (Section 4.4.1.2). The modified phagemid with LCDR3 and HCDR3 separated by 30 bases was used as a template to generate a PCR amplicon for Ion Torrent NGS analysis. Three predominant clusters were enriched from rounds 3 and 4 **(Figure 5.5**). Peptide YSYY-HAYYAGGSSHYYYYYGMDV (from cluster 1) has the highest enrichment in frequency from rounds 3 to 4. However, this peptide is thought as a non-specific Fab because it has been isolated by several members in our lab from the same Fab-library using completely different target proteins.

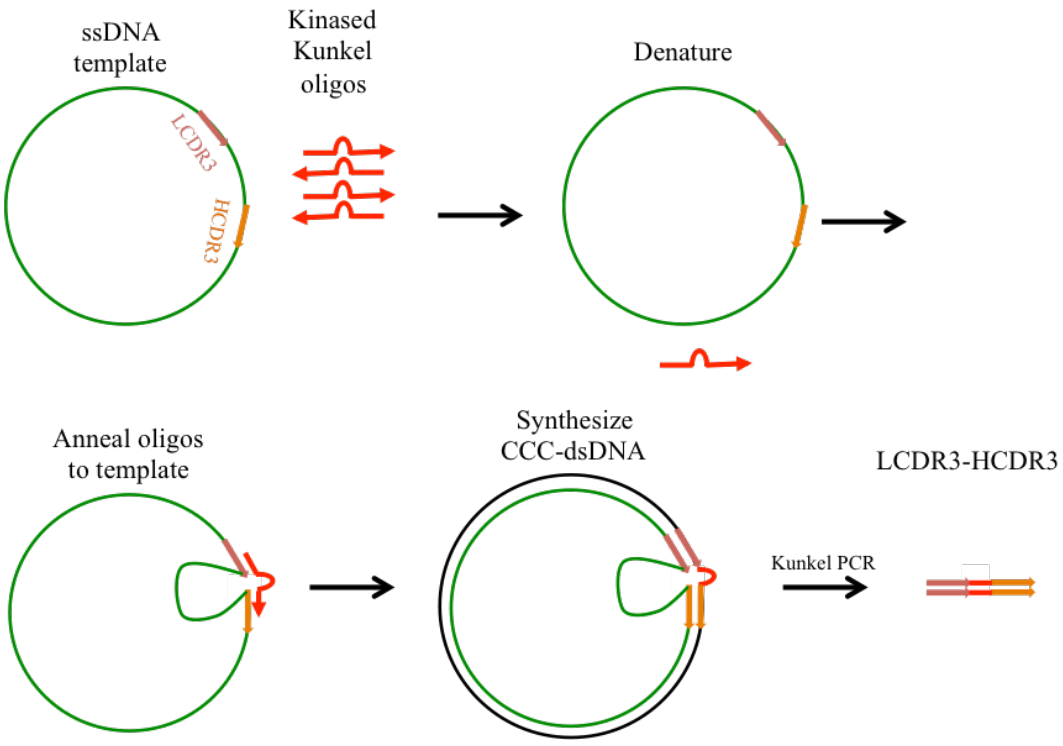

Figure 5.4 Schematic of Kunkel Reaction to Bring LCDR3 and HCDR3 Closer Together
ssDNA extracted from phage was incubated with 5'-phosphorylated Kunkel oligos followed by denaturation. Oligos were annealed to the ssDNA template, enzymatically extended, and

ligated to form heteroduplex CCC-dsDNA, which was then used as a template to PCR amplify LCDR3-HCDR3 fragments. ssDNA, single stranded DNA; LCDR3, light chain complementarity-determining region 3; HCDR3, heavy chain complementarity-determining region 3; CCC-dsDNA, covalently closed circular double stranded DNA.

(A)

(B)

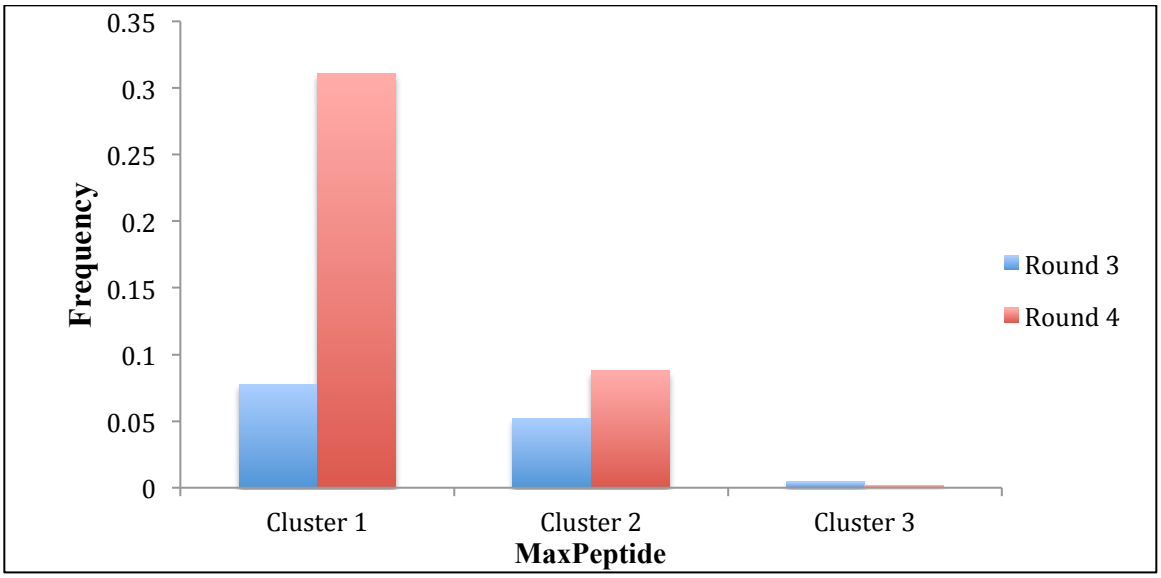

Figure 5.5 NGS Analysis for Phage-displayed Peptides Selected after Three and Four Rounds of Selection to hRad51

DNA from third and fourth round phage pools against hRad51 was used to perform Ion Torrent Next Generation Sequencing (NGS) sequencing analysis. (A) Consensus profile generated from phage-displayed LCDR3-HCDR3 peptide sequence. Three clusters were enriched after three and four rounds of phage display selection. Sequence is arranged from the N terminus to the C terminus. (B) Frequency of the MaxPeptide from each cluster for third and fourth round of selection.

5.1.4 Kinetic Analysis of hRad51 Fabs

Although potential hRad51 interaction Fabs can be enriched following phage display selection, there is the possibility that they represent false positives that do not interact with hRad51. False positive binders may refer to non-binding phage or phage binding to the polystyrene surfaces of Maxisorp plate (often referred to as background binders), or even weak binding phage. Additionally, some phage clones predominate because of their advantage in phage display propagation that allows them to outgrow other clones in the pool. Recovery of such clones is not solely dependent on their affinity to the target. To identify the true positive Fabs, it is necessary to use an additional strategy to identify true positive binders from the enriched phage display pool.

Octet® biolayer interferometry (BLI) analysis was used to identify true positive Rad51 bound Fabs by monitoring biosensor-immobilized Fabs interaction with hRad51. We expressed individual Fabs from the fourth round of enriched phage pool. First, the phagemid pool after

the fourth round of phage display was extracted from the phage-infected bacterial cells using Plasmid Miniprep Kit. DNA encoding Fab fragments containing heavy and light chains were amplified from the phagemid pool (Section 4.2.3.1) and cloned into the pCW expression vector (**Figure 4.2**) using the Gibson Assembly cloning strategy (Section 4.2.5). The resultant pCW-Fab pool was transformed into *E. coli* BL21-DE3 (Section 4.3.4) and eighteen individual transformants were isolated for small-scale Fab expression (Section 4.5.1.3). Supernatants containing Fabs were collected to determine binding to a Protein A biosensor using BLI (Section 4.5.2). Protein A binds to the first constant domain (CH1) of correctly folded Fabs (Bouvet, 1994). Three out of eighteen Fabs bound Protein A, designated Fab F_1, F_2, and F_3 (**Figure 5.6**). Plasmids for F_1, F_2, and F_3 were extracted from corresponding bacteria transformants (Section 4.3.3) and sequenced using the 3500 Genetic Analyzer (**Table 5.1**). In agreement of NGS data, the sequence showed that these three Fabs are also enriched in NGS analysis.

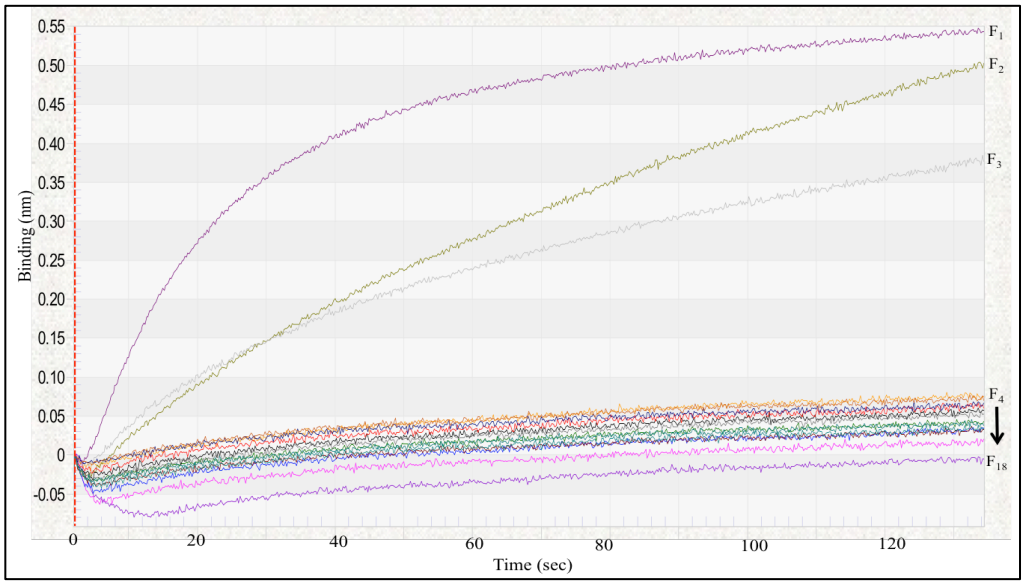

Figure 5.6 Binding of Anti-hRad51 Fabs ($F_1 – F_{18}$) to Protein A
Real-time binding of eighteen individual Fabs ($F_1 – F_{18}$) to Protein A was measured using Octet® BLI. Protein A biosensors were immersed in the wells containing Fabs, and the wavelength shift (in nm) was recorded versus time (sec).

Table 5.1 Sequence for Anti-hRad51 Fabs (F_1, F_2, and F_3).

Fab	LCDR3	HCDR3
F_1	CQQ*YSYY*PL	CAR*HAYYAGGSSHYYYYYGM*DV
F_2	CQQ*GTYL*PL	CAR*TYSYASRGWYF*DY
F_3	CQQ*YYA*PL	CAR*SWGGGSGYYAYYYYYM*DY

Fab, fragment antigen-binding; LCDR3, light chain complementarity-determining region 3; HCDR3, heavy chain complementarity-determining region 3. Variable regions are italicized.

5.2 Specific Aim 2: *In vitro* Characterization of Anti-hRad51 Fabs

5.2.1 Expression and Purification of Anti-hRad51 Fabs (F_1, F_2, and F_3)

Anti-hRad51 Fabs, Fab F_1, F_2, and F_3, were expressed and purified and their *in vitro* binding kinetics determined. Fab expression plasmids pCW-F_1, pCW-F_2, and pCW-F_3 were transfected by electroporation into BL21-DE3 cells (Section 4.3.4). Transformed cells were cultured in Overnight Express™ Instant TB Medium for 12 hours and Fabs were purified from whole cell lysates using HiTrap Protein L column. Fabs were analyzed by SDS-PAGE (**Figure 5.7**). Approximately 10 mg of each Fab was obtained from 1 L of culture.

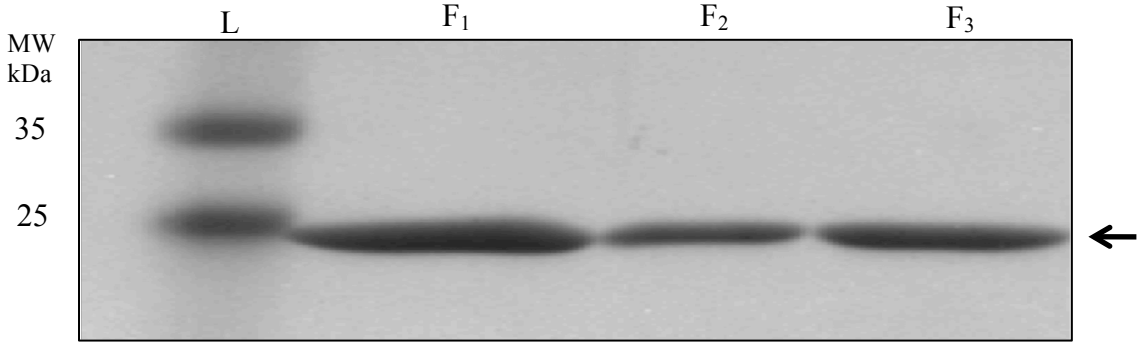

Figure 5.7 SDS-PAGE Analysis of Anti-hRad51 Fabs
Fabs F_1, F_2 and F_3 were expressed in *E. coli* BL21-DE3 strain and purified using HiTrap Protein L column. Purified Fabs were analyzed by SDS-PAGE and visualized by Coomassie blue staining. Arrow indicates the expected molecular weight (MW) of the light and heavy chain of Fabs. L is a protein MW ladder.

5.2.2 Binding Affinity of Fabs F_1, F_2, and F_3 to hRad51

To confirm that Fabs F_1, F_2, and F_3 bound hRad51, we immobilized Fabs F_1, F_2, and F_3 on Protein L biosensors. Protein L binds to kappa light chains in Fabs with a K_D less than 1 nM (Nilson *et al.*, 1992). We then immersed the biosensors in wells containing hRad51 and

analyzed the hRad51 interaction using Octet® BLI. hRad51 was preferentially bound by Fab F_2 and showed no interactions with Fab F_1 and F_3 (**Figure 5.8**). To determine the dissociation constant (K_D) of Fab F_2 with hRad51, we immobilized Fab F_2 on Protein L biosensor and immersed the biosensor in different concentrations of hRad51. By monitoring the change in wavelength (nm) versus time, we obtained the k_{on}, k_{off}, and K_D values (**Figure 5.9**). Fab F_2 bound to hRad51 with a K_D value of 8.10 ± 0.21 nM. Despite phage F_1, F_2, and F_3 being enriched from phage display selection against hRad51, Fab F_1 and F_3 were not capable of binding recombinant hRad51. These results confirmed the presence of false positive binders enriched from phage display selection.

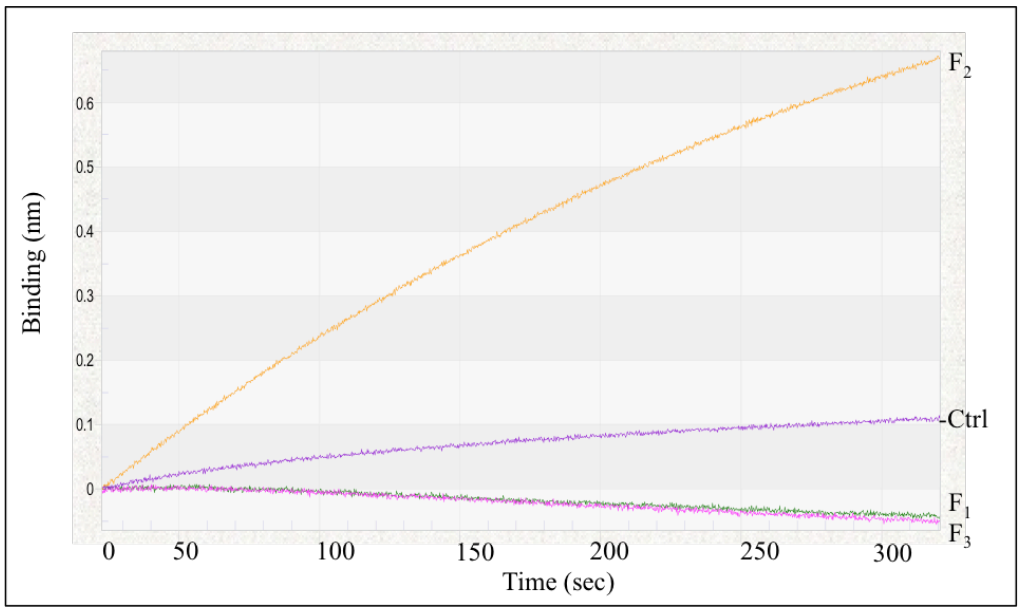

Figure 5.8 Binding of Fabs F_1, F_2 and F_3 to hRad51
Real-time binding of Fabs F_1, F_2, and F_3 to hRad51 was measured using Octet® BLI. Fabs were immobilized on Protein L biosensors and immersed in the wells containing hRad51 (500 nM). The wavelength shift (nm) was recorded versus time (sec). Empty sensor was used as negative control (-Ctrl).

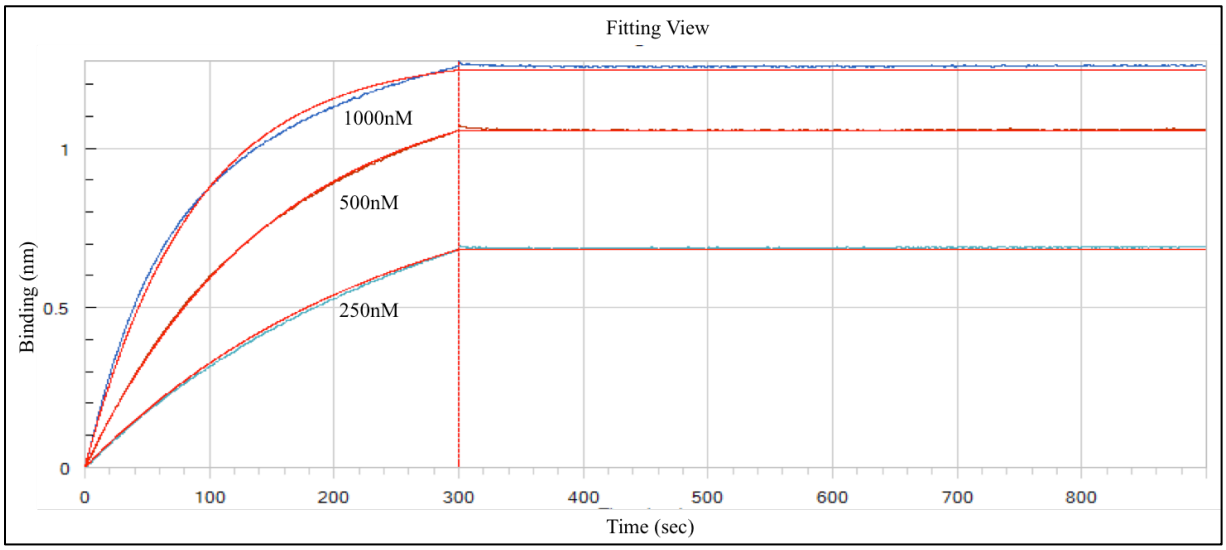

	hRad51˙F_2
k_{on} (1/Ms)	$1.93x10^{4} \pm 4.32x10^{2}$
k_{off} (1/s)	$15.63x10^{-5} \pm 3.23x10^{-6}$
K_D (nM)	8.10 ± 0.21

Figure 5.9 Kinetic Analysis of Fab F_2 Binding to hRad51
Fab F_2 was immobilized on a Protein L biosensor and the biosensor was immersed in different concentrations of hRad51. Octet® BLI measured their binding as wavelength shift (in nm) versus time (sec). Kinetic parameters (k_{on} and k_{off}) and dissociation constants (K_D) were determined by globally fitting a reference cell-subtracted concentration series to a 1:1 (Langmuir) binding model.

5.2.3 Binding Specificity of Fab F_2 to hRad51

To confirm that Fab F_2 bound hRad51 specifically (DE3)pLysS cells were transformed with empty vector or hRad51 expression plasmid. hRad51 was detected by Fab F_2 using Western analysis (Section 4.2.4) (**Figure 5.10**). RecA protein is a central bacterial recombinase that possesses 30% common sequence identity with hRad51 (Shinohara *et al.*, 1993), thus we also compared the binding of Fab F_2 to recombinant hRad51 and RecA using Western analysis (**Figure 5.10**). Fab F_2 bound hRad51 but not other proteins in *E. coli* Rosetta(DE3)pLysS, or recombinant RecA.

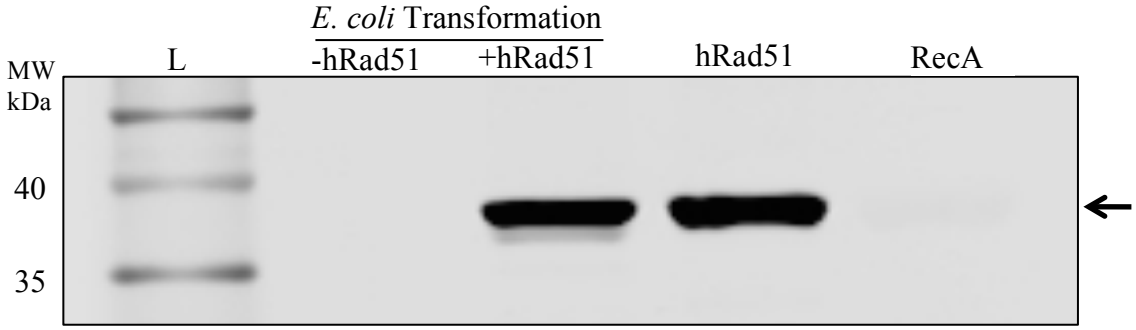

Figure 5.10 Western Analysis for hRad51 Using Fab F_2
E. coli Rosetta(DE3)pLysS cells transformed with hRad51 expression plasmid (+) were induced to express by IPTG. Cell lysates, or purified recombinant hRad51 and RecA were analyzed by polyacrylamide gel electrophoresis followed by Western analysis using IRDye® 800CW dye-labeled Fab F_2. Arrow indicates the expected molecular weight (MW) of hRad51 or RecA. L is a protein MW ladder.

5.2.4 Effect of Fab F_2 on hRad51 DNA Binding Activity

To determine whether Fab F_2 blocked the ability of hRad51 to interact with ssDNA, we used Octet® BLI. We first determined the K_D of hRad51 to ssDNA. To do this, we immobilized 5'-biotinylated oligo$(dT)_{36}$ onto a streptavidin biosensor and immersed the biosensor in different concentrations of hRad51 (**Figure 5.11**). The K_D of hRad51 for single-stranded DNA was 27.60 ± 4.75 nM, which was similar to the K_D reported previously for the interaction of hRad51 with oligo$(dT)_{50}$ (Tombline *et al.*, 2002).

Next, we developed a BLI assay to evaluate the ability of Fab F_2 to inhibit hRad51 DNA binding activity. In this assay, hRad51 was incubated with different concentrations of Fab F_2 for 30 minutes at room temperature. 5'-biotinylated oligo$(dT)_{36}$ was immobilized onto a streptavidin biosensor and the biosensor was immersed in the Fab F_2 / hRad51 mixture. The wavelength shift (until the biosensor was fully saturated) was recorded. Fab F_2 inhibited hRad51 DNA binding activity in a nanomolar range, indicating that Fab F_2 might bind near the DNA binding sites of hRad51 (**Figure 5.12**).

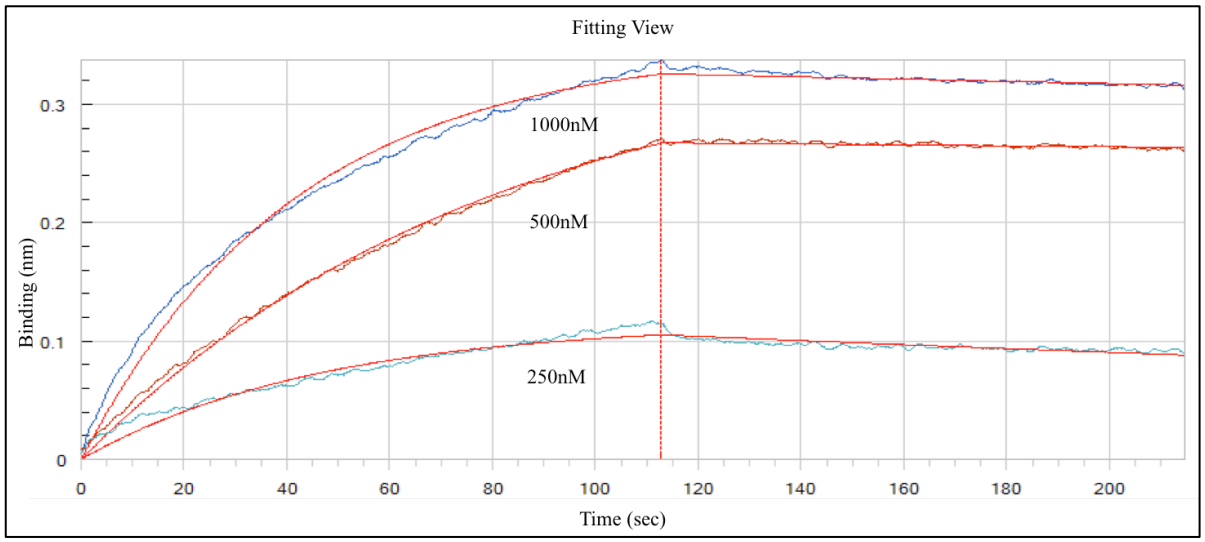

	hRad51·oligo(dT)$_{36}$
k_{on} (1/Ms)	$3.25 \times 10^{4} \pm 1.10 \times 10^{3}$
k_{off} (1/s)	$7.26 \times 10^{-4} \pm 7.36 \times 10^{-5}$
K_D (nM)	27.60 ± 4.75

Figure 5.11 Kinetic Analysis of Single Stranded DNA Binding to hRad51
5'-biotinylated oligo(dT)$_{36}$ was immobilized on a streptavidin biosensor and the biosensor was immersed in different concentrations of hRad51. Octet® BLI measured their binding as wavelength shift (in nm) versus time (sec). Kinetic parameters (k_{on} and k_{off}) and dissociation constants (K_D) were determined by globally fitting a reference cell-subtracted concentration series to a 1:1 (Langmuir) binding model.

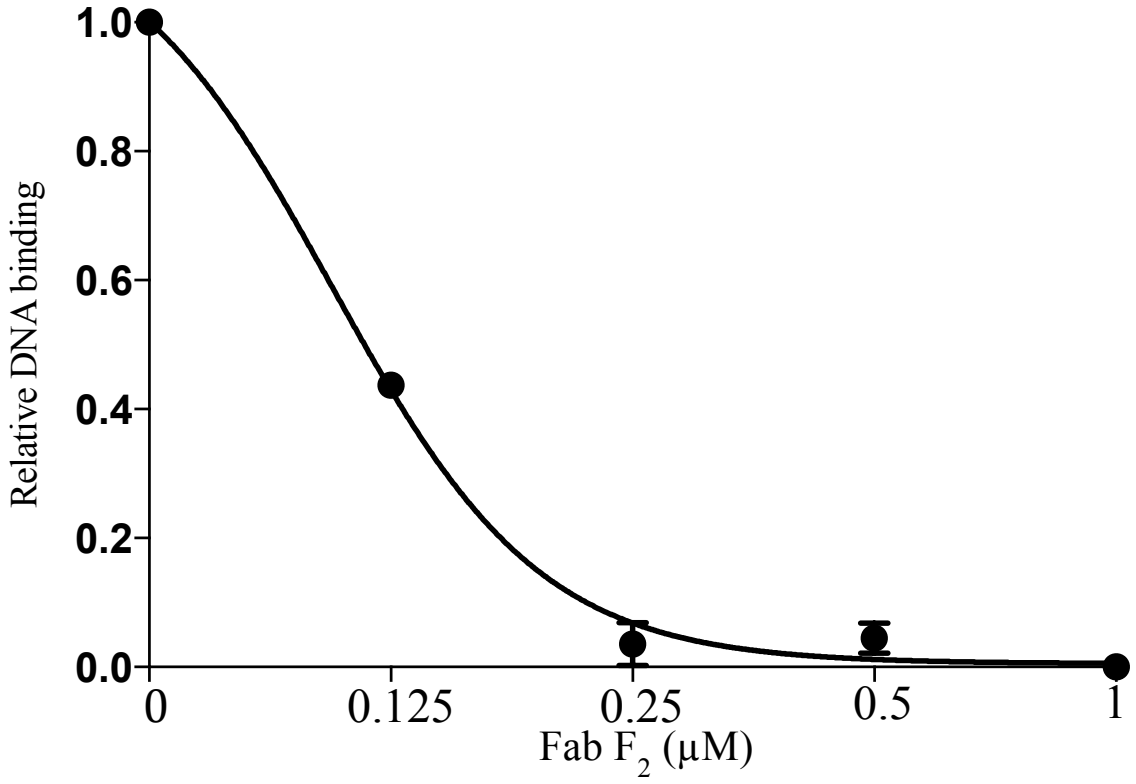

Figure 5.12 Fab F_2 Inhibits hRad51 DNA Binding
hRad51 (0.5 μM) was incubated with indicated concentrations of Fab F_2 for 30 minutes at room temperature. 5'-biotinylated oligo$(dT)_{36}$ was immobilized onto a streptavidin biosensor and the biosensor was immersed in hRad51/Fab F_2 mixtures. When the biosensor was fully saturated, the response for each condition was determined by subtracting the hRad51-free control of that condition. The response was normalized to the condition in the absence of Fab F_2, which was expressed as 1.0. Error bars represent standard deviation from three independent measurements.

5.2.5 Effect of Fab F_2 on hRad51 ATPase Activity

We investigated whether Fab F_2 inhibits hRad51 ATPase activity. To do this, we monitored the release of inorganic phosphate by ATP hydrolysis over the time using the malachite green assay as an indicator of hRad51 ATPase activity (Ishida *et al.*, 2009). We found that hRad51 ATPase activity was not inhibited by Fab F_2 in the presence or absence of DNA (**Figure 5.13**).

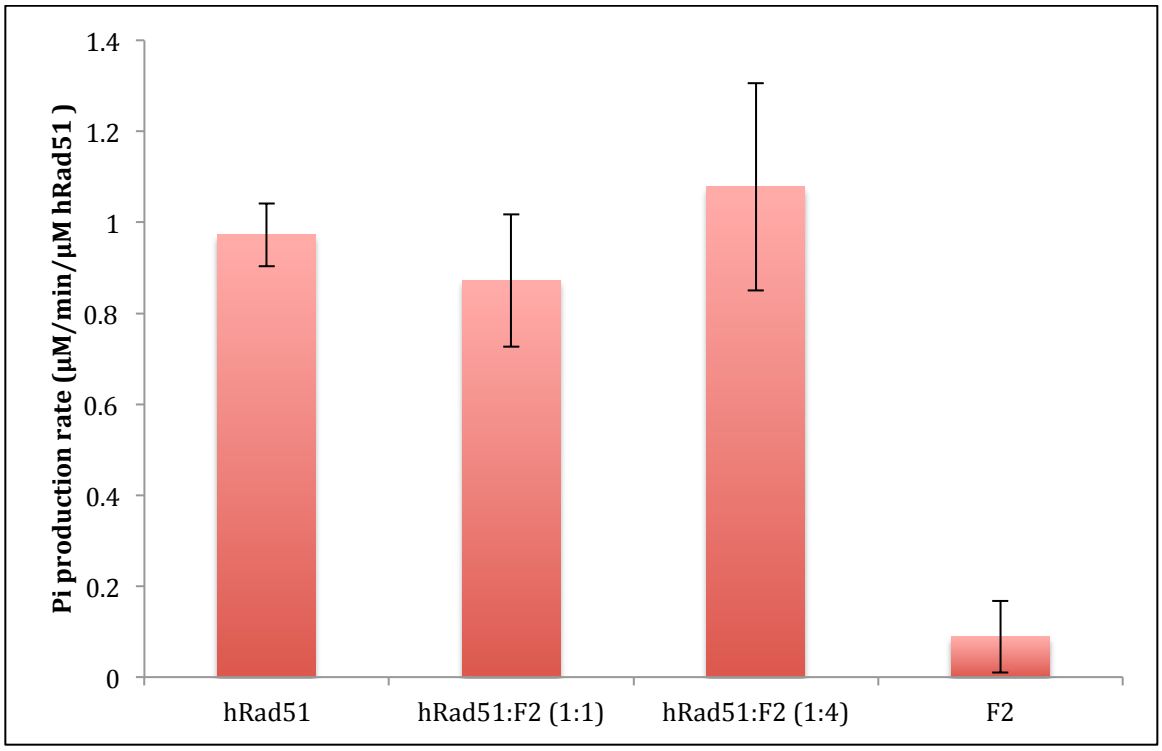

Figure 5.13 Fab F_2 does not inhibit hRad51-mediated ATP Hydrolysis
ATP hydrolysis reaction was carried out with hRad51 and Fab F_2 in different ratios. The release of inorganic phosphate by hRad51 ATP hydrolysis was monitored using the malachite green assay. Phosphate (Pi) production rate was calculated for each reaction. Fab F_2 alone did not hydrolyze ATP. Error bars represent standard deviation from at least three independent measurements. *P<0.05.

5.3 Specific Aim 3: Development of Intracellular Anti-hRad51 Antibody

So far we have demonstrated the *in vitro* specificity, affinity and the inhibitory effects of anti-hRad51 antibody on purified hRad51 protein. However, because hRad51 is an intracellular target, if anti-hRad51 antibody were to elicit its effects, it should be able to cross mammalian cell membrane. In this specific aim, our initial attempt was to express anti-hRad51 antibody in a scFv-Fc format inside HEK293T cells because scFv-Fc can increase antibody stability in a reducing intracellular environment by avoiding the formation of inter-molecular disulfide-bonds. It is likely chemotherapy will benefit more from anti-hRad51 scFv-Fc than Fab. However, our subsequent experiments showed that this anti-hRad51 svFv-Fc could not be purified when fused to a protein transduction domain, which limits the direct application of scFv-Fc. Therefore, our second attempt was to introduce anti-hRad51 Fab into the cytosol from outside the cell by fusing Fab to a protein transduction domain.

5.3.1 Effect of Anti-hRad51 scFv-Fc on HEK293T Cell Sensitivity to MMS

In collaboration with Iprogen Biotech Inc., we cloned the CDR sequences from Fab F_2 into scFv (single-chain variable fragment) format in which the VH and VL domains are joined with a flexible polypeptide linker preventing dissociation. The scFv was cloned into a mammalian expression vector as a fusion to an Fc (crystallisable fragment) domain, designated DNA837 plasmid (**Figure 4.4**). Using a Lipofectamine 2000-mediated transient cell transfection strategy (Section 4.6.2), DNA837 plasmid was transfected into HEK293T cells. Cells were cultured for 48 hours and a portion of cells were lysed for Western analysis to confirm the expression of DNA837 in HEK293T cells (**Figure 5.14**).

We examined whether DNA837 could enhance HEK293T cell sensitivity to DNA-damaging agent MMS. We used the clonogenic survival assay to assess sensitivity to MMS in the presence or absence of DNA837. DNA837-transfected HEK293T cells were treated with concentrations of MMS ranging from 0 to 100 μM. Colonies were grown for 7 days and enumerated by light microscopy. The number of colony-forming unit (cfu) was significantly decreased when HEK293T cells were transfected with DNA837 in the absence of MMS, indicating that anti-hRad51 scFv-Fc alone can inhibit HEK293T cell proliferation (**Figure 5.15**). Moreover, DNA837-transfected HEK293T cells became 4.48-fold more sensitive to 20 μM of MMS. 100 μM of MMS in combination with DNA837 completely inhibited HEK293T colony formation (**Figure 5.15**). These results indicated that anti-hRad51 scFv-Fc could significantly potentiate the activity of MMS to inhibit the cell proliferation.

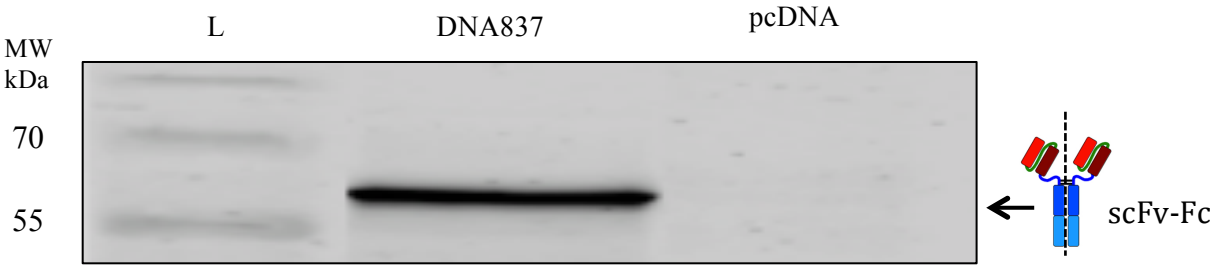

Figure 5.14 Expression of Anti-hRad51 scFv-Fc in HEK293T Cells
HEK293T cells were transfected with DNA837 encoding anti-hRad51 scFv-Fc. Western analysis was used to validate the expression of scFv-Fc. Cell lysates of the selected transfected cells were immunoblotted using Anti-IgG antibody. pcDNA-transfected 293T cell were used as control. L is a protein molecular weight (MW) ladder.

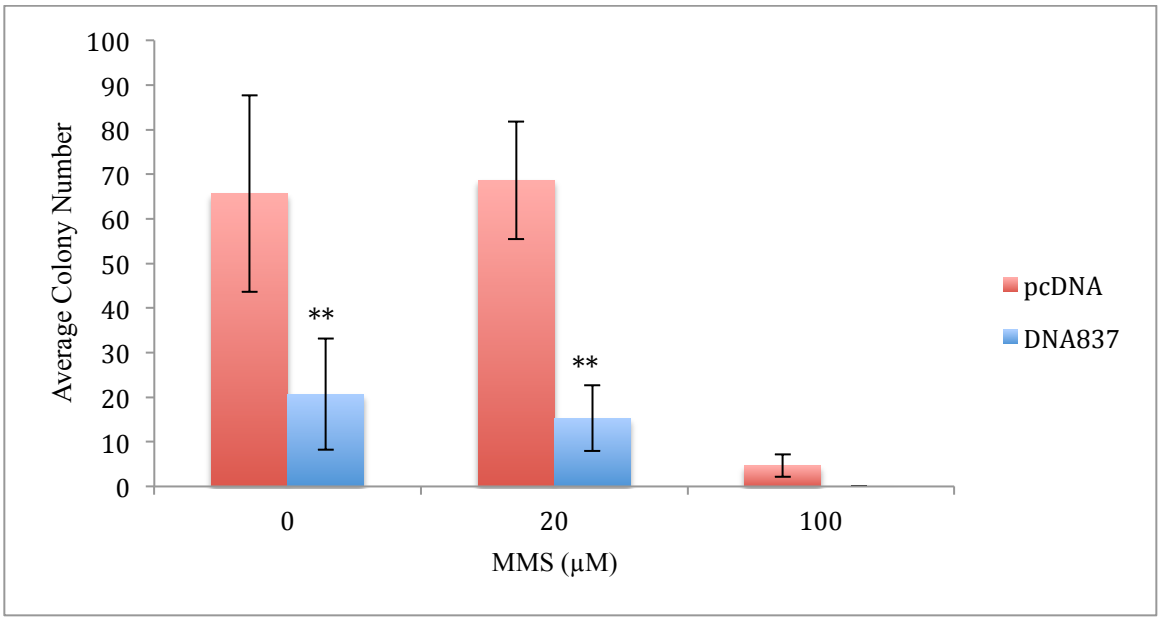

Figure 5.15 Anti-hRad51 scFv-Fc Sensitizes HEK293T Cell to Methyl Methanesulfonate HEK293T cells transiently expressed anti-hRad51 scFv-Fc DNA837 were exposed to indicated concentrations of methyl methanesulfonate (MMS). Cells were cultured for 7 days post MMS treatment. Colonies were stained with 0.3% crystal violent and enumerated by light microscopy. pcDNA transfected HEK293T cell was used as control. Error bars represent standard deviation from three independent measurements. $^{**}P<0.005$ (DNA837 with MMS 0 μM and 20 μM vs. pcDNA).

5.3.2 Fusing a Membrane Import Tag (Itag) onto C-terminus of Anti-hRad51 Fab F_2

Iprogen Biotech Inc. developed a proprietary membrane import tag (Itag), which promotes intracellular protein transduction when fused to a protein in a recombinant expression system (Patent No. WO 2014005219 A1). The Itag consists of a secretion signal peptide sequence in combination with a cleavage inhibition sequence. This combination efficiently blocks cleavage of the secretion signal peptide on a recombinant protein and halts secretion of the protein from a cell. Itag shows enhanced efficiency as a protein transduction domain when the secretion peptide sequence precedes the cleavage inhibition sequence in the N to C-terminus direction. Although the mechanism for the transduction efficiency is unknown, it appears that the intracellular delivery is achieved through receptors in a recipient cell surface. To determine whether Itag facilitates the transport of Fab F_2 across the cell plasma membrane to reach cytosol, we fused the Itag to the C-terminus of Fab F_2, designated FabItag I_2 (**Figure 5.16**). FabItag I_2 sequence was cloned into pCW-Itag vector (**Figure 4.3**), designated pCW-I_2. To overexpress FabItag I_2, plasmid pCW-I_2 was transfected by electroporation into BL21-DE3 strain. Transformed cells were cultured in Overnight Express^{TM} Instant TB Medium for 12 hours and

Fab I_2 was purified from whole cell lysates using HiTrap Protein L column. A fraction of Fab I_2 solution was analyzed by SDS-PAGE (**Figure 5.17**). Approximately 12 mg of FabItag I_2 was obtained from 1 L of culture.

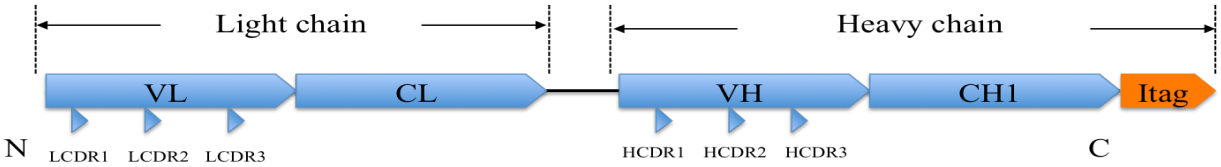

Figure 5.16 Schematic View of FabItag I_2 Molecule
The import tag (Itag) was fused to the end of C-terminus of Fab F_2. N, N-terminus; VL, variable light chain; CL, constant light chain; VH, variable heavy chain; CH1, constant heavy chain 1; C, C-terminus; LCDR, light chain complementarity-determining region; HCDR, heavy chain complementarity-determining region. Both Light chain and heavy chain contain three variable regions.

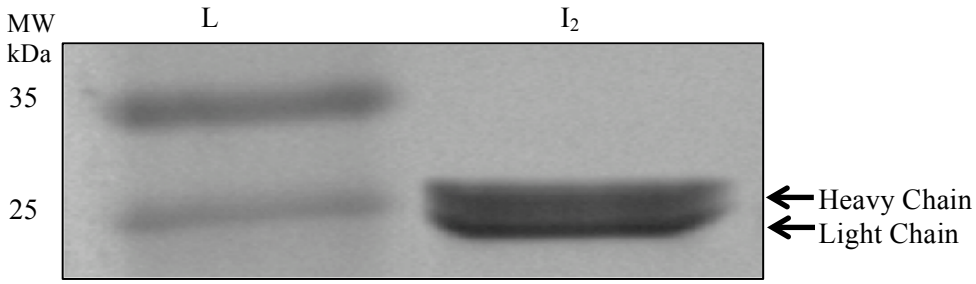

Figure 5.17 Coomassie-stained SDS-PAGE Analysis of Anti-hRad51 FabItag I_2
FabItag I_2 was expressed in *E. coli* BL21-DE3 strain and purified using HiTrap Protein L column. The purified FabItag I_2 was analyzed by polyacrylamide gel electrophoresis and visualized by Coomassie blue staining. Arrow indicates the expected size of the light and heavy chain of FabItag I_2. L is a protein molecular weight (MW) ladder.

5.3.3 Binding Affinity of FabItag I_2 to hRad51

To determine the dissociation constant (K_D) of FabItag I_2 with hRad51, we immobilized FabItag I_2 on Protein L biosensor and immersed the biosensor in different concentrations of hRad51. FabItag I_2 bound tightly to hRad51 with K_D value of 18.20 ± 0.47 nM (**Figure 5.18**), which is slightly decreased compared to Fab F_2 and hRad51 binding (8.10 ± 0.21 nM).

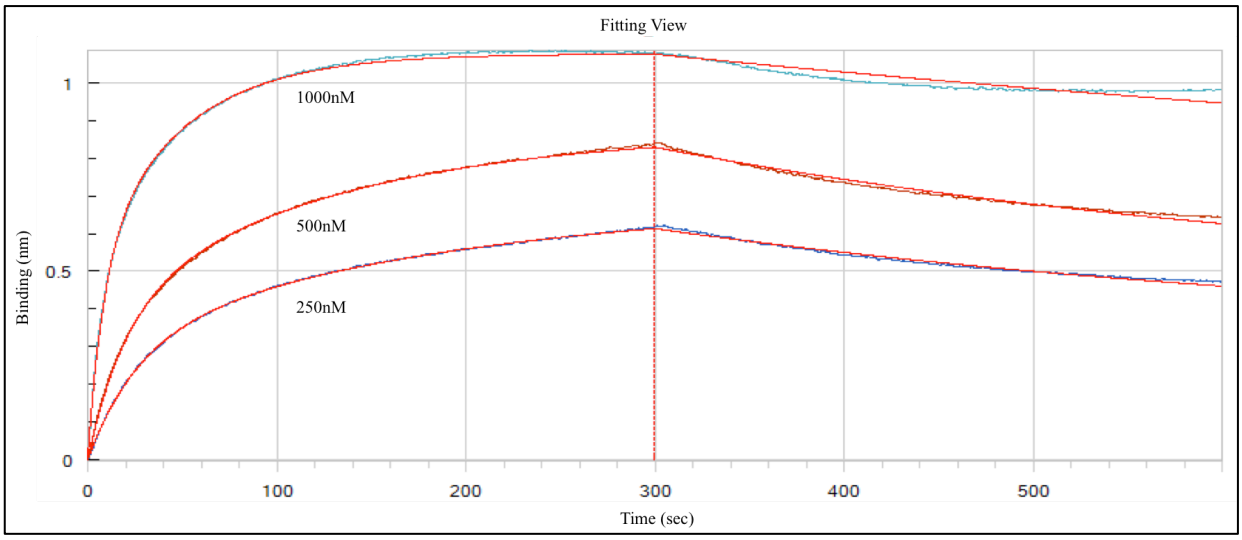

	hRad51˙I_2
k_{on} (1/Ms)	$3.71x10^{4} \pm 3.97x10^{2}$
k_{off} (1/s)	$6.58x10^{-4} \pm 1.41x10^{-5}$
K_D (nM)	18.20 ± 0.47

Figure 5.18 Kinetic Analysis of FabItag I_2 Binding to hRad51
FabItag I_2 was immobilized on a Protein L biosensor and the biosensor was immersed in different concentrations of hRad51. Octet® BLI measured their binding as wavelength shift (in nm) versus time (sec). Octet® BLI measured their binding as wavelength shift (in nm) versus time (sec). Kinetic parameters (k_{on} and k_{off}) and dissociation constants (K_D) were determined by globally fitting a reference cell-subtracted concentration series to a 1:1 (Langmuir) binding model.

5.3.2 Internalization of FabItag I_2 into HEK293T Cells

In order for anti-hRad51 FabItag I_2 to inhibit hRad51 it needs to cross mammalian cell membrane. To determine if FabItag I_2 can be internalized into HEK293T cells, we incubated cells with IRDye® 800CW dye-labeled Fab F_2 and FabItag I_2 and analyzed by fluorescent microscopy. After 2 hours of cellular exposure to the Fab F_2 and FabItag I_2, no Fab seemed to be internalized in both cases. After 8 hours an increase in FabItag I_2 fluorescence signal was observed (**Figure 5.19 I_2**). FabItag I_2 was bound to the plasma membrane while no punctuate staining of the cytosol was observed for Fab F_2 (**Figure 5.19 F_2**). After 24 hours of incubation, FabItag I_2 was not only bound to the plasma membrane but had entered the cells. Under the same condition, no Fab F_2 fluorescence signal was observed using fluorescent microscopy although flow cytometry indicated Fab F_2 might bind or enter the cells (**Figure 5.20**).

Furthermore, quantitative analysis using flow cytometry indicated that Itag significantly enhanced intracellular protein transduction efficiency (**Figure 5.20**).

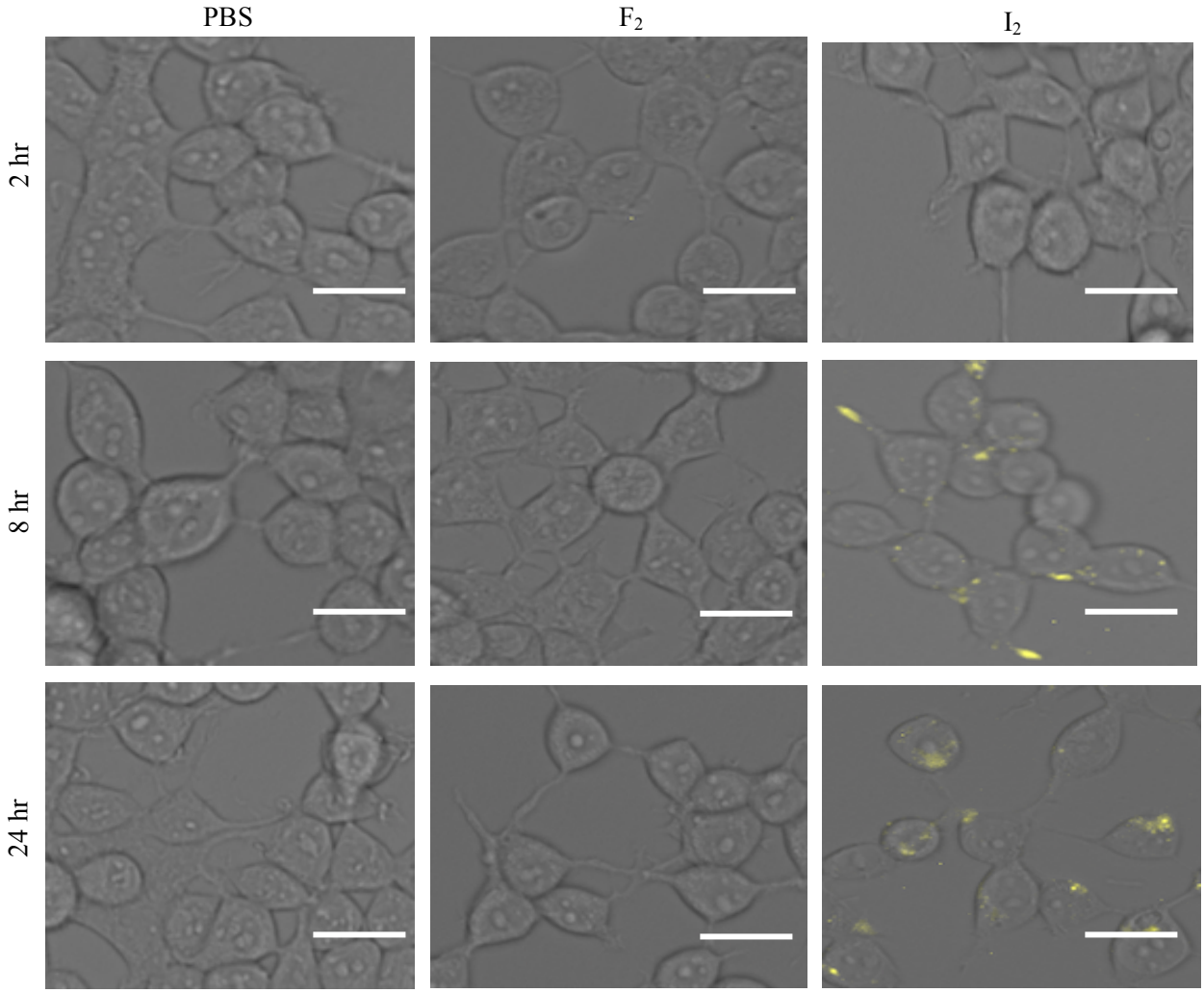

Figure 5.19 Internalization of Fab F_2 and FabItag I_2 into HEK293T Cells
HEK293T cells were incubated with IRDye® 800CW-labeled Fab F_2 (40 μM) or FabItag I_2 (40 μM), respectively, for indicated hours and fluorescence images were taken using a fluorescent microscopy. PBS was used as control. Bars indicate 200 μM.

(A)

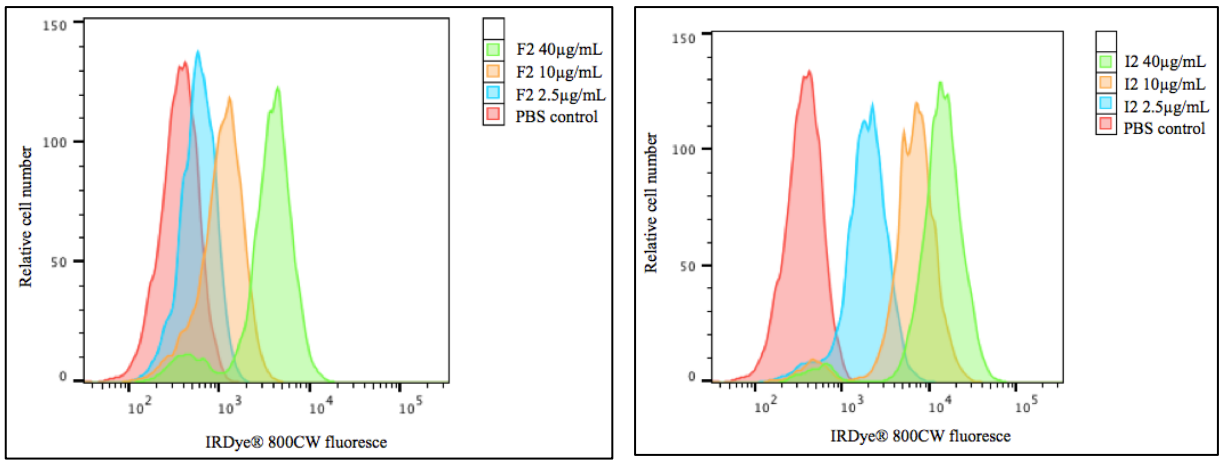

(B)

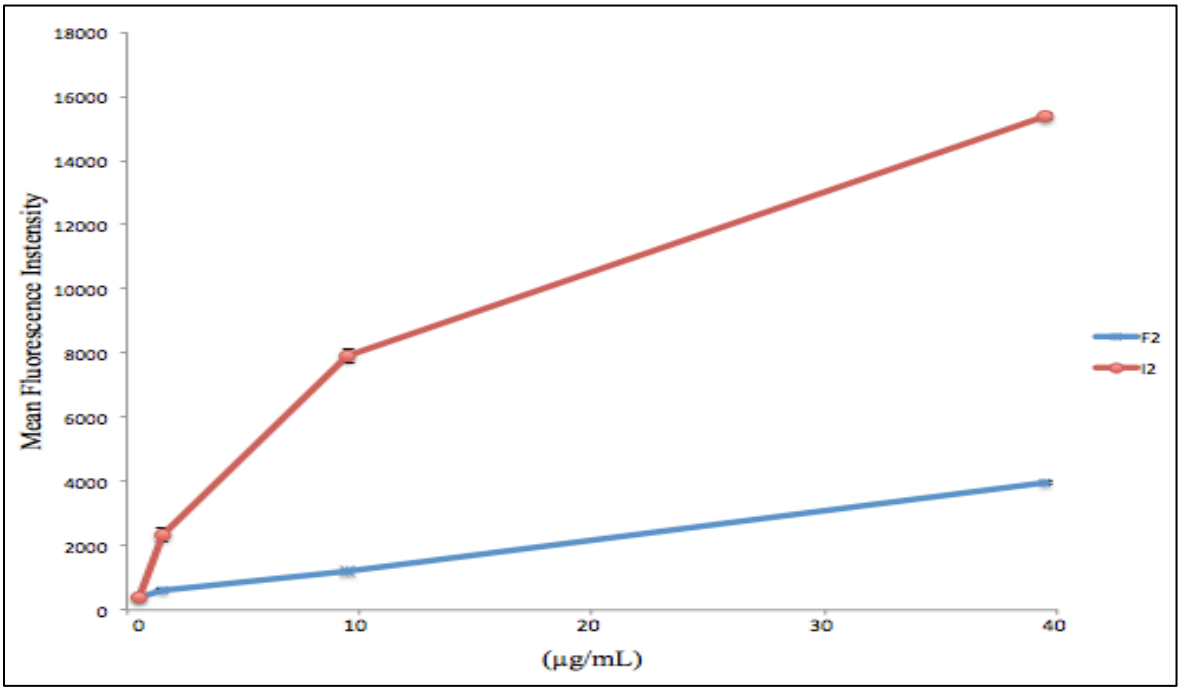

Figure 5.20 Comparison of Fab F_2 and FabItag I_2 Internalization into HEK293T Cells
HEK293T cells were incubated with indicated concentrations of IRDye® 800CW dye-labeled Fab F_2 or FabItag I_2. (A) IRDye® 800CW fluoresce was measured using flow cytometry after 24 hours. (B) Mean fluorescence intensity was compared between Fab F_2 and FabItag I_2. Error bars represent standard deviation from three independent measurements.

5.3.4 Effect of Anti-hRad51 FabItag I_2 on HEK293T Cell Sensitivity to MMS

We examined whether FabItag I_2 could enhance HEK293T cell sensitivity to the DNA-damaging agent MMS. HEK293T cells were treated with 80 μM of MMS and concentrations of FabItag I_2 ranging from 0 to 40 μM, both alone and in combination. We used the clonogenic survival assay to assess sensitivity to MMS in the presence or absence of hRad51 Fabs. Colonies were allowed to grow for 7 days and were enumerated by light microscopy. Although the number of colony-forming unit (cfu) was not changed significantly when HEK293T cells were treated with FabItag I_2 alone, a decreasing trend in the number of cfus was observed when HEK293T cells were treated with FabItag I_2 and MMS. Moreover, 10 and 40 μM FabItag I_2 in combination with MMS significantly inhibited colony formation, indicating that FabItag I_2 enhances the cell sensitivity to MMS (**Figure 5.21**).

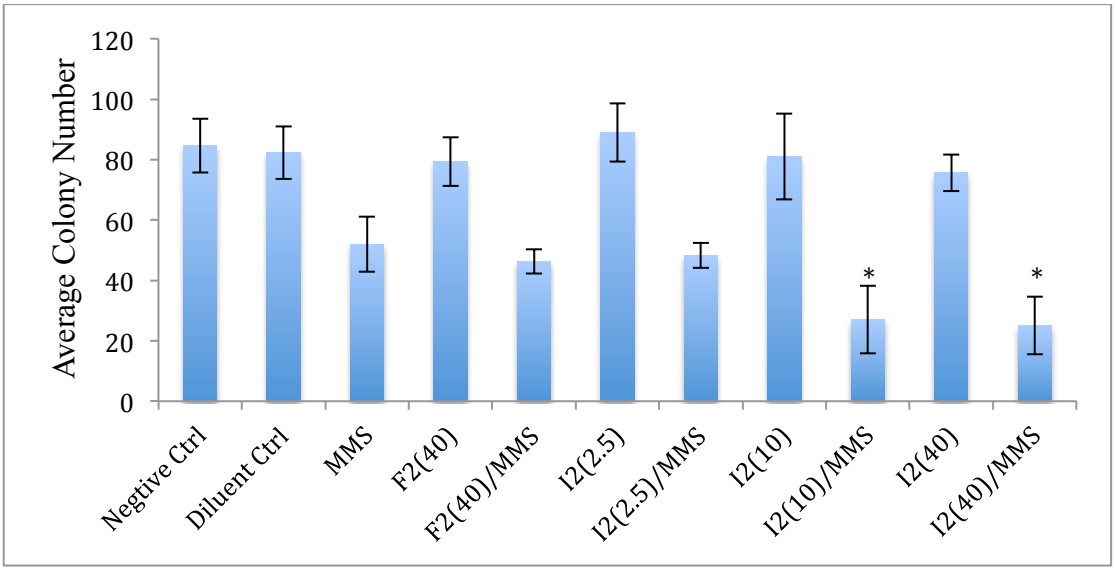

Figure 5.21 Anti-hRad51 FabItag I_2 Sensitizes HEK293T Cell to Methyl Methanesulfonate

HEK293T were treated with methyl methanesulfonate (MMS) alone, or in combination with Fab F_2 (or FabItag I_2) with indicated concentration in parentheses (μM). Cells were cultured for 7 days and colonies were stained with 0.3% crystal violent and enumerated by light microscopy. Cells without addition or with PBS addition were used as negative and diluent control, respectively. Error bars represent standard deviation from three independent measurements.

Chapter 6 Discussion

Approximately 40% of Canadians are expected to develop cancer during their lifetimes and chemotherapy is currently the predominant therapeutic strategy for many cancer treatments (www.cancer.ca). The efficacy of many chemotherapeutics is based on damaging the DNA of cancer cells by inducing adducts or single- or double-strand breaks (DSBs) in DNA. However, in ~50% of cases cancer cells survive the chemotherapy via varieties of mechanisms, including upregulation of DNA repair proteins (Hannay *et al.*, 2007). It was reported that hRad51, a central DNA repair and recombinase factor in homologous recombination (HR), is almost ubiquitously overexpressed in cancer cells (Maacke, Jost*, et al.*, 2000; Hannay *et al.*, 2007; Klein, 2008). hRad51 overexpression is implicated with the required drug resistance after chemotherapy (Vispe *et al.*, 1998). Therefore, targeted inhibition of hRad51 has been explored as a way to enhance the anticancer activity of the chemotherapeutics and slow down drug resistance.

Although several small molecule hRad51 inhibitors have been isolated by screening large collections of commercialized chemical compounds, most of them are limited to *in vitro* applications. The aim of this thesis work was to generate a specific antibody with high affinity to hRad51 because target-specific antibodies are reported to have the potential to neutralize antigen proteins *in vivo* (Antman and Livingston, 1980). We used phage display as a central technique to identify anti-hRad51 antibodies because this technique can generate specific antibodies more efficiently and cost-effectively compared to conventional mouse hybridoma technique. Although antibody library diversities may be impaired as a result from loss of DNA during library construction, the final antibody library - by virtue of its ability to screen up to 10^{10} phage to select those with antigen binding – offers sufficient depth of coverage to find antigen-specific antibodies even if they are rare in the natural repertoire.

To generate Fabs using phage display, we first expressed and purified hRad51. In our initial attempts, we found that hRad51 was expressed at very high levels in BL21-DE3, however most of the expressed protein was found in inclusion bodies. The remaining soluble protein resulted in relatively low yield. In order to increase the yield of soluble protein from bacteria we used Rosetta (DE3) *E. coli* for hRad51 expression under different IPTG induction conditions. Rosetta (DE3) strain is BL21 derivative designed to enhance the expression of

eukaryotic proteins that contain codons rarely used in *E. coli*. Using this strain, more than 90% of the protein was still found in the insoluble fraction. However, the soluble fraction contained 2-4 mg of protein per 900 mL of bacterial culture. The DNA binding and ATPase activities of hRad51 were characterized, confirming the correct hRad51 activity.

After four rounds of antibody phage selection, approximately one thousand unique potential binders were retained from the *naïve* Fab library containing 10^9 -10^{10} different clones. A great majority of initial clones that do not bind to the target protein or any other components of the screening system were removed during multiple washing steps. However, the selected binders may still represent false positive clones binding to other components of the screening system that predominate during rounds of panning selection. Those false positive clones can be classified as selection-related target-unrelated clones, and were categorized into three main groups in our study, including contaminants in the target sample, solid phase (Maxisorp plate) and propagation-related target-unrelated clones. One possible explanation for the presence of non-specific binders is the presence of impurities in the target protein preparations, such as cell debris including DNA, protein aggregates or other components of cell growth media. A second possibility for non-specific binders is that to some extent virtually all proteins or non-protein targets absorb nonspecifically and noncovalently to polystyrene surfaces of Maxsorp plate via hydrogen bonds and nonpolar interactions (Adey *et al.*, 1995). Likewise, phage clones displaying certain Fab fragments show greater affinity for plastic surface. To prevent interactions between library phage and solid surface, we blocked the target-immobilized surface with BSA. However, blocking unoccupied surfaces did not necessarily prevent the predominance of background binders. For example, peptide YSYY-HAYYAGGSSHYYYYYGMDV (from NGS cluster 1) has the highest enrichment in frequency from round three to round four. However, this peptide is thought as a background binder because it has been isolated by several members in our lab from the same Fab-library using completely different target proteins. Another possibility is that some phage clones predominate because of their advantage in propagation that allows them to outgrow other clones in the pool. Therefore, recovery of such non-specific clones is independent of their affinity binding to the target. During the panning, we concluded that for some clones the faster propagation was because a small DNA fragment was deleted in the phagemid, which might be shortening the DNA replication time, accelerating the process of phage particle assembly.

Within three or four rounds of selection, these clones predominated although they were not related to hRad51 or even more, they lose the capability to correctly express Fab on the surface of phage particles (**Figure 5.6**).

The next aim of this thesis was to characterize the specificity and affinity of the Fab to hRad51 selected during the phage display selection using recombinant hRad51 as target. Three potential phage clones (F_1, F_2 and F_3) were predominant from numerous background clones after several rounds of panning selection. Sequence analysis showed that these three phage clones came from those three predominant clusters identified by NGS. However, kinetic assay showed that only Fab F_2 possesses high binding affinity for hRad51. When comparing the kinetic assay with NGS results, there was some correlation. The Fab (GTYL-TYSYASRGWYFDY from cluster 2) that had a higher frequency was more likely to bind hRad51 compared to the Fab from cluster 3 (SYSY-YYHYVYGYYSSPYYYDY). This result suggests that following phage display selection with NGS analysis can accelerate the identification of specific antibodies.

Because hRad51 mediated homologous recombination involves two hRad51 domains, a ssDNA and dsDNA binding N-terminal domain and an ATP binding C-terminal domain (Aihara *et al.*, 1999), we can inhibit hRad51 by targeting its DNA binding site and ATPase activity. The DNA binding assay showed that Fab F_2 inhibited hRad51 DNA binding activity, indicating that Fab F_2 might bind near the DNA binding sites of hRad51.

When analyzing the ATPase activity of hRad51, we found that the ATPase activity was not inhibited by Fab F_2 in either the presence or absence of DNA. One possible explanation could be that, for panning selection, we employed the most straightforward approach to immobilize antigen where hRad51 protein was directly absorbed onto the surface of Maxisorp plate. This approach does not depend on any protein modification, but requires some conformational change of protein. When the protein is absorbed to the Maxisorp plate surface, it exposes hydrophobic residues toward the plastic (Butler *et al.*, 1992). Crystal structure of a *Saccharomyces cerevisiae* Rad51, sharing conserved core domain with hRad51, shows that ATPase site is located at the interface between two protomers (Conway *et al.*, 2004). It is highly possible that the ATPase site is hidden from exposure or changed conformation to some extend when immobilized onto plate. Therefore, the antibody raised in the panning selection may not recognize the ATPase active site. The fact that hRad51 was denatured and recognized

by Fab F_2 in the Western analysis might also indicated that Fab F_2 recognizes an structural epitope in hRad51 rather than a conformational epitope in hRad51.

As part of the *in vitro* characterization of Fab F_2 in this thesis work, we have demonstrated the specificity, affinity and the inhibitory effects of Fab F_2 on hRad51. However, if anti-hRad51 antibodies were to elicit their effects, they should be able to cross mammalian cell membrane in order to physically interact with hRad51. To test the efficacy of Fab F_2 to inhibit the hRad51 activity intracellularly, we used clonogenic survival assay to monitor the cell response to DNA damage. First, we cloned the CDR sequences from Fab F_2 into a mammalian expression vector in a scFv format in which the VH and VL domains are joined with a flexible polypeptide linker preventing dissociation. The scFv was cloned into a mammalian expression vector as a fusion to an Fc (crystallisable fragment) domain, designated DNA837 plasmid. Western analysis confirmed the expression of anti-hRad51 scFv-Fc from DNA837 in HEK293T cells. The number of colony-forming unit (cfu) was significantly decreased when HEK293T cells were transfected with DNA837 in the absence of MMS, indicating that anti-hRad51 scFv-Fc alone can inhibit HEK293T cell proliferation. Moreover, DNA837-transfected HEK293T cells became significantly more sensitive to low concentration of MMS. High concentration of MMS in combination with DNA837 completely inhibited HEK293T colony formation. These results indicate that anti-hRad51 scFv-Fc can significantly potentiate the activity MMS to inhibit the cell proliferation.

Despite the insights that the above clonogenic survival assay has provided for anti-hRad51 antibody, expressing antibodies inside cells is inconvenient for application. For intracellular antibody to become a broadly applicable technology it requires a direct means of introducing antibodies into large cell populations. However, because of the selective permeability of the cell membrane, a larger molecule like a Fab is not able to cross the cell membrane under normal conditions. Therefore, a delivery system to transport Fabs inside cells is necessary. To achieve this goal, Fab F_2 was fused with a membrane import tag designated as FabItag I_2. Itag shows intracellular protein transduction properties when fused to a protein (Patent No. WO 2014005219 A1). It consists of a secretion signal peptide sequence in combination with a cleavage inhibition sequence. This combination efficiently blocks cleavage of secretion signal peptide in a recombinant protein and also halts secretion of the protein from a cell. Moreover, Itag can work efficiently as a protein transduction domain when the secretion

signal peptide sequence precedes the cleavage inhibition sequence in an N- to C-terminus direction. Although a particular theory for the superior transduction efficiency is unknown, it appears that the intracellular delivery is achieved through receptors in a recipient cell surface. BLI binding analysis showed that FabItag I_2 retained Fab F_2 affinity to hRad51, indicating that the binding capacity of a Fab was not affected by the fusion of Itag. In order to ensure that FabItag I_2 crosses the cell membrane, HEK293T cells were incubated with IRDye® 800CW dye-labeled FabItag I_2 and signal detected by fluorescent microscopy. The results show that FabItag I_2 started internalization into HEK293T cells after 8 hours and accumulated inside cytoplasm after 24 hours. In agreement with this result, quantitative analysis using flow cytometry indicated that Itag significantly promotes intracellular protein transduction efficiency. Importantly, clonogenic survival assays showed that when HEK293T cells were treated with FabItag I_2 and MMS simultaneously, the number of colony formed decreased significantly. Since colony formation is a measure of cell proliferation, this result indicates that anti-hRad51 antibody may have the ability to sensitize those cancer cells with hRad51 overexpression to DNA damaging therapies.

Recently several hRad51 inhibitors were reported to exhibit inhibitory effect on the biochemical activities of hRad51 (Ishida *et al.*, 2009; Takaku *et al.*, 2011; Budke *et al.*, 2012; Budke *et al.*, 2013). However, their *in vivo* experiments were not continued either because of inhibitor non-specificity or high cellular toxicity. In this project, we developed more potent, specific, and less toxic anti-Rad51 antibody using phage display technology. Our data demonstrate that anti-hRad51 antibody potentiates the anti-cancer activity of MMS *in vivo*. Although more experiments are needed for anti-hRad51 antibody in hRad51 overexpressing cancer cells, our data have shown that anti-hRad51 antibody has the potential to improve the efficacy of chemotherapies of cancer and development of novel combination cancer therapies.

From the methodology perspective, we have demonstrated a number of things in this project. First, we show that phage display technology is feasible and efficient to discover novel inhibitors for intracellular targets. Second, phage display combined with NGS and BLI analysis significantly accelerates the selection process, which can provide an insight to establish standard protocol for discovery of antibody inhibitors. Third, we provide evidence that Fab can be introduced into the cytosol from outside the cell by fusing Fab to a protein transduction

domain, and function as intracellular inhibitors of protein activity. The techniques described in development of these Fabs could be transferable to a variety of intracellular targets.

Chapter 7 Conclusions and Future Directions

hRad51 protein was successfully over-expressed, purified from *E. coli* Rosetta (DE3) cells using nickel affinity column. Combined with technology of NGS, we were able to select a hRad51 specific Fab F_2 from a large synthetic Fab-phage library (~$1x10^{10}$ independent clones) using phage display technology. We found that Fab F_2 has high binding affinity and specificity to hRad51. *In vitro* ATPase studies showed that Fab F_2 does not inhibit hRad51 ATPase activity in the presence or absence of DNA. However, DNA binding assay showed that Fab F_2 inhibits hRad51 DNA binding activity, indicating that Fab F_2 may bind near the DNA binding sites of hRad51. In addition, we cloned the CDR sequences from Fab F_2 into a mammalian expression vector as a format of scFv-Fc. Clonogenic survival assay showed that anti-hRad51 scFv-Fc increases sensitivity of HEK293T cells to DNA-damage agent MMS. Importantly, we were able to transport Fab across the cell membrane into cytoplasm by fusing Fab into a membrane import tag. We found that anti-hRad51 Fab F_2 significantly increased the sensitivity of HEK293T cells to MMS.

Despite the encouraging results, many questions could be addressed for the future improvements. First, the yield of recombinant hRad51 protein is relatively low until *E. coli* Rosetta (DE3) is used for protein expression. Also DNA may remain bound hRad51 protein during purification. The expression conditions and purification procedures need to be optimized. We can try a wide spectrum of bacterial strains, like BL21(DE3)-pLysS, BL21 Star-pLysS, or Rosetta pLysS, to determine which strain produces the best yield of recombinant hRad51. Besides, after the cell pellet was homogenized but before nickel affinity purification, DNase enzyme should be added into hRad51 protein solution to degrade any remaining bacterial DNA in the solution.

Furthermore, direct absorption of the purified hRad51 on a Maxisorp plate may change the original protein conformation. As was investigated in this study, hRad51 ATP binding site may be hidden from exposure or changed conformation to some extend when immobilized onto plate. To address this question, we can try to covalently immobilize hRad51 to the solid phase using chemistry reactive on accessible lysine at the protein surface. Alternatively, we can perform selection against biotinylated antigen to avoid the adsorption process as described previously by Habicht (Habicht *et al.*, 2007). Both approaches have the potential to select

hRad51 specific binders able to bind a structural epitope of the target.

Since the membrane import tag from iProgen significantly promotes Fab F_2 transduction efficiency into HEK293T cells, studies should be performed to investigate the internalization of Fab across a wider spectrum of cancer cell lines. Also intracellular effects of Fab F_2 in hRad51-related cancer cells should be investigated, such as breast cancer, pancreatic cancer, head and neck, invasive breast cancer as well as non-small cell lung cancer. Since these cancer cells are all reported to exhibit elevated levels of hRad51 expression, and hRad51 is the target of Fab F_2, the activity of Fab F_2 in these cells are worth investigation.

Finally, the intracellular activity of other forms of anti-hRad51 antibody should be investigated. As was performed in this study, when CDR sequences from Fab F_2 were cloned into a mammalian expression plasmid in an scFv-Fc format followed by expression inside HEK293T cells, the cells exhibited elevated sensitivity to DNA-damaging agent. Although we have difficulties in producing scFv-Fc with a protein transduction domain in mammalian cells, we can try to engineer smaller antibody fragment scFv to improve production in bacterial expression system. Similar to scFv-Fc, scFv can increase antibody stability in a reducing intracellular environment by avoiding the formation of inter-molecular disulfide-bonds. It is likely chemotherapy will benefit more from anti-hRad51 scFv.

Chapter 8 References

Adey, N.B., Mataragnon, A.H., Rider, J.E., Carter, J.M., and Kay, B.K. (1995). Characterization of phage that bind plastic from phage-displayed random peptide libraries. Gene *156*, 27-31.

Adimoolam, S., Sirisawad, M., Chen, J., Thiemann, P., Ford, J.M., and Buggy, J.J. (2007). HDAC inhibitor PCI-24781 decreases RAD51 expression and inhibits homologous recombination. Proceedings of the National Academy of Sciences of the United States of America *104*, 19482-19487.

Aihara, H., Ito, Y., Kurumizaka, H., Yokoyama, S., and Shibata, T. (1999). The N-terminal domain of the human Rad51 protein binds DNA: structure and a DNA binding surface as revealed by NMR. Journal of molecular biology *290*, 495-504.

Anderson, D.C., Nichols, E., Manger, R., Woodle, D., Barry, M., and Fritzberg, A.R. (1993). Tumor cell retention of antibody Fab fragments is enhanced by an attached HIV TAT protein-derived peptide. Biochemical and biophysical research communications *194*, 876-884.

Antman, K.H., and Livingston, D.M. (1980). Intracellular neutralization of SV40 tumor antigens following microinjection of specific antibody. Cell *19*, 627-635.

Aplan, P.D. (2006). Causes of oncogenic chromosomal translocation. Trends in genetics : TIG *22*, 46-55.

Arias-Lopez, C., Lazaro-Trueba, I., Kerr, P., Lord, C.J., Dexter, T., Iravani, M., Ashworth, A., and Silva, A. (2006). p53 modulates homologous recombination by transcriptional regulation of the RAD51 gene. EMBO reports *7*, 219-224.

Arkin, M.R., and Wells, J.A. (2004). Small-molecule inhibitors of protein-protein interactions: progressing towards the dream. Nature reviews. Drug discovery *3*, 301-317.

Ashworth, A. (2008). A synthetic lethal therapeutic approach: poly(ADP) ribose polymerase inhibitors for the treatment of cancers deficient in DNA double-strand break repair. Journal of clinical oncology : official journal of the American Society of Clinical Oncology *26*, 3785-3790.

Ayriss, J., Woods, T., Bradbury, A., and Pavlik, P. (2007). High-throughput screening of single-chain antibodies using multiplexed flow cytometry. J Proteome Res *6*, 1072-1082.

Baker, K.P., Edwards, B.M., Main, S.H.*, et al.* (2003). Generation and characterization of LymphoStat-B, a human monoclonal antibody that antagonizes the bioactivities of B lymphocyte stimulator. Arthritis Rheum *48*, 3253-3265.

Barbano, R., Copetti, M., Perrone, G.*, et al.* (2011). High RAD51 mRNA expression characterize estrogen receptor-positive/progesteron receptor-negative breast cancer and is associated with patient's outcome. International journal of cancer. Journal international du cancer *129*, 536-545.

Barbas, C.F., 3rd (1995). Synthetic human antibodies. Nat Med *1*, 837-839.

Barbas, C.F., 3rd, Bain, J.D., Hoekstra, D.M., and Lerner, R.A. (1992). Semisynthetic combinatorial antibody libraries: a chemical solution to the diversity problem. Proc Natl Acad Sci U S A *89*, 4457-4461.

Barbas, C.F., 3rd, and Burton, D.R. (1996). Selection and evolution of high-affinity human anti-viral antibodies. Trends Biotechnol *14*, 230-234.

Barbas, C.F., 3rd, Kang, A.S., Lerner, R.A., and Benkovic, S.J. (1991). Assembly of combinatorial antibody libraries on phage surfaces: the gene III site. Proc Natl Acad Sci U S A *88*, 7978-7982.

Barbas, C.F., 3rd, Languino, L.R., and Smith, J.W. (1993). High-affinity self-reactive human antibodies by design and selection: targeting the integrin ligand binding site. Proc Natl Acad Sci U S A *90*, 10003-10007.

Baumann, P., Benson, F.E., and West, S.C. (1996). Human Rad51 protein promotes ATP-dependent homologous pairing and strand transfer reactions in vitro. Cell *87*, 757-766.

Bearss, D.J., Lee, R.J., Troyer, D.A., Pestell, R.G., and Windle, J.J. (2002). Differential effects of p21(WAF1/CIP1) deficiency on MMTV-ras and MMTV-myc mammary tumor properties. Cancer research *62*, 2077-2084.

Benson, F.E., Stasiak, A., and West, S.C. (1994). Purification and characterization of the human Rad51 protein, an analogue of E. coli RecA. The EMBO journal *13*, 5764-5771.

Bertrand, P., Lambert, S., Joubert, C., and Lopez, B.S. (2003). Overexpression of mammalian Rad51 does not stimulate tumorigenesis while a dominant-negative Rad51 affects centrosome fragmentation, ploidy and stimulates tumorigenesis, in p53-defective CHO cells. Oncogene *22*, 7587-7592.

Better, M., Chang, C.P., Robinson, R.R., and Horwitz, A.H. (1988). Escherichia coli secretion of an active chimeric antibody fragment. Science *240*, 1041-1043.

Biocca, S., Neuberger, M.S., and Cattaneo, A. (1990). Expression and targeting of intracellular antibodies in mammalian cells. The EMBO journal *9*, 101-108.

Birtalan, S., Zhang, Y., Fellouse, F.A., Shao, L., Schaefer, G., and Sidhu, S.S. (2008). The intrinsic contributions of tyrosine, serine, glycine and arginine to the affinity and specificity of antibodies. J Mol Biol *377*, 1518-1528.

Bishop, A.J., and Schiestl, R.H. (2003). Role of homologous recombination in carcinogenesis. Experimental and molecular pathology *74*, 94-105.

Bjorklund, J., Biverstahl, H., Graslund, A., Maler, L., and Brzezinski, P. (2006). Real-time transmembrane translocation of penetratin driven by light-generated proton pumping. Biophysical journal *91*, L29-31.

Blasiak, J., Przybylowska, K., Czechowska, A., Zadrozny, M., Pertynski, T., Rykala, J., Kolacinska, A., Morawiec, Z., and Drzewoski, J. (2003). Analysis of the G/C polymorphism in the 5'-untranslated region of the RAD51 gene in breast cancer. Acta biochimica Polonica *50*, 249-253.

Bond, C.J., Wiesmann, C., Marsters, J.C., Jr., and Sidhu, S.S. (2005). A structure-based database of antibody variable domain diversity. J Mol Biol *348*, 699-709.

Bouvet, J.P. (1994). Immunoglobulin Fab fragment-binding proteins. International journal of immunopharmacology *16*, 419-424.

Bradbury, A.R., and Marks, J.D. (2004). Antibodies from phage antibody libraries. J Immunol Methods *290*, 29-49.

Brooks, H., Lebleu, B., and Vives, E. (2005). Tat peptide-mediated cellular delivery: back to basics. Advanced drug delivery reviews *57*, 559-577.

Budke, B., Kalin, J.H., Pawlowski, M., Zelivianskaia, A.S., Wu, M., Kozikowski, A.P., and Connell, P.P. (2013). An optimized RAD51 inhibitor that disrupts homologous recombination without requiring Michael acceptor reactivity. Journal of medicinal chemistry *56*, 254-263.

Budke, B., Logan, H.L., Kalin, J.H., Zelivianskaia, A.S., Cameron McGuire, W., Miller, L.L., Stark, J.M., Kozikowski, A.P., Bishop, D.K., and Connell, P.P. (2012). RI-1: a chemical inhibitor of RAD51 that disrupts homologous recombination in human cells. Nucleic acids research *40*, 7347-7357.

Butler, J.E., Ni, L., Nessler, R., Joshi, K.S., Suter, M., Rosenberg, B., Chang, J., Brown, W.R., and Cantarero, L.A. (1992). The physical and functional behavior of capture antibodies adsorbed on polystyrene. Journal of immunological methods *150*, 77-90.

Carlson, J.R. (1993). A new use for intracellular antibody expression: inactivation of human immunodeficiency virus type 1. Proceedings of the National Academy of Sciences of the United States of America *90*, 7427-7428.

Chen, B.X., and Erlanger, B.F. (2002). Intracellular delivery of monoclonal antibodies. Immunology letters *84*, 63-67.

Chen, B.X., and Erlanger, B.F. (2006). Cell cycle inhibition by an anti-cyclin D1 antibodychemically modified for intracellular delivery. Cancer letters *244*, 71-75.

Chen, F., Nastasi, A., Shen, Z., Brenneman, M., Crissman, H., and Chen, D.J. (1997). Cell cycle-dependent protein expression of mammalian homologs of yeast DNA double-strand break repair genes Rad51 and Rad52. Mutation research *384*, 205-211.

Christodoulopoulos, G., Malapetsa, A., Schipper, H., Golub, E., Radding, C., and Panasci, L.C. (1999). Chlorambucil induction of HsRad51 in B-cell chronic lymphocytic leukemia. Clinical cancer research : an official journal of the American Association for Cancer Research *5*, 2178-2184.

Cohen, B.A., Colas, P., and Brent, R. (1998). An artificial cell-cycle inhibitor isolated from a combinatorial library. Proceedings of the National Academy of Sciences of the United States of America *95*, 14272-14277.

Collis, S.J., Tighe, A., Scott, S.D., Roberts, S.A., Hendry, J.H., and Margison, G.P. (2001). Ribozyme minigene-mediated RAD51 down-regulation increases radiosensitivity of human prostate cancer cells. Nucleic acids research *29*, 1534-1538.

Connell, P.P., Jayathilaka, K., Haraf, D.J., Weichselbaum, R.R., Vokes, E.E., and Lingen, M.W. (2006). Pilot study examining tumor expression of RAD51 and clinical outcomes in human head cancers. International journal of oncology *28*, 1113-1119.

Conway, A.B., Lynch, T.W., Zhang, Y., Fortin, G.S., Fung, C.W., Symington, L.S., and Rice, P.A. (2004). Crystal structure of a Rad51 filament. Nature structural & molecular biology *11*, 791-796.

Cortes, J., Lipton, J.H., Rea, D., Digumarti, R., Chuah, C., Nanda, N., Benichou, A.C., Craig, A.R., Michallet, M., Nicolini, F.E., Kantarjian, H., and Omacetaxine 202 Study, G. (2012). Phase 2 study of subcutaneous omacetaxine mepesuccinate after TKI failure in patients with chronic-phase CML with T315I mutation. Blood *120*, 2573-2580.

Courtenay-Luck, N.S., Epenetos, A.A., Moore, R., Larche, M., Pectasides, D., Dhokia, B., and Ritter, M.A. (1986). Development of primary and secondary immune responses to mouse monoclonal antibodies used in the diagnosis and therapy of malignant neoplasms. Cancer Res *46*, 6489-6493.

den Broeder, A., van de Putte, L., Rau, R., Schattenkirchner, M., Van Riel, P., Sander, O., Binder, C., Fenner, H., Bankmann, Y., Velagapudi, R., Kempeni, J., and Kupper, H. (2002). A single dose, placebo controlled study of the fully human anti-tumor necrosis factor-alpha antibody adalimumab (D2E7) in patients with rheumatoid arthritis. J Rheumatol *29*, 2288-2298.

Dickson, M.A., and Schwartz, G.K. (2009). Development of cell-cycle inhibitors for cancer therapy. Current oncology *16*, 36-43.

Dong, X., Stothard, P., Forsythe, I.J., and Wishart, D.S. (2004). PlasMapper: a web server for drawing and auto-annotating plasmid maps. Nucleic acids research *32*, W660-664.

Du, L.Q., Du, X.Q., Bai, J.Q., Wang, Y., Yang, Q.S., Wang, X.C., Zhao, P., Wang, H., Liu, Q., and Fan, F.Y. (2012). Methotrexate-mediated inhibition of RAD51 expression and homologous recombination in cancer cells. Journal of cancer research and clinical oncology *138*, 811-818.

Duchardt, F., Fotin-Mleczek, M., Schwarz, H., Fischer, R., and Brock, R. (2007). A comprehensive model for the cellular uptake of cationic cell-penetrating peptides. Traffic *8*, 848-866.

Edwards, B.M., Barash, S.C., Main, S.H., Choi, G.H., Minter, R., Ullrich, S., Williams, E., Du Fou, L., Wilton, J., Albert, V.R., Ruben, S.M., and Vaughan, T.J. (2003). The remarkable flexibility of the human antibody repertoire; isolation of over one thousand different antibodies to a single protein, BLyS. J Mol Biol *334*, 103-118.

Elbing, K.L., and Brent, R. (2001). Media preparation and bacteriological tools. Current protocols in protein science / editorial board, John E. Coligan ... [et al.] *Appendix 4*, Appendix 4A.

Essers, J., Hendriks, R.W., Swagemakers, S.M., Troelstra, C., de Wit, J., Bootsma, D., Hoeijmakers, J.H., and Kanaar, R. (1997). Disruption of mouse RAD54 reduces ionizing radiation resistance and homologous recombination. Cell *89*, 195-204.

Farmer, H., McCabe, N., Lord, C.J., Tutt, A.N., Johnson, D.A., Richardson, T.B., Santarosa, M., Dillon, K.J., Hickson, I., Knights, C., Martin, N.M., Jackson, S.P., Smith, G.C., and Ashworth, A. (2005). Targeting the DNA repair defect in BRCA mutant cells as a therapeutic strategy. Nature *434*, 917-921.

Fellouse, F.A., Wiesmann, C., and Sidhu, S.S. (2004). Synthetic antibodies from a four-amino-acid code: a dominant role for tyrosine in antigen recognition. Proc Natl Acad Sci U S A *101*, 12467-12472.

Ferguson, D.O., and Holloman, W.K. (1996). Recombinational repair of gaps in DNA is asymmetric in Ustilago maydis and can be explained by a migrating D-loop model. Proceedings of the National Academy of Sciences of the United States of America *93*, 5419-5424.

Fischer, N. (2011). Sequencing antibody repertoires: the next generation. mAbs *3*, 17-20.

Frisch, C., Brocks, B., Ostendorp, R., Hoess, A., von Ruden, T., and Kretzschmar, T. (2003). From EST to IHC: human antibody pipeline for target research. J Immunol Methods *275*, 203-212.

Fuchs, S.M., and Raines, R.T. (2004). Pathway for polyarginine entry into mammalian cells. Biochemistry *43*, 2438-2444.

Futaki, S. (2005). Membrane-permeable arginine-rich peptides and the translocation mechanisms. Advanced drug delivery reviews *57*, 547-558.

Futaki, S. (2006). Oligoarginine vectors for intracellular delivery: design and cellular-uptake mechanisms. Biopolymers *84*, 241-249.

Griffiths, A.D., Malmqvist, M., Marks, J.D., Bye, J.M., Embleton, M.J., McCafferty, J., Baier, M., Holliger, K.P., Gorick, B.D., Hughes-Jones, N.C., and et al. (1993). Human anti-self antibodies with high specificity from phage display libraries. EMBO J *12*, 725-734.

Gump, J.M., June, R.K., and Dowdy, S.F. (2010). Revised role of glycosaminoglycans in TAT protein transduction domain-mediated cellular transduction. The Journal of biological chemistry *285*, 1500-1507.

Habicht, G., Haupt, C., Friedrich, R.P., Hortschansky, P., Sachse, C., Meinhardt, J., Wieligmann, K., Gellermann, G.P., Brodhun, M., Gotz, J., Halbhuber, K.J., Rocken, C., Horn, U., and Fandrich, M. (2007). Directed selection of a conformational antibody domain that prevents mature amyloid fibril formation by stabilizing Abeta protofibrils. Proceedings of the National Academy of Sciences of the United States of America *104*, 19232-19237.

Hanahan, D., and Weinberg, R.A. (2000). The hallmarks of cancer. Cell *100*, 57-70.

Hannay, J.A., Liu, J., Zhu, Q.S., Bolshakov, S.V., Li, L., Pisters, P.W., Lazar, A.J., Yu, D., Pollock, R.E., and Lev, D. (2007). Rad51 overexpression contributes to chemoresistance in human soft tissue sarcoma cells: a role for p53/activator protein 2 transcriptional regulation. Molecular cancer therapeutics *6*, 1650-1660.

Hastings, P.J. (1988). Recombination in the eukaryotic nucleus. BioEssays : news and reviews in molecular, cellular and developmental biology *9*, 61-64.

Heng, B.C., and Cao, T. (2005). Making cell-permeable antibodies (Transbody) through fusion of protein transduction domains (PTD) with single chain variable fragment (scFv) antibodies: potential advantages over antibodies expressed within the intracellular environment (Intrabody). Medical hypotheses *64*, 1105-1108.

Hine, C.M., Li, H., Xie, L., Mao, Z., Seluanov, A., and Gorbunova, V. (2014). Regulation of Rad51 promoter. Cell cycle *13*, 2038-2045.

Hine CM, S.A., Gorbunova V. (2008). Use of the Rad51 promoter for targeted anti-cancer therapy. Proceedings of the National Academy of Sciences of the United States of America *105*, 20810-20815.

Hitz, T., Iten, R., Gardiner, J., Namoto, K., Walde, P., and Seebach, D. (2006). Interaction of alpha-and beta-oligoarginine-acids and amides with anionic lipid vesicles: a mechanistic and thermodynamic study. Biochemistry *45*, 5817-5829.

Hoogenboom, H.R. (2005). Selecting and screening recombinant antibody libraries. Nat Biotechnol *23*, 1105-1116.

Hoogenboom, H.R., and Winter, G. (1992). By-passing immunisation. Human antibodies from synthetic repertoires of germline VH gene segments rearranged in vitro. J Mol Biol *227*, 381-388.

Huang, F., Mazina, O.M., Zentner, I.J., Cocklin, S., and Mazin, A.V. (2012). Inhibition of homologous recombination in human cells by targeting RAD51 recombinase. Journal of medicinal chemistry *55*, 3011-3020.

Huang, F., Motlekar, N.A., Burgwin, C.M., Napper, A.D., Diamond, S.L., and Mazin, A.V. (2011). Identification of specific inhibitors of human RAD51 recombinase using high-throughput screening. ACS chemical biology *6*, 628-635.

Humphreys, D.P. (2003). Production of antibodies and antibody fragments in Escherichia coli and a comparison of their functions, uses and modification. Curr Opin Drug Discov Devel *6*, 188-196.

Ishida, T., Takizawa, Y., Kainuma, T., Inoue, J., Mikawa, T., Shibata, T., Suzuki, H., Tashiro, S., and Kurumizaka, H. (2009). DIDS, a chemical compound that inhibits RAD51-mediated homologous pairing and strand exchange. Nucleic acids research *37*, 3367-3376.

Ito, M., Yamamoto, S., Nimura, K., Hiraoka, K., Tamai, K., and Kaneda, Y. (2005). Rad51 siRNA delivered by HVJ envelope vector enhances the anti-cancer effect of cisplatin. The journal of gene medicine *7*, 1044-1052.

Jackson, A.L., Bartz, S.R., Schelter, J., Kobayashi, S.V., Burchard, J., Mao, M., Li, B., Cavet, G., and Linsley, P.S. (2003). Expression profiling reveals off-target gene regulation by RNAi. Nature biotechnology *21*, 635-637.

Jackson, A.L., and Linsley, P.S. (2010). Recognizing and avoiding siRNA off-target effects for target identification and therapeutic application. Nature reviews. Drug discovery *9*, 57-67.

Jackson, S.P., and Bartek, J. (2009). The DNA-damage response in human biology and disease. Nature *461*, 1071-1078.

Jalal, S., Earley, J.N., and Turchi, J.J. (2011). DNA repair: from genome maintenance to biomarker and therapeutic target. Clinical cancer research : an official journal of the American Association for Cancer Research *17*, 6973-6984.

Jespers, L., Schon, O., James, L.C., Veprintsev, D., and Winter, G. (2004). Crystal structure of HEL4, a soluble, refoldable human V(H) single domain with a germ-line scaffold. J Mol Biol *337*, 893-903.

Judge, A.D., Sood, V., Shaw, J.R., Fang, D., McClintock, K., and MacLachlan, I. (2005). Sequence-dependent stimulation of the mammalian innate immune response by synthetic siRNA. Nature biotechnology *23*, 457-462.

Kabir, M.E., Krishnaswamy, S., Miyamoto, M., Furuichi, Y., and Komiyama, T. (2009). An improved phage-display panning method to produce an HM-1 killer toxin anti-idiotypic antibody. BMC biotechnology *9*, 99.

Kachhap, S.K., Rosmus, N., Collis, S.J., Kortenhorst, M.S., Wissing, M.D., Hedayati, M., Shabbeer, S., Mendonca, J., Deangelis, J., Marchionni, L., Lin, J., Hoti, N., Nortier, J.W., DeWeese, T.L., Hammers, H., and Carducci, M.A. (2010). Downregulation of homologous recombination DNA repair genes by HDAC inhibition in prostate cancer is mediated through the E2F1 transcription factor. PloS one *5*, e11208.

Kameyama, S., Okada, R., Kikuchi, T., Omura, T., Nakase, I., Takeuchi, T., Sugiura, Y., and Futaki, S. (2006). Distribution of immunoglobulin Fab fragment conjugated with HIV-1 REV peptide following intravenous administration in rats. Molecular pharmaceutics *3*, 174-180.

Kato, M., Yano, K., Matsuo, F., Saito, H., Katagiri, T., Kurumizaka, H., Yoshimoto, M., Kasumi, F., Akiyama, F., Sakamoto, G., Nagawa, H., Nakamura, Y., and Miki, Y. (2000). Identification of Rad51 alteration in patients with bilateral breast cancer. Journal of human genetics *45*, 133-137.

Kiyohara, E., Tamai, K., Katayama, I., and Kaneda, Y. (2012). The combination of chemotherapy with HVJ-E containing Rad51 siRNA elicited diverse anti-tumor effects and synergistically suppressed melanoma. Gene therapy *19*, 734-741.

Klein, H.L. (2008). The consequences of Rad51 overexpression for normal and tumor cells. DNA repair *7*, 686-693.

Knappik, A., Ge, L., Honegger, A., Pack, P., Fischer, M., Wellnhofer, G., Hoess, A., Wolle, J., Pluckthun, A., and Virnekas, B. (2000). Fully synthetic human combinatorial antibody libraries (HuCAL) based on modular consensus frameworks and CDRs randomized with trinucleotides. J Mol Biol *296*, 57-86.

Kowalczykowski, S.C. (1991). Biochemistry of genetic recombination: energetics and mechanism of DNA strand exchange. Annual review of biophysics and biophysical chemistry *20*, 539-575.

Krejci, L., Altmannova, V., Spirek, M., and Zhao, X. (2012). Homologous recombination and its regulation. Nucleic acids research *40*, 5795-5818.

Krogh, B.O., and Symington, L.S. (2004). Recombination proteins in yeast. Annual review of genetics *38*, 233-271.

Kunkel, T.A., Roberts, J.D., and Zakour, R.A. (1987). Rapid and efficient site-specific mutagenesis without phenotypic selection. Methods in enzymology *154*, 367-382.

Laemmli, U.K. (1970). Cleavage of structural proteins during the assembly of the head of bacteriophage T4. Nature *227*, 680-685.

Lee, C.V., Liang, W.C., Dennis, M.S., Eigenbrot, C., Sidhu, S.S., and Fuh, G. (2004). High-affinity human antibodies from phage-displayed synthetic Fab libraries with a single framework scaffold. J Mol Biol *340*, 1073-1093.

Lengauer, C., Kinzler, K.W., and Vogelstein, B. (1998). Genetic instabilities in human cancers. Nature *396*, 643-649.

Lin, F.L., Sperle, K., and Sternberg, N. (1984). Model for homologous recombination during transfer of DNA into mouse L cells: role for DNA ends in the recombination process. Molecular and cellular biology *4*, 1020-1034.

Lloyd, C., Lowe, D., Edwards, B., Welsh, F., Dilks, T., Hardman, C., and Vaughan, T. (2009). Modelling the human immune response: performance of a 1011 human antibody repertoire against a broad panel of therapeutically relevant antigens. Protein Eng Des Sel *22*, 159-168.

Lundin, C., Schultz, N., Arnaudeau, C., Mohindra, A., Hansen, L.T., and Helleday, T. (2003). RAD51 is involved in repair of damage associated with DNA replication in mammalian cells. Journal of molecular biology *328*, 521-535.

Maacke, H., Hundertmark, C., Miska, S., Voss, M., Kalthoff, H., and Sturzbecher, H.W. (2002). Autoantibodies in sera of pancreatic cancer patients identify recombination factor Rad51 as a tumour-associated antigen. Journal of cancer research and clinical oncology *128*, 219-222.

Maacke, H., Jost, K., Opitz, S., Miska, S., Yuan, Y., Hasselbach, L., Luttges, J., Kalthoff, H., and Sturzbecher, H.W. (2000). DNA repair and recombination factor Rad51 is over-expressed in human pancreatic adenocarcinoma. Oncogene *19*, 2791-2795.

Maacke, H., Opitz, S., Jost, K., Hamdorf, W., Henning, W., Kruger, S., Feller, A.C., Lopens, A., Diedrich, K., Schwinger, E., and Sturzbecher, H.W. (2000). Over-expression of wild-type Rad51 correlates with histological grading of invasive ductal breast cancer. International journal of cancer. Journal international du cancer *88*, 907-913.

Mae, M., and Langel, U. (2006). Cell-penetrating peptides as vectors for peptide, protein and oligonucleotide delivery. Current opinion in pharmacology *6*, 509-514.

Magzoub, M., Pramanik, A., and Graslund, A. (2005). Modeling the endosomal escape of cell-penetrating peptides: transmembrane pH gradient driven translocation across phospholipid bilayers. Biochemistry *44*, 14890-14897.

Malkova, A., Ivanov, E.L., and Haber, J.E. (1996). Double-strand break repair in the absence of RAD51 in yeast: a possible role for break-induced DNA replication. Proceedings of the National Academy of Sciences of the United States of America *93*, 7131-7136.

Marks, J.D., Hoogenboom, H.R., Bonnert, T.P., McCafferty, J., Griffiths, A.D., and Winter, G. (1991). By-passing immunization. Human antibodies from V-gene libraries displayed on phage. J Mol Biol *222*, 581-597.

Martinez, S.F., Renodon-Corniere, A., Nomme, J., Eveillard, D., Fleury, F., Takahashi, M., and Weigel, P. (2010). Targeting human Rad51 by specific DNA aptamers induces inhibition of homologous recombination. Biochimie *92*, 1832-1838.

McCabe, N., Turner, N.C., Lord, C.J., Kluzek, K., Bialkowska, A., Swift, S., Giavara, S., O'Connor, M.J., Tutt, A.N., Zdzienicka, M.Z., Smith, G.C., and Ashworth, A. (2006). Deficiency in the repair of DNA damage by homologous recombination and sensitivity to poly(ADP-ribose) polymerase inhibition. Cancer research *66*, 8109-8115.

Menendez, A., and Scott, J.K. (2005). The nature of target-unrelated peptides recovered in the screening of phage-displayed random peptide libraries with antibodies. Anal Biochem *336*, 145-157.

Mersmann, M., Meier, D., Mersmann, J., Helmsing, S., Nilsson, P., Graslund, S., Colwill, K., Hust, M., Dubel, S., and Consortium, S.G. (2010). Towards proteome scale antibody selections using phage display. New Biotechnology *27*, 118-128.

Moreland, N.J., Susanto, P., Lim, E., Tay, M.Y., Rajamanonmani, R., Hanson, B.J., and Vasudevan, S.G. (2012). Phage display approaches for the isolation of monoclonal antibodies against dengue virus envelope domain III from human and mouse derived libraries. International journal of molecular sciences *13*, 2618-2635.

Morrison, C., Shinohara, A., Sonoda, E., Yamaguchi-Iwai, Y., Takata, M., Weichselbaum, R.R., and Takeda, S. (1999). The essential functions of human Rad51 are independent of ATP hydrolysis. Molecular and cellular biology *19*, 6891-6897.

Moynahan, M.E., and Jasin, M. (2010). Mitotic homologous recombination maintains genomic stability and suppresses tumorigenesis. Nature reviews. Molecular cell biology *11*, 196-207.

Muller, S., Zhao, Y., Brown, T.L., Morgan, A.C., and Kohler, H. (2005). TransMabs: cell-penetrating antibodies, the next generation. Expert opinion on biological therapy *5*, 237-241.

Munshi, N.C., Hideshima, T., Carrasco, D., Shammas, M., Auclair, D., Davies, F., Mitsiades, N., Mitsiades, C., Kim, R.S., Li, C., Rajkumar, S.V., Fonseca, R., Bergsagel, L., Chauhan, D., and Anderson, K.C. (2004). Identification of genes modulated in multiple myeloma using genetically identical twin samples. Blood *103*, 1799-1806.

Nagathihalli, N.S., and Nagaraju, G. (2011). RAD51 as a potential biomarker and therapeutic target for pancreatic cancer. Biochimica et biophysica acta *1816*, 209-218.

Nassif, N., Penney, J., Pal, S., Engels, W.R., and Gloor, G.B. (1994). Efficient copying of nonhomologous sequences from ectopic sites via P-element-induced gap repair. Molecular and cellular biology *14*, 1613-1625.

Nelson, B., and Sidhu, S.S. Synthetic antibody libraries. Methods Mol Biol *899*, 27-41.

Niesner, U., Halin, C., Lozzi, L., Gunthert, M., Neri, P., Wunderli-Allenspach, H., Zardi, L., and Neri, D. (2002). Quantitation of the tumor-targeting properties of antibody fragments conjugated to cell-permeating HIV-1 TAT peptides. Bioconjugate chemistry *13*, 729-736.

Nilson, B.H., Solomon, A., Bjorck, L., and Akerstrom, B. (1992). Protein L from Peptostreptococcus magnus binds to the kappa light chain variable domain. The Journal of biological chemistry *267*, 2234-2239.

Nissim, A., Hoogenboom, H.R., Tomlinson, I.M., Flynn, G., Midgley, C., Lane, D., and Winter, G. (1994). Antibody fragments from a 'single pot' phage display library as immunochemical reagents. EMBO J *13*, 692-698.

Ohnishi, T., Taki, T., Hiraga, S., Arita, N., and Morita, T. (1998). In vitro and in vivo potentiation of radiosensitivity of malignant gliomas by antisense inhibition of the RAD51 gene. Biochemical and biophysical research communications *245*, 319-324.

Orr-Weaver, T.L., and Szostak, J.W. (1983). Yeast recombination: the association between double-strand gap repair and crossing-over. Proceedings of the National Academy of Sciences of the United States of America *80*, 4417-4421.

Orr-Weaver, T.L., Szostak, J.W., and Rothstein, R.J. (1981). Yeast transformation: a model system for the study of recombination. Proceedings of the National Academy of Sciences of the United States of America *78*, 6354-6358.

Pershad, K., Pavlovic, J.D., Graslund, S., Nilsson, P., Colwill, K., Karatt-Vellatt, A., Schofield, D.J., Dyson, M.R., Pawson, T., Kay, B.K., and McCafferty, J. (2010). Generating a panel of highly specific antibodies to 20 human SH2 domains by phage display. Protein Engineering Design & Selection *23*, 279-288.

Poungpair, O., Pootong, A., Maneewatch, S., Srimanote, P., Tongtawe, P., Songserm, T., Tapchaisri, P., and Chaicumpa, W. (2010). A human single chain transbody specific to matrix protein (M1) interferes with the replication of influenza A virus. Bioconjugate chemistry *21*, 1134-1141.

Prochiantz, A. (2000). Messenger proteins: homeoproteins, TAT and others. Current opinion in cell biology *12*, 400-406.

Qiao, G.B., Wu, Y.L., Yang, X.N., Zhong, W.Z., Xie, D., Guan, X.Y., Fischer, D., Kolberg, H.C., Kruger, S., and Stuerzbecher, H.W. (2005). High-level expression of Rad51 is an independent prognostic marker of survival in non-small-cell lung cancer patients. British journal of cancer *93*, 137-143.

Radding, C.M. (1991). Helical interactions in homologous pairing and strand exchange driven by RecA protein. The Journal of biological chemistry *266*, 5355-5358.

Raderschall, E., Stout, K., Freier, S., Suckow, V., Schweiger, S., and Haaf, T. (2002). Elevated levels of Rad51 recombination protein in tumor cells. Cancer research *62*, 219-225.

Rajan, S., and Sidhu, S.S. (2012). Simplified synthetic antibody libraries. Methods in enzymology *502*, 3-23.

Richard, J.P., Melikov, K., Vives, E., Ramos, C., Verbeure, B., Gait, M.J., Chernomordik, L.V., and Lebleu, B. (2003). Cell-penetrating peptides. A reevaluation of the mechanism of cellular uptake. The Journal of biological chemistry *278*, 585-590.

Richardson, C., and Jasin, M. (2000). Frequent chromosomal translocations induced by DNA double-strand breaks. Nature *405*, 697-700.

Richardson, C., Moynahan, M.E., and Jasin, M. (1998). Double-strand break repair by interchromosomal recombination: suppression of chromosomal translocations. Genes & development *12*, 3831-3842.

Ristic, D., Modesti, M., van der Heijden, T., van Noort, J., Dekker, C., Kanaar, R., and Wyman, C. (2005). Human Rad51 filaments on double- and single-stranded DNA: correlating regular and irregular forms with recombination function. Nucleic acids research *33*, 3292-3302.

Roovers, R.C., van der Linden, E., Zijlema, H., de Bruine, A., Arends, J.W., and Hoogenboom, H.R. (2001). Evidence for a bias toward intracellular antigens in the local humoral anti-tumor immune response of a colorectal cancer patient revealed by phage display. Int J Cancer *93*, 832-840.

Rothbard, J.B., Jessop, T.C., Lewis, R.S., Murray, B.A., and Wender, P.A. (2004). Role of membrane potential and hydrogen bonding in the mechanism of translocation of guanidinium-rich peptides into cells. Journal of the American Chemical Society *126*, 9506-9507.

San Filippo, J., Sung, P., and Klein, H. (2008). Mechanism of eukaryotic homologous recombination. Annual review of biochemistry *77*, 229-257.

Schenone, S., Brullo, C., and Botta, M. (2010). New opportunities to treat the T315I-Bcr-Abl mutant in chronic myeloid leukaemia: tyrosine kinase inhibitors and molecules that act by alternative mechanisms. Current medicinal chemistry *17*, 1220-1245.

Shin, I., Edl, J., Biswas, S., Lin, P.C., Mernaugh, R., and Arteaga, C.L. (2005). Proapoptotic activity of cell-permeable anti-Akt single-chain antibodies. Cancer research *65*, 2815-2824.

Shinohara, A., Ogawa, H., Matsuda, Y., Ushio, N., Ikeo, K., and Ogawa, T. (1993). Cloning of human, mouse and fission yeast recombination genes homologous to RAD51 and recA. Nature genetics *4*, 239-243.

Short, S.C., Giampieri, S., Worku, M., Alcaide-German, M., Sioftanos, G., Bourne, S., Lio, K.I., Shaked-Rabi, M., and Martindale, C. (2011). Rad51 inhibition is an effective means of targeting DNA repair in glioma models and CD133+ tumor-derived cells. Neuro-oncology *13*, 487-499.

Slupianek, A., Hoser, G., Majsterek, I., Bronisz, A., Malecki, M., Blasiak, J., Fishel, R., and Skorski, T. (2002). Fusion tyrosine kinases induce drug resistance by stimulation of homology-dependent recombination repair, prolongation of G(2)/M phase, and protection from apoptosis. Molecular and cellular biology *22*, 4189-4201.

Smith, G.P. (1985). Filamentous fusion phage: novel expression vectors that display cloned antigens on the virion surface. Science *228*, 1315-1317.

Sonoda, E., Sasaki, M.S., Buerstedde, J.M., Bezzubova, O., Shinohara, A., Ogawa, H., Takata, M., Yamaguchi-Iwai, Y., and Takeda, S. (1998). Rad51-deficient vertebrate cells accumulate chromosomal breaks prior to cell death. The EMBO journal *17*, 598-608.

Stein, S., Weiss, A., Adermann, K., Lazarovici, P., Hochman, J., and Wellhoner, H. (1999). A disulfide conjugate between anti-tetanus antibodies and HIV (37-72)Tat neutralizes tetanus toxin inside chromaffin cells. FEBS letters *458*, 383-386.

Stocks, M. (2005). Intrabodies as drug discovery tools and therapeutics. Current opinion in chemical biology *9*, 359-365.

Strathern, J.N., Klar, A.J., Hicks, J.B., Abraham, J.A., Ivy, J.M., Nasmyth, K.A., and McGill, C. (1982). Homothallic switching of yeast mating type cassettes is initiated by a double-stranded cut in the MAT locus. Cell *31*, 183-192.

Sung, P., and Klein, H. (2006). Mechanism of homologous recombination: mediators and helicases take on regulatory functions. Nature reviews. Molecular cell biology *7*, 739-750.

Sung, P., and Robberson, D.L. (1995). DNA strand exchange mediated by a RAD51-ssDNA nucleoprotein filament with polarity opposite to that of RecA. Cell *82*, 453-461.

Takaku, M., Kainuma, T., Ishida-Takaku, T., Ishigami, S., Suzuki, H., Tashiro, S., van Soest, R.W., Nakao, Y., and Kurumizaka, H. (2011). Halenaquinone, a chemical compound that specifically inhibits the secondary DNA binding of RAD51. Genes to cells : devoted to molecular & cellular mechanisms *16*, 427-436.

Taki, T., Ohnishi, T., Yamamoto, A., Hiraga, S., Arita, N., Izumoto, S., Hayakawa, T., and Morita, T. (1996). Antisense inhibition of the RAD51 enhances radiosensitivity. Biochemical and biophysical research communications *223*, 434-438.

Tjandra, J.J., Ramadi, L., and McKenzie, I.F. (1990). Development of human anti-murine antibody (HAMA) response in patients. Immunol Cell Biol *68 (Pt 6)*, 367-376.

Tombline, G., Heinen, C.D., Shim, K.S., and Fishel, R. (2002). Biochemical characterization of the human RAD51 protein. III. Modulation of DNA binding by adenosine nucleotides. The Journal of biological chemistry *277*, 14434-14442.

Tonikian, R., Zhang, Y., Boone, C., and Sidhu, S.S. (2007). Identifying specificity profiles for peptide recognition modules from phage-displayed peptide libraries. Nature protocols *2*, 1368-1386.

Torchilin, V.P. (2008). Tat peptide-mediated intracellular delivery of pharmaceutical nanocarriers. Advanced drug delivery reviews *60*, 548-558.

Tsuzuki, T., Fujii, Y., Sakumi, K., Tominaga, Y., Nakao, K., Sekiguchi, M., Matsushiro, A., Yoshimura, Y., and MoritaT (1996). Targeted disruption of the Rad51 gene leads to lethality in embryonic mice. Proceedings of the National Academy of Sciences of the United States of America *93*, 6236-6240.

Vispe, S., Cazaux, C., Lesca, C., and Defais, M. (1998). Overexpression of Rad51 protein stimulates homologous recombination and increases resistance of mammalian cells to ionizing radiation. Nucleic acids research *26*, 2859-2864.

Wang, J.Y., Ho, T., Trojanek, J., Chintapalli, J., Grabacka, M., Stoklosa, T., Garcia, F.U., Skorski, T., and Reiss, K. (2005). Impaired homologous recombination DNA repair and enhanced sensitivity to DNA damage in prostate cancer cells exposed to anchorage-independence. Oncogene *24*, 3748-3758.

Ward, A., Khanna, K.K., and Wiegmans, A.P. (2015). Targeting homologous recombination, new pre-clinical and clinical therapeutic combinations inhibiting RAD51. Cancer treatment reviews *41*, 35-45.

Watters, D., Khanna, K.K., Beamish, H., Birrell, G., Spring, K., Kedar, P., Gatei, M., Stenzel, D., Hobson, K., Kozlov, S., Zhang, N., Farrell, A., Ramsay, J., Gatti, R., and Lavin, M. (1997). Cellular localisation of the ataxia-telangiectasia (ATM) gene product and discrimination between mutated and normal forms. Oncogene *14*, 1911-1921.

Wertman, K.F., Wyman, A.R., and Botstein, D. (1986). Host/vector interactions which affect the viability of recombinant phage lambda clones. Gene *49*, 253-262.

Wiegmans, A.P., Al-Ejeh, F., Chee, N., Yap, P.Y., Gorski, J.J., Da Silva, L., Bolderson, E., Chenevix-Trench, G., Anderson, R., Simpson, P.T., Lakhani, S.R., and Khanna, K.K. (2014). Rad51 supports triple negative breast cancer metastasis. Oncotarget *5*, 3261-3272.

Willats, W.G. (2002). Phage display: practicalities and prospects. Plant Mol Biol *50*, 837-854.

Winter, G. (1998). Making antibody and peptide ligands by repertoire selection technologies. J Mol Recognit *11*, 126-127.

Winter, G., and Milstein, C. (1991). Man-made antibodies. Nature *349*, 293-299.

Wulff, H. (2008). New light on the "old" chloride channel blocker DIDS. ACS chemical biology *3*, 399-401.

Xia, S.J., Shammas, M.A., and Shmookler Reis, R.J. (1997). Elevated recombination in immortal human cells is mediated by HsRAD51 recombinase. Molecular and cellular biology *17*, 7151-7158.

Xie, C., Drenberg, C., Edwards, H., Caldwell, J.T., Chen, W., Inaba, H., Xu, X., Buck, S.A., Taub, J.W., Baker, S.D., and Ge, Y. (2013). Panobinostat enhances cytarabine and daunorubicin sensitivities in AML cells through suppressing the expression of BRCA1, CHK1, and Rad51. PloS one *8*, e79106.

Yamamoto, A., Taki, T., Yagi, H., Habu, T., Yoshida, K., Yoshimura, Y., Yamamoto, K., Matsushiro, A., Nishimune, Y., and Morita, T. (1996). Cell cycle-dependent expression of the mouse Rad51 gene in proliferating cells. Molecular & general genetics : MGG *251*, 1-12.

Yoshikawa, K., Ogawa, T., Baer, R., Hemmi, H., Honda, K., Yamauchi, A., Inamoto, T., Ko, K., Yazumi, S., Motoda, H., Kodama, H., Noguchi, S., Gazdar, A.F., Yamaoka, Y., and Takahashi, R. (2000). Abnormal expression of BRCA1 and BRCA1-interactive DNA-repair proteins in

breast carcinomas. International journal of cancer. Journal international du cancer *88*, 28-36.

Zhao, Y., Brown, T.L., Kohler, H., and Muller, S. (2003). MTS-conjugated-antiactive caspase 3 antibodies inhibit actinomycin D-induced apoptosis. Apoptosis : an international journal on programmed cell death *8*, 631-637.

Zhao, Y., Lou, D., Burkett, J., and Kohler, H. (2001). Chemical engineering of cell penetrating antibodies. Journal of immunological methods *254*, 137-145.

Zhu, J., Zhou, L., Wu, G., Konig, H., Lin, X., Li, G., Qiu, X.L., Chen, C.F., Hu, C.M., Goldblatt, E., Bhatia, R., Chamberlin, A.R., Chen, P.L., and Lee, W.H. (2013). A novel small molecule RAD51 inactivator overcomes imatinib-resistance in chronic myeloid leukaemia. EMBO molecular medicine *5*, 353-365.